



RAIN

PROJECT

Security Sensitivity Committee Deliverable Evaluation

Deliverable Reference	D 2.2 version 2.0 final
Deliverable Name	Past cases of Extreme Weather Impact on Critical Infrastructure in Europe
Contributing Partners	ESSL as correspondence author
Date of Submission	2015-02-28

Evaluation is based on version 1.0 dated 2015-03-19 of the proposal for the SSC evaluation:

- The content is not related to general project management
- The content is not related to general outcomes as dissemination and communication
- The content is related to critical infrastructure vulnerability or sensitivity
- The content is publicly available or commonly known
- The content does not add new information on vulnerabilities, sensitivities or incident scenario's on specific objects or transport systems or assets in general
- There are no uncertainties that need to be discussed with a NSA

Diagram path: 1-2-3-4-5.1-5.2-9. Therefore the evaluation is: Public.

Decision of Evaluation	Public	Confidential
	Restricted	

Evaluator Name	P.L. Prak, MSSM
Evaluator Signature	
Date of Evaluation	2015-05-22





Past Cases of Extreme Weather Impact on Critical Infrastructure in Europe

Authors

Pieter Groenemeijer* (ESSL)	Ilari Lehtonen (FMI)
Nico Becker (FU-Berlin)	Hanna Mäkelä (FMI)
Matilda Djidara (GDG)	Oswaldo Morales Napoles (TU-Delft)
Kenneth Gavin (GDG)	Katrin Nissen (FU-Berlin)
Timo Hellenberg (Hellenberg)	Dominik Paprotny (TU-Delft)
Alois M. Holzer (ESSL)	Peter Prak (PSJ)
Ilkka Juga (FMI)	Tomáš Púčik (ESSL)
Pauli Jokinen (FMI)	Lars Tijssen (ESSL)
Kirsti Jylhä (FMI)	Andrea Vajda (FMI)

***Correspondence author:**

Dr. Pieter Groenemeijer, European Severe Storms Laboratory e.V.
c/o DLR Institute for Atmospheric Physics, Münchner Str. 20, Geb. 20, 82234 Wessling, Germany,
pieter.groenemeijer@essl.org, +49 151 59031839

Date: 23/04/2015

Dissemination level: (PU, PP, RE, CO): PU

This project has received funding from the European Union's Seventh Framework Programme for research, technological development and demonstration under grant agreement no 608166



This project is funded by
the European Union

DOCUMENT HISTORY

Index	Date	Author(s)	Main modifications
0.0	16 January 2015	Pieter Groenemeijer* (ESSL), Nico Becker (FU-Berlin), Matilda Djidara (GDG), Kenneth Gavin (GDG), Timo Hellenberg (Hellenberg), Alois M. Holzer (ESSL), Ilkka Juga (FMI), Pauli Jokinen (FMI), Kirsti Jylhä (FMI), Ilari Lehtonen (FMI), Hanna Mäkelä (FMI), Oswaldo Morales Napoles (TU-Delft), Katrin Nissen (FU-Berlin), Dominik Paprotny (TU-Delft), Peter Prak (PSJ), Tomáš Půčik (ESSL), Lars Tijssen (ESSL), Andrea Vajda (FMI)	First Draft, compiled from contributions.
1.0	25 February 2015	“	Second Draft, improved after round of feedback.
2.0	23 April 2015	“	Final version, improved after project internal review, ready for submission to Commission.

Document Name: Past Impacts of Extreme Weather Impact on Critical Infrastructure in Europe (List of Past Cases)

Work Package: 2

Task: 2.1

Deliverable: 2.2

Deliverable scheduled date: 28 February 2014

Responsible Partner: ESSL

Table of Contents

1.	Executive Summary	7
2.	Introduction.....	8
3.	List of Past Cases	10
3.1	Windstorms	11
3.1.1	Windstorms Lothar and Martin, Western Europe, December 1999	11
3.1.2	Windstorm Kyrill, West, Central and East Europe, January 2007	14
3.2	Heavy rainfall and flash floods	17
3.2.1	Flash flood, Berlin, 4 August 2013	17
3.2.2	Flash flood, Madeira, 20 February 2010	18
3.2.1	Flash flood, Grand-Bornand (Haute-Savoie), 14 July 1987.....	23
3.3	Landslides	27
3.3.1	Landslides, Scotland, August 2004	27
3.3.2	Landslide, Switzerland, 13 August 2014.....	28
3.3.3	Landslide, Croatia, 12 September 2014	29
3.4	River floods.....	30
3.4.1	River floods, England, 2007	30
3.4.2	River floods, Central Europe, May and June 2013	34
3.4.3	River flood, Dublin-Belfast railway, 21 August 2009.....	37
3.5	Thunderstorm gusts	38
3.5.1	Convective windstorm, Northrhine-Westphalia (Germany), 9 June 2014.....	38
3.6	Tornado	43
3.6.1	Tornado outbreak, South Poland, 15 August 2008	43
3.7	Hail.....	47
3.7.1	Hail, Stuttgart (Germany), 15 August 1972	47
3.8	Lightning	49
3.8.1	Lightning, Jistebnik (Czech Republic), 2009.....	49
3.9	Snow and snow storms	51
3.9.1	Heavy snowfall, Helsinki metropolitan area, 17 March 2005	51
3.9.2	Snow storm, South and central Finland, 23-24 November 2008	55
3.9.3	Heavy snow loading, Finland, 31 October – 1 November 2001	58
3.10	Freezing rain	64
3.10.1	Freezing rain, Slovenia, 31 January – 3 February 2014	64

- 3.11 Wildfire 68
 - 3.11.1 Wildfire event in Västmanland, Sweden, 31 July 2014 - 11 September 2014 68
- 3.12 Coastal Flood 72
 - 3.12.1 Storm surge with coastal flood, France, February 2010 72
- 4. Synthesis of stakeholder interviews and past cases 78
 - 4.1 Stakeholder interviews..... 78
 - 4.2 Impact of the various extreme weather phenomena 79
 - 4.3 Impact of wind storms..... 81
 - 4.3.1 Affected sectors..... 81
 - 4.3.2 Impacts 81
 - 4.3.3 Preventive and response measures 82
 - 4.4 Impact of thunderstorm gusts..... 83
 - 4.4.1 Affected sectors..... 83
 - 4.4.2 Impacts 83
 - 4.4.3 Preventive and response measures 83
 - 4.5 Impact of heavy precipitation and consequential phenomena 85
 - 4.5.1 Affected sectors..... 85
 - 4.5.2 Impacts 85
 - 4.5.3 Preventive and response measures 85
 - 4.6 Impact of river floods 86
 - 4.6.1 Affected sectors..... 86
 - 4.6.2 Impacts 86
 - 4.6.3 Preventive and response measures 86
 - 4.6.4 Conclusions..... 86
 - 4.7 Coastal floods 86
 - 4.7.1 Affected sectors..... 86
 - 4.7.2 Impacts 87
 - 4.7.3 Preventive and response measures 87
 - 4.7.4 Conclusions..... 87
 - 4.8 Impact of hail..... 87
 - 4.8.1 Affected sectors..... 87
 - 4.8.2 Impacts 87
 - 4.8.3 Preventive and response measures 87

- 4.9 Impact of snow (storms) and freezing precipitation 88
 - 4.9.1 Affected sectors..... 88
 - 4.9.2 Impacts 88
 - 4.9.3 Thresholds 88
 - 4.9.4 Preventive and response measures 89
 - 4.9.5 Conclusions..... 90
- 4.10 Impact of wildfires..... 90
 - 4.10.1 Affected sectors..... 90
 - 4.10.2 Impacts 90
 - 4.10.3 Preventive and response measures 91
 - 4.10.4 Conclusions..... 91
- 4.11 Impact of tornadoes..... 91
 - 4.11.1 Affected sectors..... 91
 - 4.11.2 Impacts 91
 - 4.11.3 Preventive and response measures 92
- 4.12 Impact of lightning 92
 - 4.12.1 Affected sectors..... 92
 - 4.12.2 Impacts 92
 - 4.12.3 Preventive and response measures 92
- 5. Method Development for the detection of Extreme Weather Impact..... 93
 - 5.1 Physical and statistical flood risk analysis methods 93
 - 5.1.1 Introduction..... 93
 - 5.1.2 Physical methods..... 93
 - 5.1.3 Statistical methods 98
 - 5.2 Windstorm impact identification methods 100
 - 5.2.1 Introduction..... 100
 - 5.2.2 Estimation of return levels 102
 - 5.2.3 Towards the application of the modified Storm Severity Index 105
 - 5.2.4 Outlook..... 106
 - 5.3 Hazardous precipitation identification methods 106
 - 5.3.1 Introduction..... 106
 - 5.3.2 Calculation of critical thresholds 106
 - 5.3.3 Detection of heavy precipitation events 108

6. Conclusions and recommendations	111
6.1 Conclusions.....	111
6.2 Recommendations	113
7. References.....	115
Appendix A. Technical details of physical and statistical methods to be used by TU-Delft.....	126
Appendix B: Interview guideline	128

1. Executive Summary

This report presents the results of three components of the identification of extreme weather hazards to critical infrastructure (CI) carried out within the RAIN project. The focus was on four types of CI: i) **roads**, ii) **railways**, iii) **electrical power supply infrastructure** and iv) **telecommunication infrastructure**. Firstly, a list of past cases of extreme weather affecting critical infrastructure was compiled. Second, 28 semi-structured interviews with stakeholders (mostly operators of CI or emergency management officials) were carried out in person or by telephone during November and December 2014. These stakeholders include managers of infrastructure and emergency managers that were selected based using the existing contact networks of the RAIN partners. Last, new hazard identification methods were developed by the RAIN project partners.

The efforts were carried out with the aim of addressing the following questions:

- How CI is impacted by severe weather?
- Which severe weather events impact CI the most?
- Which CI are most vulnerable to extreme weather?
- Which measures have CI operators taken to prevent or reduce the impact of extreme weather?

The results indicate that CI operators are most concerned about the impacts of **freezing precipitation, snowfall, snow loading and snow storms, windstorms** and **heavy precipitation**, especially if the latter lead to **river floods**. In addition, particular CI types are especially sensitive to a particular type of severe weather that is of lower concern to other types of CI. For instance, telecommunication is very vulnerable to lightning, road transportation to coastal floods, and rail transportation to landslides.

Operators and managers of CI systems concerning road and rail transport judge their systems to be vulnerable to more types of severe weather than power and telecommunications. For instance floods, landslides or heavy snowfall (which does not freeze onto wires) are of less concern to these modes, whereas they can paralyze rail and road transport.

In important way for CI operators to prepare for severe weather is by seeking tailored (hydro)meteorological advice, which 22 out of 28 do. Based on this advice, measures are taken such as temporarily operating the system in a more resilient, but more costly mode, e.g. by creating more redundancy in a power network or introducing speed limits to vehicles and trains. Vulnerable components (such as wind turbines) may temporarily be taken out of use. In addition, CI operators often request additional personnel to be on stand-by to mitigate impact as it occurs and commission additional checks of protective measures (e.g. the heating system of railway switches) prior to the event. Furthermore, CI managers review their action plans and communicate them to all relevant parties.

Some CI operators not only worry about the time scale of weather forecasting, but also prepare for changes in risk of extreme weather on the time-scale of climatic changes. They have established platforms of cooperation with climate scientists, where they jointly seek to find how CI systems can be best adapted to cope with expected changes.

2. Introduction

The RAIN project aims to develop an operational analysis framework that identifies critical infrastructure components impacted by extreme weather events, with the ultimate objective to minimise those impacts. An important aim of the RAIN project is to evaluate the present and future risk to critical infrastructure posed by various extreme weather events. The threefold approach that was taken consisted of

1. Compiling a list of past events of critical infrastructure failures caused by severe weather.
2. Interviewing operators of critical infrastructure and emergency managers to obtain direct information about extreme weather impacts.
3. Developing new technical methods to assist in the identification of hazards.

This report contains the results of these efforts in three subsequent chapters.

The purpose of this report is to present an overview of the ways in which extreme weather impacts on different forms of critical infrastructure (CI). It is important to note here that the CI considered in detail within the RAIN project are i.) roads, ii.) railways, iii.) electrical power grids and iv.) telecommunication networks. A key objective is to identify the severe weather phenomena to which each of these CI are more and to which they are less vulnerable. Furthermore, we report on the CI operators' estimate of useful threshold values for severe weather intensity, which is relevant for subsequent work. Finally we made an inventory of the ways CI infrastructures operators mitigate and prepare for extreme weather.

The RAIN partners were involved in this work according to their field of expertise: The Finnish Meteorological Institute (FMI) addressed snowfall and snow storms, freezing precipitation as well as wildfires. The Free University of Berlin (FU-Berlin) contributed with respect to heavy precipitation and windstorms. The European Severe Storms Laboratory (ESSL) addressed thunderstorm-related hazards, The TU Delft (TU-Delft) river and coastal flooding, Gavin and Doherty Geosolutions (GDG) contributed with regard to landslides. Additionally, Hellenberg and PSJ Advies contributed in giving advice and designing the stakeholder interviews.

The List of Past Cases presented in Chapter 3 was compiled by the partners who each used the expertise at their respective institution to provide a description of one or more events of the phenomenon. Often this was done by summarizing or extending prior studies or perusing data sets their institution owns. Each case consists of a description of the (hydro-)meteorological background of the event and of the impact on CI, and, where appropriate, some key findings were summarized.

In Chapter 4, the findings from the stakeholder interviews are summarized. These interviews were carried out, generally in person or by telephone, by all partners during October and November 2014. The chapter starts with a quantitative analysis of the results, then summarizes the main findings categorized with respect to CI mode, and finally again categorized with respect to extreme weather phenomena.

Chapter 5 describes the development of new methods to benefit hazard identification. These methods are to be used in subsequent work with the aim to quantify the distribution of the various hazards

across Europe. In addition, they will be used to address the effects of climate change on the frequency and intensity of the extreme weather events. Three different methods are described. The first section describes the methods used by TU-Delft to analyse flood risk. The second section presents FU-Berlin's work to develop a new method of identifying the impact of wind storms using a wind field tracking algorithm including an integrative storm severity index (SSI). The last section reports on new identification procedures for hazardous precipitation events developed at FU-Berlin. Finally, Chapter 6 presents the conclusions of the work.

The authors would like to thank all stakeholders who have contributed to the research we report on here by allowing us to interview them. In addition, we thank Dr. Chiara Bianchizza of the Institute of International Sociology in Gorizia for her helpful review of a draft of the report.

3.1 Windstorms

3.1.1 Windstorms Lothar and Martin, Western Europe, December 1999

Type of event	windstorm
Date	25 – 28 December 1999
Location	West and Central Europe
Total damage	€ 9 billion
Fatalities	140
Affected critical infrastructure	
Type of damage to infrastructure	Broken power lines, blocked roads, railways

In December 1999 a series of five windstorms affected Europe. The two extreme storms Lothar and Martin occurred within a period of 36 hours and affected mainly Western and Central Europe, in particular France and South Germany (Figure 3.2). These two windstorms had a major impact on the French energy system and caused blackouts affecting 3.4 million people. Lothar and Martin caused 140 fatalities and an economic loss of more than 15 billion dollars (MunichRe 2002).

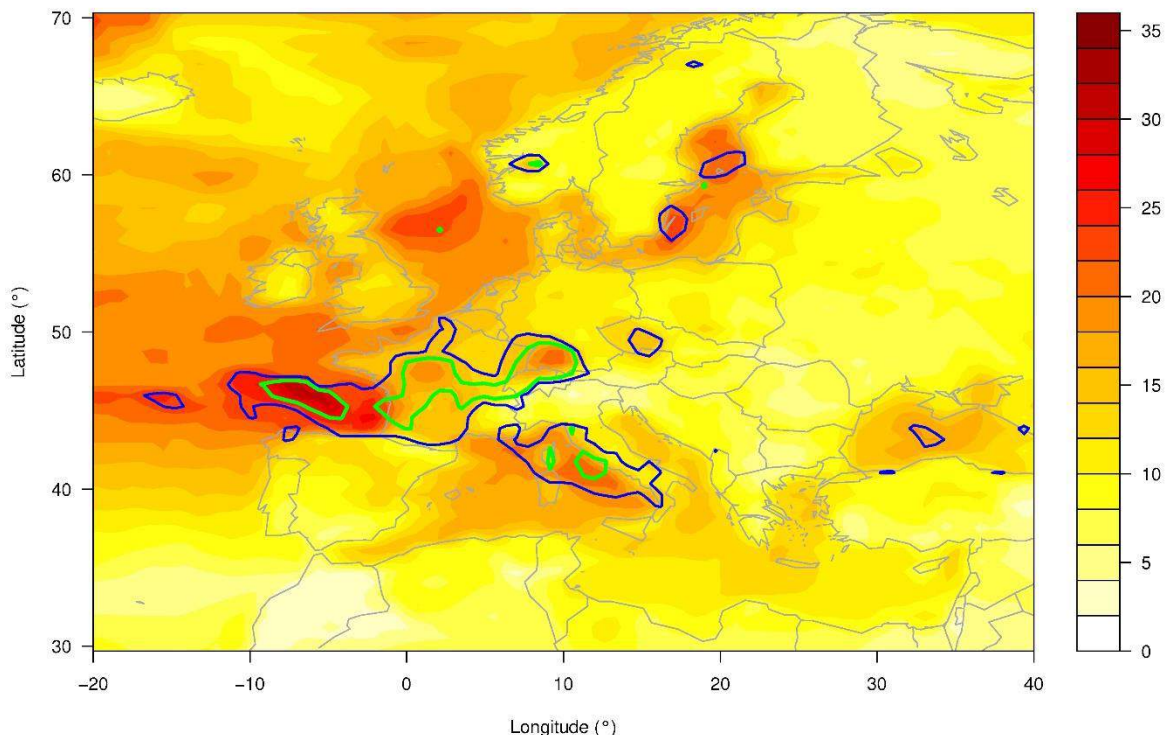


Figure 3.2. Maximum 10m wind speeds in m/s which occurred during the passage of windstorms "Lothar" and "Martin" within the period from 25 to 28 Dec. 1999, derived from ERA interim reanalysis data (shading). The contours encircle areas where the 5-year (blue) and the 50-year (green) return levels are exceeded by the 10m wind speeds

3.1.1.1 Meteorological Description

The prevailing large-scale atmospheric conditions during the formation of the two storms Lothar and Martin were characterized by a high level of baroclinicity and an intense zonal upper-level jet (Ulbrich et al. 2001). Lothar initially developed close to the North American east coast on 24 December 1999 at 00 UTC. In the beginning, the system was restricted to the lower troposphere. While travelling towards the European continent, it crossed the area of high baroclinicity with an intense jet stream and strong temperature gradients (Figure 3.3). Usually, these regions of high baroclinicity provide optimal conditions for an explosive development of extra-tropical storms. However, such growth did not occur until Lothar reached the European region on 26 December at 00 UTC. Reasons for the suppressed development of Lothar are the shallow structure and the relatively small size of the system, which possibly inhibited significant baroclinic growth (Ulbrich et al. 2001). Lothar reached Europe without altering the general characteristics of the upper-level conditions over the North Atlantic. When reaching Europe an additional factor finally initiated the rapid intensification of the pressure system. Between Brittany and Cornwall the upper-level flow exhibited a region with strong divergence caused by a diffluent flow at the eastern exit-region of the jet-stream. An extraordinary pressure drop of 28 hPa within 3 hours was recorded at stations in northern France and the English Channel. While crossing France, Germany and Poland, Lothar was characterized by a high propagation speed and a relatively small diameter.

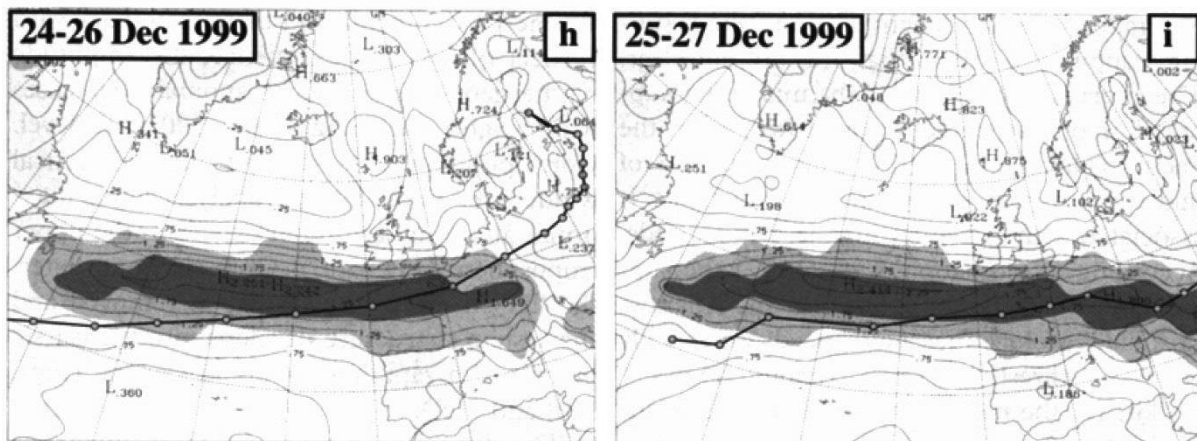


Figure 3.3. Cyclone-tracks of “Lothar” (left) and “Martin” (right) with 6-hourly time steps. Contours show the 3-day averaged upper-level (500 - 300 hPa) Eady growth rate (per day), a measure for baroclinicity quantifying the large-scale conditions for the potential growth of extratropical cyclones. Grid points where the Eady growth rate exceed the local 95th and 99th percentile are shaded. (from Ulbrich et al. 2001)

As early as 25 December, the successor system of Lothar, named Martin, had formed over North America and moved rapidly across the North Atlantic. While Lothar was relatively small in size and therefore did not interact with the strong baroclinic environment in the North Atlantic region, Martin was a larger system and could profit from the baroclinic conditions, which led to a strong intensification of the storm on its way across the North Atlantic. Martin’s track, which was located slightly further southward than Lothar, affected both France and Spain.

Windstorm Lothar was poorly predicted by several operational forecast models (Leutbecher et al. 2002). One reason was that rapidly falling pressure values which were recorded by ships on the North Atlantic did not go into the initialization procedures of the model prediction runs. Instead these

measurements were rejected by the model system, because the extreme pressure drop was regarded as a measurement error by the automatic consistency checks (Inness and Dorling 2012). Additionally, the results of an ensemble simulation showed that the atmospheric conditions during windstorm Lothar were “exceptionally unpredictable” (Palmer and Hagedorn 2006).

3.1.1.2 *Impacts on Critical Infrastructure*

The highest impact caused by Lothar and Martin was experienced by the electricity network of Electricité de France (EdF). The damages and consequences were summarized by the Union of the Electricity Industry (2006). While EdF was well prepared for the effects of freezing rain and snow on the power lines, the effects of such a severe wind situation was not anticipated. 35 extra-high voltage lines were tripped by the two storms, which amounts to 25% of the total number. 180 high-voltage lines were destroyed and more than 100 high- and medium-voltage substations were out of order. Additionally, a large number of low-voltage lines were destroyed by falling trees. In total, more than 3.4 million customers were affected by the resulting blackouts. After the passage of the storms, exceptional measures were taken in order to rebuild the power grid. Among others, 19 800 operators specialized in grid maintenance, 40 000 logistic and commercial employees of EdF were engaged in the efforts to restore the energy supply of the French population. They were supported by operators with electrical ability from other companies and countries. Estimated costs resulting from the damages of the power grid alone amount to € 1.4 billion.

Power generation was affected by the storms as well. The combination of the rising tides and exceptionally high winds caused by Martin led to a flooding of the Blayais Nuclear Power Plant, located on the Gironde estuary in western France. The flooding resulted in a Level 2 event on the International Nuclear Event Scale (Mattéi et al. 2001). A level 2 (on the 8 point Scale) is called an “*Incident*”.

The storms strongly disturbed both fixed and mobile telecommunication networks within the affected areas (MunichRe 2002). These disturbances were caused by the failures of the power supply as well as by damages to the transmission facilities. In some cases the disruption of the telecommunication system lasted for several days.

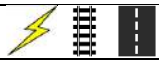
3.1.1.3 *Conclusions*

The series of winter storms in December 1999 caused a change in the perception of European windstorms (Tatge 2009). In contrast to the earlier perception of windstorms as rather local phenomena, Lothar and Martin increased the sensitivity to the Europe-wide effects of extreme extra-tropical cyclones.

As a result from the flooding of the Blayais Nuclear Power Plant a number of projects were initiated by the French and German operators to study the circumstances which led to the critical situation and to draw conclusions on how to improve the flood defenses in Blayais and at other sites (Mattéi et al. 2001).

The case of Lothar has become an example for the failure of weather forecast models and has since then been used for model evaluation and improvement (e.g. Caron et al. 2002, Hoskins and Coutinho 2005).

3.1.2 Windstorm Kyrill, West, Central and East Europe, January 2007

Type of event	Windstorm
Date	17 – 18 January 2007
Location	West, Central and East Europe
Total damage	€ 4 - 7 billion
Fatalities	47
Affected critical infrastructure	
Type of damage to infrastructure	falling trees leading to blocked roads and railways; damage to power lines

Kyrill was an extratropical cyclone which developed into an intense European windstorm in January 2007. It caused extensive damages of up to 7 billion Euros within large parts of Europe (Figure 3.4) and led to 47 fatalities. Kyrill had an exceptionally strong impact on the public transport system and caused widespread power outages.

3.1.2.1 Meteorological Description

The genesis and development of Kyrill was typical for an extreme European windstorm. The pressure system formed in the western North Atlantic close to Newfoundland around 16 January 2014. Optimal growth conditions were created by two previous low pressure systems, which transported cold polar air southward and created a strong temperature gradient opposed to warm and humid air of the subtropics. The upper tropospheric flow showed a strong jet stream with widespread areas of divergent flow in the European region. Within two days, Kyrill crossed the North Atlantic with increasing speed. It reached the Irish coast in the morning of the 18 January, where it caused wind speeds of up to 120 km/h. Similar to windstorm Lothar, described above, Kyrill entered an area of upper-level divergence, which contributed to the intensification of Kyrill and delayed the weakening of the storm after landfall (Fink et al. 2009). Around noon, minimum pressure fell below 960 hPa across the southern North Sea. The resulting strong pressure gradients led to widespread hurricane force wind gusts up to 150 km/h throughout Central Europe. During the passage of the cold front, thunderstorms with heavy precipitation occurred. At many stations in North-East Germany the 24h precipitation sums exceeded the mean January accumulation of rainfall. In northern and western Germany, hurricane force winds were recorded throughout the whole afternoon of 18 January. The 18 UTC radiosonde measurement in Lindenberg, Germany, revealed an intrusion of dry air at levels above 400 hPa, which may have led to an increase in convective instability (Fink et al. 2009). Lifting associated with the cold front apparently caused strong convective activity, leading to the formation of thunderstorms and high lightning rates. During the night, the windstorm affected Poland, the Czech Republic, Austria and Switzerland, where it caused an all-time wind speed record for a lowland station in Wolfsegg am Hausruck. Despite the heavy precipitation related to Kyrill, no heavy flooding occurred in the German low mountain ranges, due to little precipitation in the previous days and due to the lack of snow cover. In summary, Kyrill was an extreme windstorm, because it affected unusually widespread areas including Germany and most of its neighbouring states.

In contrast to Lothar, Kyrill was well forecasted by the numerical prediction models and the related gusts and heavy precipitation were predicted already 5-6 day before the arrival of the storm. This can be attributed to the fact that Kyrill developed rather from an upper-tropospheric pressure perturbation over North-America, than from a near surface depression as it was the case for Lothar, for example (Willis 2007). It also displays the increasing abilities of medium range weather forecasting systems. However, a storm surge which was expected for the German Bight did not occur, because Kyrill moved quicker than expected further eastward and did not coincide with the high tide.

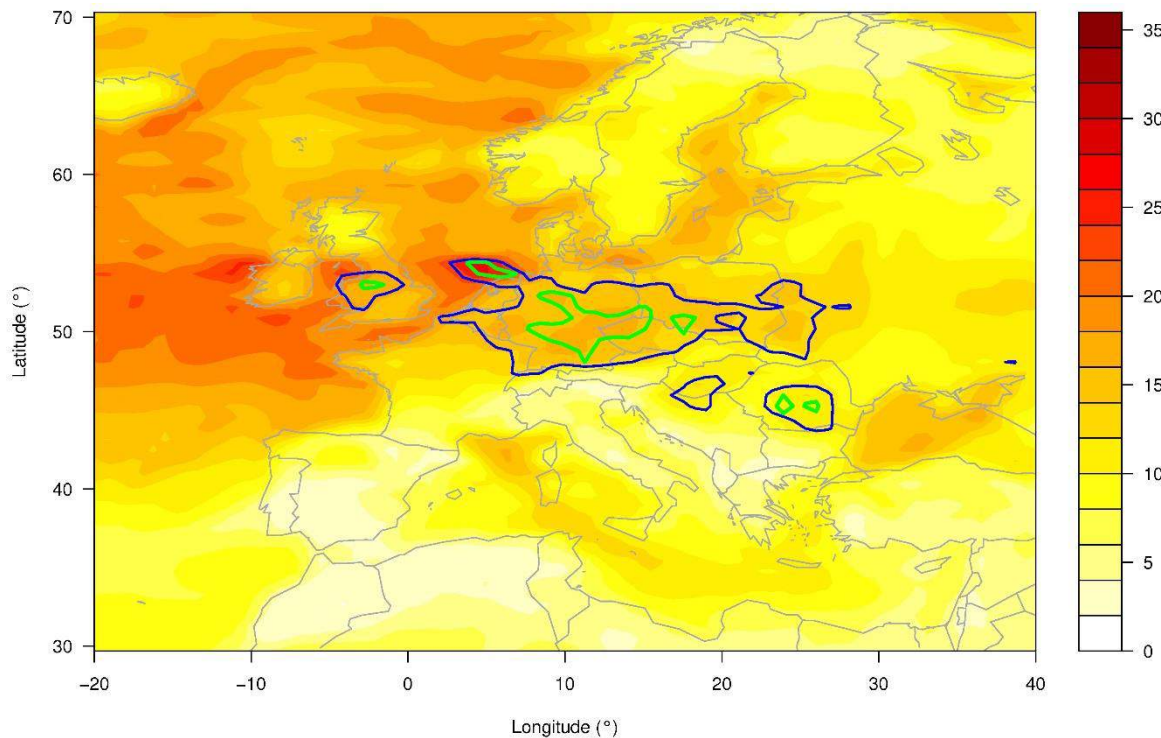


Figure 3.4. Maximum 10m wind speeds in m/s which occurred during the passage of windstorm "Kyrill" within the period from 16 to 19 Jan. 2007, derived from ERA interim reanalysis data (shading). The contours encircle areas where the 5-year (blue) and the 50-year (green) return levels are exceeded by the 10m wind speeds.

3.1.2.2 Impacts on Critical Infrastructure

Kyrill had major effects on the transportation infrastructure within large parts of Europe. Many roads and motorways were blocked due to fallen trees and overturned high-sided vehicles. Many motorways and especially bridges across rivers or valleys were closed because of the high wind speeds, leading to long queues. This was for instance the case for several Rhine bridges.

Also the train system was heavily disturbed in the affected countries. After wind speeds started to increase prior to the arrival of the storm, speed limits were imposed to trains in order to minimise damages due to fallen trees. This already caused delays of the trains. On the 18 January 2014 at 21:00 h CET, the German long-distance train traffic was shut down completely for the first time in history. The shutdown of the train services lasted for a period of 9 hours, in order to assure the security of the passengers. Additionally, parts of the regional train connections were cancelled. Other countries like Great Britain and the Netherlands reduced or stopped their train services. Furthermore, many train stations were heavily damaged, including those in London, Delft, Amsterdam and Berlin. As a consequence, they partly had to be evacuated and were closed for safety reasons.

In Germany, the telecommunication network was largely unaffected by the storm (Wilkins 2007). Vodafone and T-Mobile stated that mobile network congestions only occurred at train stations, where people lost their train connections and tried to reach their relatives. Batteries and power generator could maintain the function of important parts of the telecommunication system also within periods of power blackouts. Telecommunication provider E-Plus mentioned single cases of damaged telecommunication antennas, however none were completely destroyed.

Furthermore, blackouts affected more than 100.000 customers (EQECAT 2007), however, the impacts on the energy sector were substantially lower than in the case of the storms Lothar and Martin.



Figure 3.5. Damages caused by the windstorm "Kyrill" between the 18th and 19th January 2007. (from left to right) An overturned truck in the Harz Mountains, Germany, damaged rail ways in Sutton Coldfield, Great Britain (Focus 2007) and a toppled power pylon near Magdeburg-Ottersleben, Germany (Wikipedia 2009).

3.1.2.3 Conclusions

Compared to Lothar and Martin, Kyrill did not cause as much damage. There are several possible reasons for that. First, the higher quality of the weather forecast made possible by the higher predictability of the storm, which allowed for a better preparation and precautionary measures. Second, it is likely that the infrastructure was improved based on the experiences from the windstorms of the previous decades, such as Lothar.

3.2 Heavy rainfall and flash floods

3.2.1 Flash flood, Berlin, 4 August 2013

Type of event	Flash flood (thunderstorm-related)
Date	4 – 5 August 2013
Location	Berlin
Total damage	Unknown
Victims	No fatalities
Affected critical infrastructure	
Type of damage to infrastructure	Flooding of roads and subway station

After a period of extreme heat, thunderstorms developed over Germany (e.g. MA, 2013). These were associated with strong wind gusts, lightning and extreme precipitation. Several of these convective cells were associated with damage to infrastructure. Several people were injured. One of the events hit the South-West of Berlin, where it flooded streets and a subway station (MP, 2013).

3.2.1.1 Meteorological and Hydrological Description

At the back of a high pressure system, warm and humid air masses were transported into Central Europe. Temperatures in Berlin on 4 August 2013 reached almost 30 °C. During the afternoon severe thunderstorms developed in many places over Germany especially in Bavaria and Baden-Württemberg. During the night between the 4th and 5th of August, the South West of Berlin was hit by a thunderstorm. In some places, more than 13 mm of rain were recorded within 15 minutes. The radar image (Figure 3.6) shows a cluster of convective cells over Berlin.

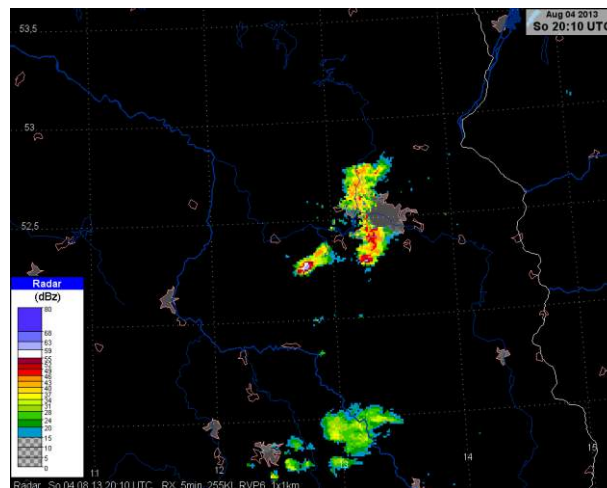


Figure 3.6. Radar image of 4 of August 2013 at 2010 UTC. A thunderstorm over Berlin. Data source: DWD.

3.2.1.2 Impact on Critical Infrastructure

The event has flooded several streets and a subway station. The line had to be closed but could be opened again after the water masses receded. There was no long-term damage to the streets and the station.

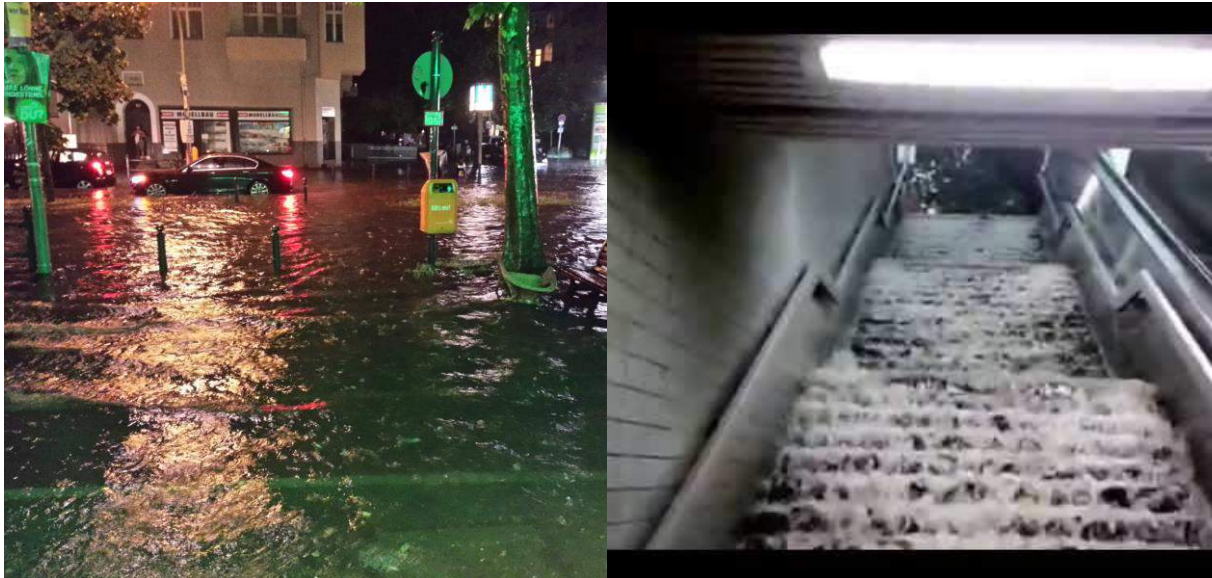


Figure 3.7. Rain has flooded streets and a subway station in the South West of Berlin. Left figure courtesy Thomas Schubert, right figure was taken from youtube video (MP 2013).

3.2.1.3 Conclusions

Localized small-scale events can cause disruptions and damage to infrastructure, if they hit a critical infrastructure element. The effect is usually smaller than for large-scale events. Certain weather situations, such as the one presented here, favor the occurrence of numerous severe precipitation events. In the current case a high number of local events associated with thunderstorms have hit regions all over Germany and the neighboring countries. Even though the impact of the individual events may be modest, in total they can cause severe damage to different parts of the infrastructure network.

3.2.2 Flash flood, Madeira, 20 February 2010

Type of event	Flash flood (thunderstorm-related)
Date	20 February 2010
Location	Central, southern and eastern parts of the island of Madeira, Portugal
Total damage	1.5 billion EUR
Victims	45 fatalities; 6 persons missing
Affected critical infrastructure	
Type of damage to infrastructure	Blocked roads, disrupted electricity and telecommunication, closed airport, cut water supplies

On 20 February 2010 during the morning and noon hours, severe storms devastated the communities of Tabua, Ribeira Brava, Curral Das Freiras, Santo António, São Roque, Canico, Santa Cruz, São Martinho, Monte, and as one of the worst hit towns also the capital Funchal (Figure 3.8).

Flash floods caused damage of 1.5 billion EUR. 51 people died in the event, making it the deadliest hydro-meteorological catastrophe in Portugal in the last four decades and since 1803 in Madeira. On 9 October 1803 a flash-flood event caused 800 to 1000 casualties in Funchal. The southern coastal

strip of Madeira is densely populated with 150 000 inhabitants alone in the Funchal district. Madeira is a mountainous island with steep slopes. This might be the reason why flash-floods and their streams own a local common name: “aluvião”.

Several types of critical infrastructure were heavily damaged or destroyed by the flashfloods: streets, power and water supplies and telecommunication lines. The airport had to be temporarily closed.



Figure 3.8. Event report (blue dot near the capital town of Funchal) from the European Severe Weather Database ESWD for 20 February 2010, and overview map of the island of Madeira

3.2.2.1 Meteorological Description

The episode of the given event was preceded by a very wet winter season, largely exceeding the 95th percentile of Funchal’s historical precipitation records, dating back to the year 1865.

On 20 February 2010 at 0 UTC, a quasi-stationary low was situated over the central north Atlantic with a core pressure of 982 hPa. An associated warm front passed the island of Madeira in the early morning of this day. During the severe event in the morning hours Madeira was situated in the warm sector with a temperature of just below 20 degrees at the southern coastline. The occlusion point of the warm front and cold front was close to the island, just a little north. The models produced a high amount of precipitation in forecasts and hindcasts for this day around the Madeira archipelago.

The direction of the wind was onshore and therefore perpendicular to the orientation of the mountain chain that covers the inner part of the island from WNW to ESE. This setup enhanced the already large amounts of precipitation (caused by the mesoscale weather setting) by local orographic lift of the very moist marine air.

The radiosounding of Funchal (12 UTC on 20 February 2010; Figure 3.9) shows moisture-saturated air from the sea surface up to about 2.5 km, and it shows unidirectional southwesterly wind in the lowest 2 km of the troposphere, but at the same time extreme speed shear with an increase of nearly 30 m/s in the lowest km. Already 300 m above sea level the wind was 20 m/s from SW, causing extreme uplift and condensation along the southern mountain slopes. The same radiosounding indicates a convective available potential energy (CAPE) of about 300 J/kg (which cannot be seen in the re-analysis maps).

It must be noted that this sounding was launched a few hours after the peak of the event, and that some of the meteorological standard data (Funchal observatory reports and 12 UTC radiosounding)

was not transferred via the GTS, because of the event itself. This fact might have an effect on the ECMWF re-analyses.

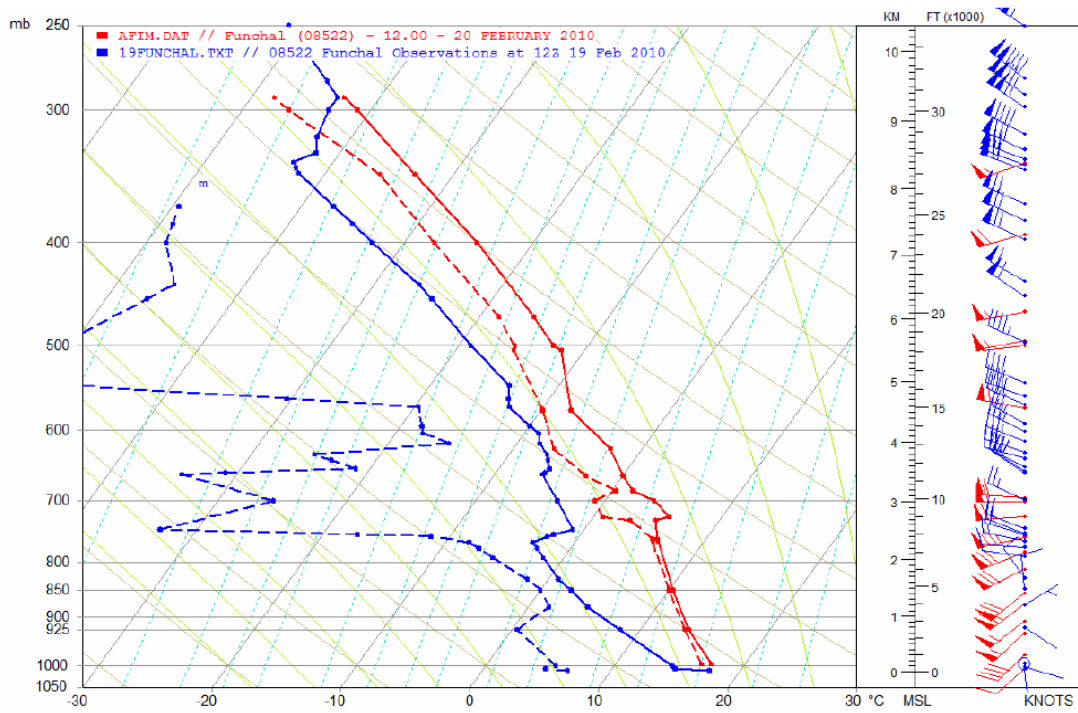


Figure 3.9. Radiosounding of Funchal, projection on a skew-T diagram of the 19 February 2010 (12:00 UTC) in blue, and of 20 February 2010 (12:00 UTC) in red. From Fragoso et al (2012).

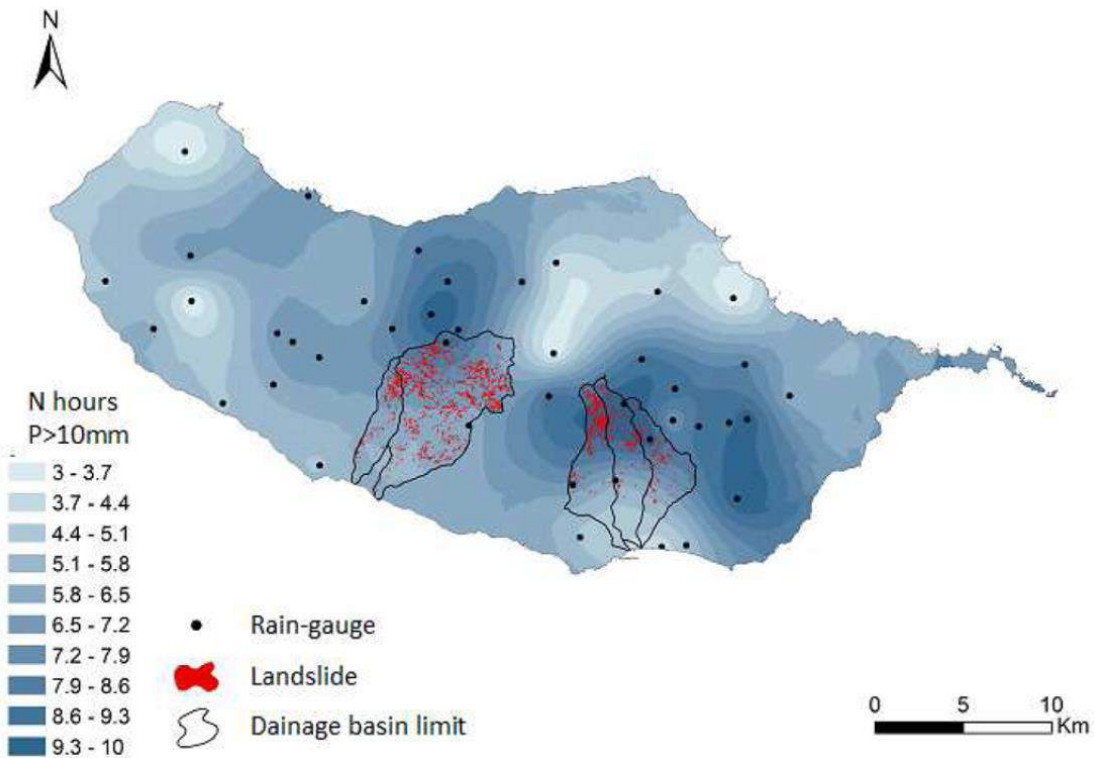


Figure 3.10. Number of hours with precipitation above 10mm and landslides distribution on Funchal and Ribeira Brava areas. This map is based on a subset of the hydrographical network stations. From Fragoso et al (2012).

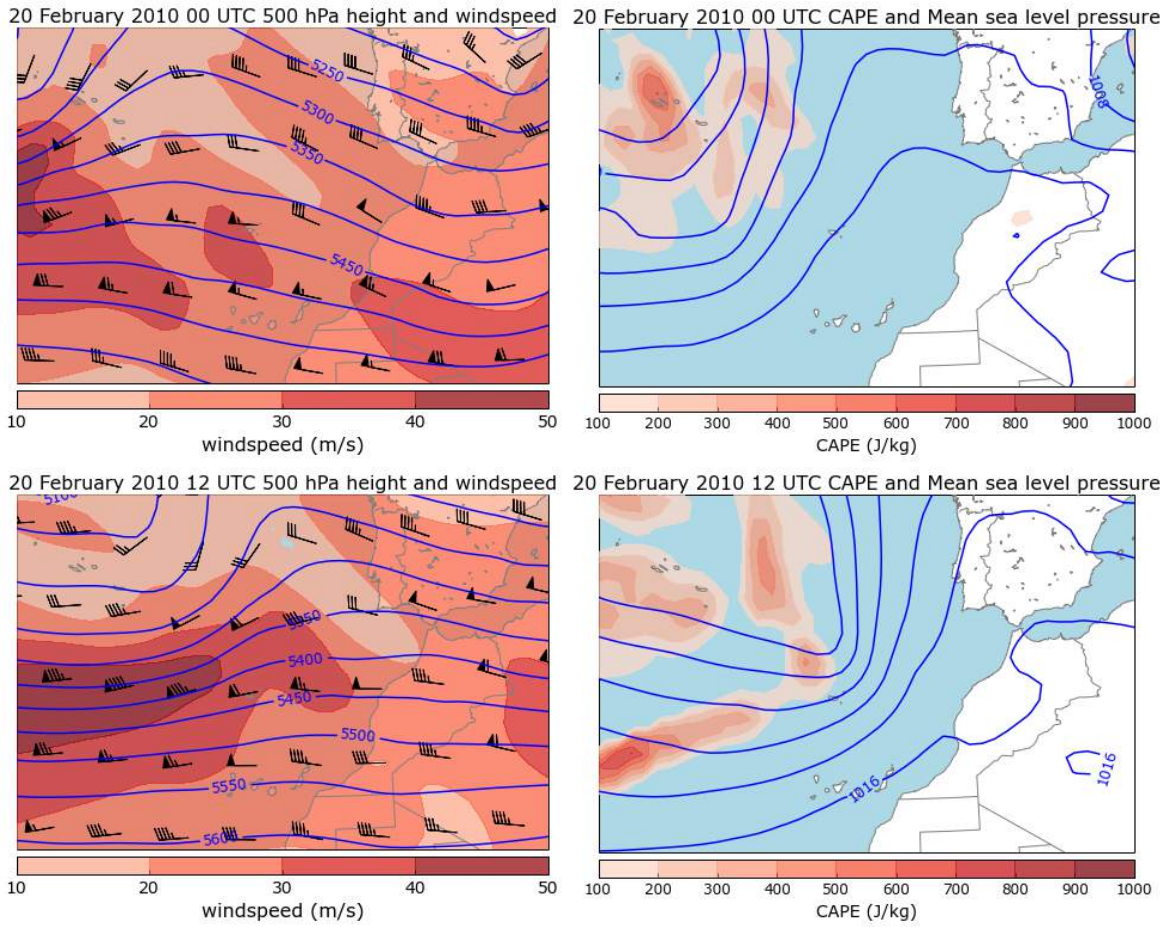


Figure 3.11. Wind and geopotential height at 500 hPa on 20 February 00 UTC and 12 UTC (left), Convective Available Potential Energy (CAPE in J/kg) and mean sea level pressure (in hPa) (right). Data: ERA-Interim.

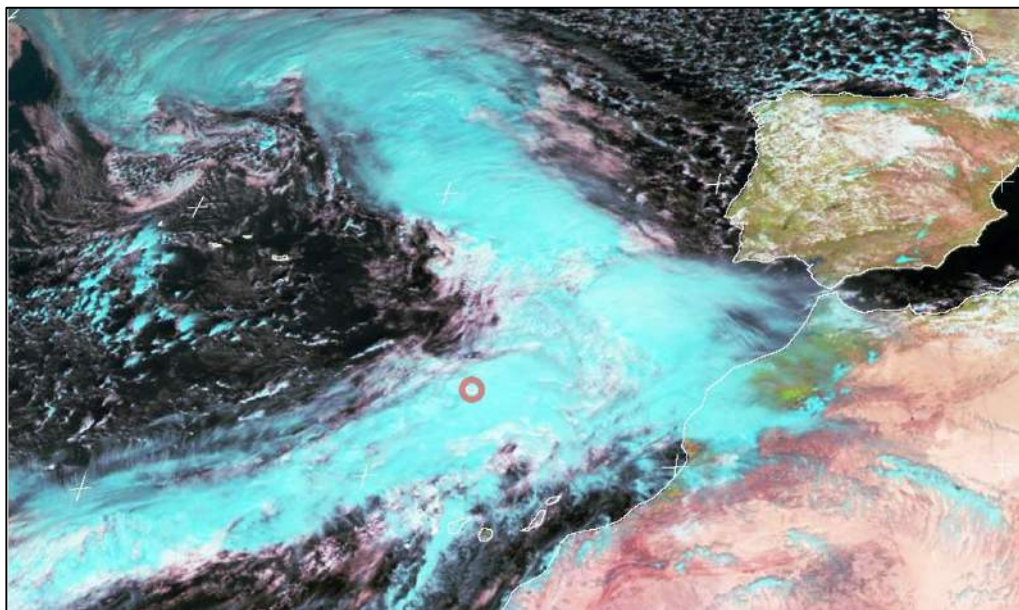


Figure 3.12. RGB composite satellite imagery of 12 UTC on 20 February 2010 (towards the end of the flash-flood episode). Red ring denotes the location of the island of Madeira. Source: EUMETSAT and Dundee Satellite receiving station.

At the same time a strongly divergent wind field was observed in the upper troposphere, supporting strong lift. Total column precipitable water: 37 mm. Most of the island experienced 14 consecutive hours of rainfall from 3 to 17 UTC, peaking around 9 UTC with intensities of 60 mm per hour.

333.8 mm were recorded within 24 hours at the mountain station Areeiro (an estimated return period of 90 years), while in Funchal 146.9 mm were recorded (a statistically estimated return period of 290 years). Only the scientific report of Fragoso et al. (2012) reveals the true maximum measured 24 hour accumulated rain amount of 333.8 mm. This strongly contrasts with the much lower values that circulated in the media directly after the event. Apparently the most accurate data were not immediately available and distributed by the weather service. No satellite wind data was available for this day in the vicinity of Madeira. Therefore potentially existing near surface wind convergence lines could not be identified.

3.2.2.2 Impacts to Critical Infrastructure

The total damage was estimated to be 1.5 billion Euro. Many streets were impassable for hours or even completely destroyed (massively eroded or covered by rocks). Blockages were widespread in the capital and its surroundings, mainly to the west. Because of so many blocked streets, emergency services were massively handicapped in their ability to reach the most affected areas. Widespread telecommunication and power supply failures affected mainly the southern parts of the island. As Madeira is a touristic island, many families could not reach their relatives in the affected area. Media were reporting worldwide about the event, attracting high attention for the event. Because of the massive soil erosion together with the flash floods, water pipes were destroyed and water supply therefore disrupted in some of the areas.

3.2.2.3 Conclusions

The flash flood event seems to be the worst on the island of Madeira since the year 1803, when flash floods even caused more damage and much more fatalities in the Funchal area than in 2010.

Several hydrological and meteorological factors contributed to the extremeness of the event:

- a very rainy winter season causing wet soil preconditioning
- very favorable synoptic-scale conditions for heavy precipitation (upper level divergence, very moist tropical air, instability)
- extremely moist lower troposphere on the mesoscale
- very strong upslope winds from the southwest, causing the moisture to precipitate on the southern side of the intra-island mountains

Up to 333.8 mm of rain were measured on the mountain range in the inner parts of the island, causing flashfloods, landslides and rockfalls. Land-use in the flash-flood and erosion endangered areas was problematic. In total 51 people died in the event and damage to critical infrastructure was extensive in several infrastructure sectors.

3.2.1 Flash flood, Grand-Bornand (Haute-Savoie), 14 July 1987

Type of event	Flashflood with excessive amounts of rain
Date	14 July 1987
Location	Grand-Bornand, Haute-Savoie, France
Total damage	unknown
Victims	21 fatalities, 2 persons missing
Affected critical infrastructure	
Type of damage to infrastructure	National road destroyed for 700 m length, bridge washed away, campsite devastated

On 14 July 1987 during the late afternoon and early evening hours, severe and quasi-stationary storms devastated streets and a campsite in the community of Grand-Bornand in the French Département Haute-Savoie. 23 people died in the event.

The village of Grand-Bornand has about 2000 inhabitants and is situated in the valley of the small river Le Borne. It is a touristic mountain region with skiing resorts and a golf site, with hotels, chalets and with a campsite situated in the river floodplain of the valley. At the event the national road was destroyed over a stretch of 700 m and therefore impassable for a long period. A bridge was swept away.

3.2.1.1 Meteorological Description

14 of July 1987 was a hot day in eastern France. 31 degrees were measured in low-lying locations like in Thonon-les-Bains. In Grand-Bornand, in an altitude of about 1000 m above sea level, the temperature reached 25 degrees on this day.

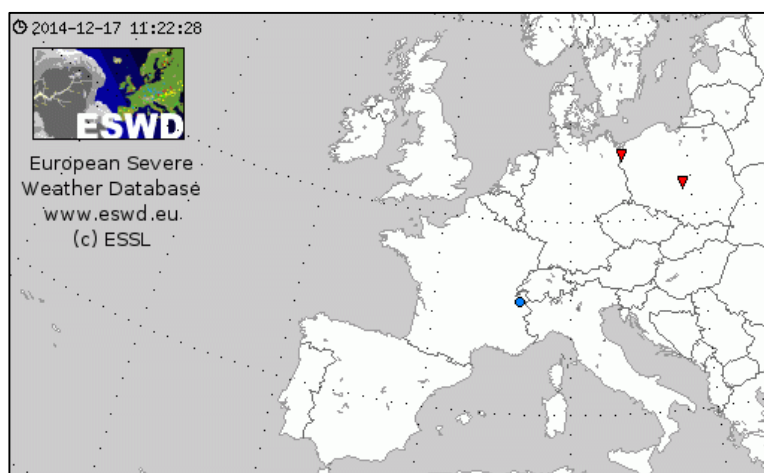


Figure 3.13. Event reports from the European Severe Weather Database ESWD for 14 July 1987. The blue dot marks the flash flood event in the French Alps, red triangles mark two tornadoes over Poland on the same day.

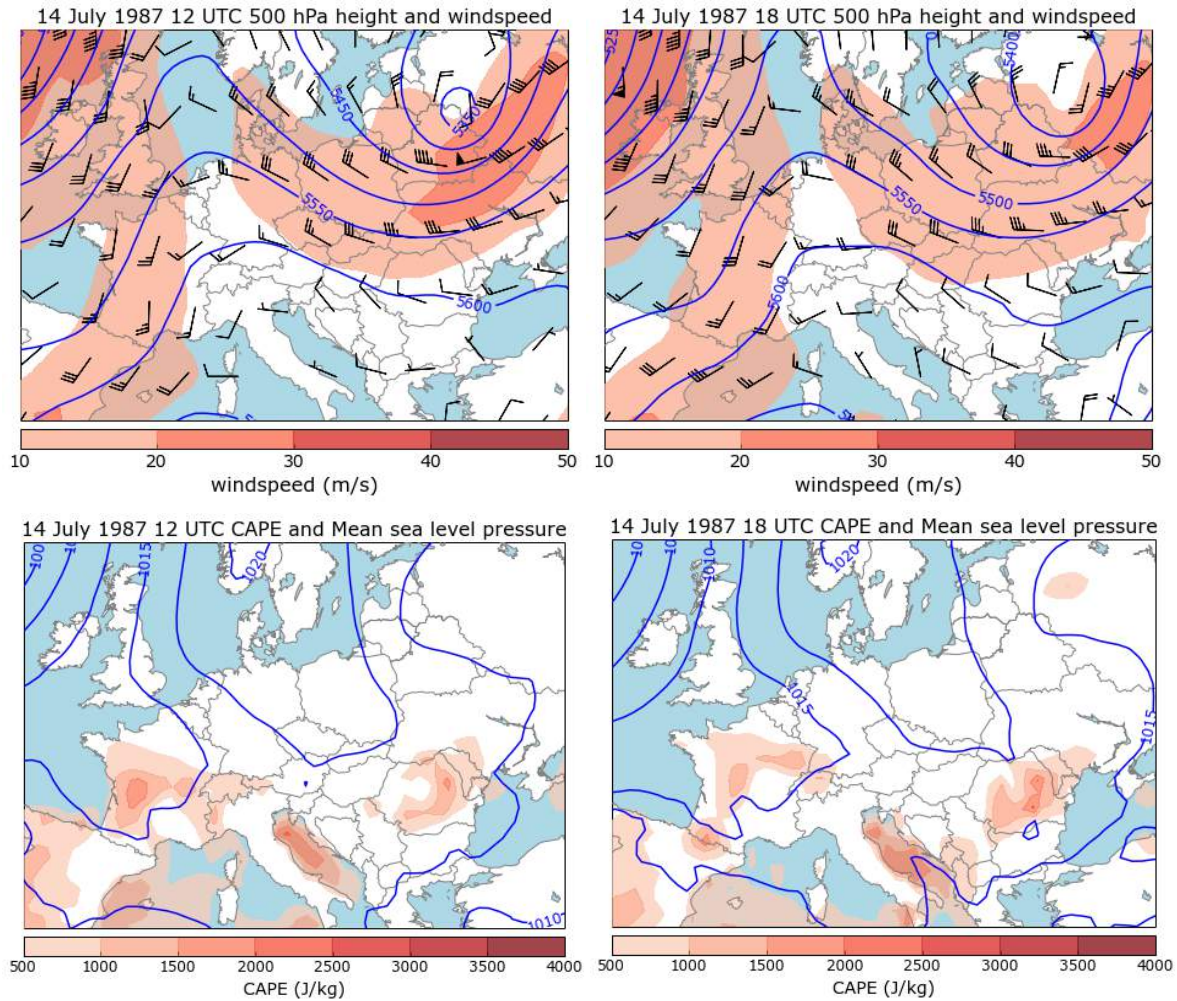


Figure 3.14. Top: Wind and geopotential height at 500 hPa on 14 July 1987 at 12 UTC (left) and at 18 UTC (right). Bottom: Convective Available Potential Energy (CAPE in J/kg) and mean sea level pressure (hPa) at 12 UTC (left) and at 18 UTC (right).

A shallow area of low pressure was situated over western France, a shallow high pressure area over north-central Europe. In the mid-troposphere (500 hPa) a weak short-wave trough swept over southwestern France, while easternmost France was still under the ridge, slightly west of the ridge axis.

The closest available radiosounding of Payerne (western Switzerland, Figure 3.15) showed at 12 UTC a near surface temperature of about 25 degrees and a dewpoint temperature of about 18 degrees, slight southwesterly winds in all heights and high instability (MUCAPE of 2300 and MLCAPE of 1200 J/kg), but little convective inhibition. The total column precipitable water amounted to 34 mm.

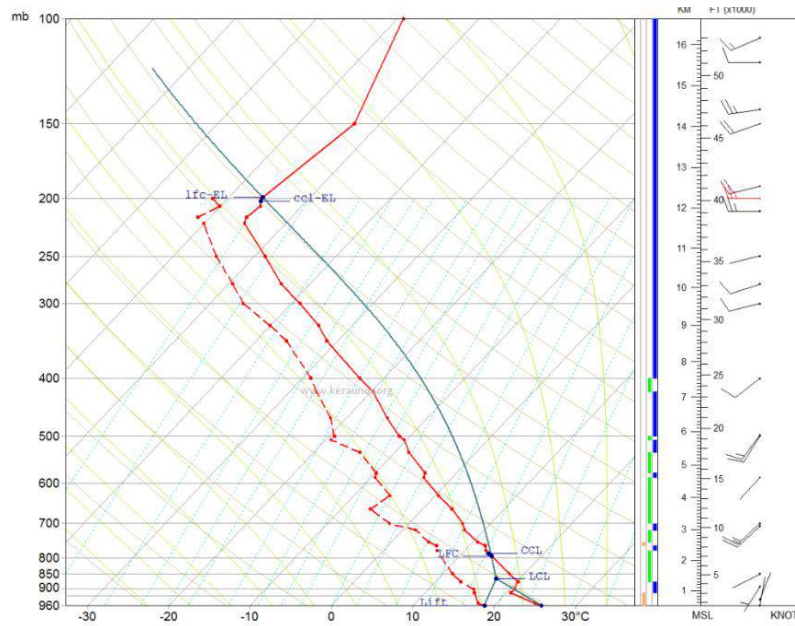


Figure 3.15. Radiosounding of Payerne (14th July 1987, 12 UTC), Source: KERAUNOS, Observatoire français des tornades et orages violents.

The first thunderstorms hit the mountain peaks surrounding Grand-Bornand around 15 h local time (or 13 UTC). Even stronger storms formed over the mountain chain of Aravis at 17:30 h local time (or 15:30 UTC). Both small rivers that merge in the village, le Chinailon and le Borne, experienced simultaneously extreme high runoff, resulting in an exceptional flash flood downstream. At 18:30 a 1 m high flood wave knocked down trees and reached the campsite of Grand-Bornand. By the high current of the flashflood, cars and camping cars were swept away. Around 20:30 local time the thunderstorms dissipate

The local orientation of the valley (SW-NE) may have favored and channeled the inflow into the storms over the mountain range, because of the general flow from the SW. Lift was provided by the upslope flow towards the mountains.



Figure 3.16. RGB composite satellite imagery of 14:47 UTC on 14 July 1987 (when storms started to form). Copyright: NERC, Dundee Satellite receiving station. Red ring: location of Grand-Bornand

3.2.1.2 *Impacts to Critical Infrastructure*

The total monetary damage is unknown, 700 meters of national road were eroded and a bridge was washed away. This rendered the camp site where the human disaster occurred very difficult to reach for emergency services. 26 people were rescued by helicopter immediately after the event. In 1997, 10 years after the event, the municipality of Grand-Bornand was sentenced in the court of Lyon to reimburse the victims of the flashflood, because the campsite was located in an area known to be a flood prone plain.

3.2.1.3 *Conclusions*

The hydro-meteorological event is of a type that can be observed several times in Europe each year, in different mountainous locations, that is quasi stationary or so-called back-building storms punching heavy rain for several hours over the same area, resulting in flash floods that destroy local streets and bridges. The maximum rain is rarely directly measured in such events, but seems often to be well above 100 mm within one or two hours. In this Grand-Bornand case, only a valley-measurement is available (93.4 mm; Keraunos, 2015), but no measurement from the source region of the flash-flood.

The high number of fatalities (23) resulted from a) an extreme risk-exposure of the people in a campsite, located in a known flood-plain, and b) the fact that the people in the campsite were not warned before the event. Such a warning would have allowed them to reach higher ground on the nearby valley slopes. In addition, soil characteristics (mainly the process of soil consolidation) may have contributed to the extremeness of the flash-flood event as parts of the area were transformed into skiing resorts. This probably resulted in enhanced water runoff and soil erosion.

3.3 Landslides

3.3.1 Landslides, Scotland, August 2004

Type of event	Landslide (caused by heavy precipitation)
Date	August 2004
Location	Multiple rainfall induced landslides in Scotland, specifically on the A83, A9 and A85 Trunk Roads
Total damage	Unknown
Fatalities	0
Affected critical infrastructure	
Type of damage to infrastructure	Roads blocked by debris from slopes. Local damage

In August 2004, following a period of sustained heavy rainfall and localised storms, a series of landslides and debris flows occurred over a wide area of Scotland. These had major impacts on sections of the A9, A83 and A89 highway.

3.3.1.1 Meteorological Description

Rainfall intensities experienced in Scotland during August 2004 were substantially above average values, with amounts in some areas being in excess of 300% of the 30-year average August rainfall. The areas of Perth and Kinross experienced rainfall amounts of between 250% and 300% above normal, whilst areas including Stirling and Argyll & Bute, although experiencing less severe rainfall, still received amounts of between 200% and 250% of the monthly average.

3.3.1.2 Impacts to Critical Infrastructure

Whilst no major injuries occurred, the trunk road was blocked at a number of locations. The occurrence of two debris flows in close proximity on the A85 at Glen Ogle (Figure 3.17) resulted in the requirement to airlift 57 people to safety. The major impact was to traffic as a result of road closures. The A85, which carries 5,600 vehicles a day, was closed for four days, whilst the A83 and A9 which carry 5,000 and 13,500 vehicles per day respectively, were closed for two days.



Figure 3.17. The A85 Glen Ogle. Source: www.transportscotland.gov.uk.

3.3.2 Landslide, Switzerland, 13 August 2014

Type of event	Landslide (caused by heavy rainfall)
Date	13 August 2014
Location	Railway line near the town of Tiefencastel, Switzerland.
Total damage	Unknown
Fatalities	11 injured, no fatalities
Affected critical infrastructure	
Type of damage to infrastructure	Slopes. Train derailed

On 13 August 2014, a landslide which blocked a 15 m section of the rail track of between Tiefencastel and Solis, south-east of Zurich, caused three train cars to derail, with one sliding down a steep valley before coming to rest against trees. Of the two hundred people on board the train 11 people were injured.

3.3.2.1 Meteorological Description

The landslide occurred at a time of extremely heavy rainfall on the morning of the failure which had been preceded by several weeks of rainfall. The rainfall was particularly heavy on the day preceding the failure with rainfall of 55 mm following over 12 hours. This is equivalent to approximately one-third of the average monthly rainfall levels for the area.

3.3.2.2 Impacts to Critical Infrastructure

The carriage which slid down the slope was prevented from entering a river in flood, by hitting heavy woodland. The line was closed for three days.



Figure 3.18. Derailment of a train near the Swiss Ski resort of St. Moritz on 13th August 2014. (image www.bbc.com)

3.3.3 Landslide, Croatia, 12 September 2014

Type of event	Rockfall (caused by heavy rainfall)
Date	12 September 2014
Location	Railway line near Kastel Stari on the Zagreb to Split Railway, Croatia
Total damage	Unknown
Fatalities	0
Affected critical infrastructure	
Type of damage to infrastructure	Slopes, rockfall. Train derailed

On 12 September 2014, a boulder which became dislodged from cutting slope landed on the rail track and caused the derailment of a passenger train carrying 30 passengers. There were no serious injuries.

3.3.3.1 Meteorological Description

Rain gauges positioned on a road construction site close to the slope recorded rainfall in 1 minute intervals. These revealed that heavy rainfall occurred the day before the derailment, see Figure 3.19. The measured rate of rainfall was typically between 75mm/hr and 140 mm/hr with the highest measured rate approaching 166 mm/hr and the total rainfall for this one hour period being 56 mm.

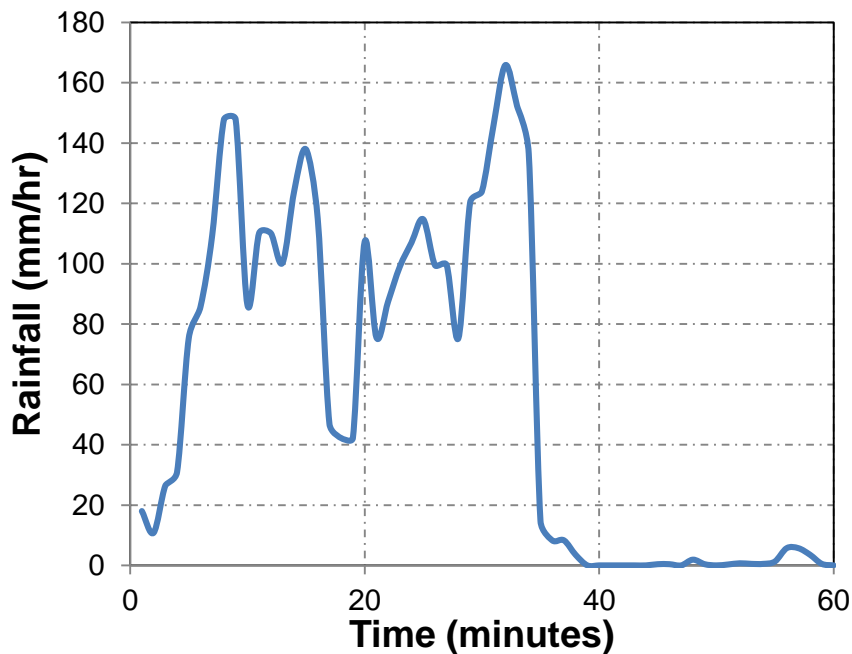
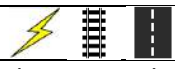


Figure 3.19. Rainfall measured at 1 minute time intervals between 18:00 and 19:00 on 11/09/2014 near the location of the rock fall

3.4 River floods

3.4.1 River floods, England, 2007

Type of event	river floods
Date	May–July 2007
Location	England, United Kingdom
Total damage	£3.2 billion (official estimate)
Victims	13 fatalities
Affected critical infrastructure	
Type of damage to infrastructure	direct damage and destruction by floodwater, disruption of traffic, cessation of services. Flood defences, water and waste water systems also affected.

The United Kingdom was severely affected by a series of floods that occurred in late spring and summer of 2007. Three heavy downpours causing flash floods appeared on top of an exceptionally wet three-month period resulting in extensive river floods. England was most heavily affected by those events.

3.4.1.1 Meteorological and hydrological description

After a warm winter of 2006/2007 and previous year’s drought, the soil moisture in April 2007 was the lowest since records began in 1961. However, in May heavy rainfall started and by mid-June the soil was already saturated (Environment Agency 2007, Marsh and Hannaford 2007). Between 12 and 15 June, a downpour affected mainly the central part of England with 70–140 mm of rain recorded during that period. A record 98 mm of rainfall was recorded during a single day at Harlow Hill Reservoir. After a few days of less intense rainfall, another round of downpours struck most of England and Wales on 24 and 25 June (60–120 mm of rain in total). At Winestead Booster 120 mm of rain occurred in only 24 hours. A third wave of heavy rain covered most of British Isles on 19 and 20 July (70–120 mm of rain). The most intense rain was recorded at Pershore College near Birmingham, where 143 mm of rain fell in 24 hours. By end of July soil moisture was the highest on record (Blackburn et al. 2008, Hanna et al. 2008, Marsh and Hannaford 2007, MetOffice 2012).

Overall, England and Wales experienced the highest May-July precipitation since records began 1766. The total (415 mm, or 223% of 1971–2000 average) was 19% higher than the previous maximum recorded in 1789 and 35% higher than the maximum recorded during the last century (in 1924). It was not, however, the wettest three-month period on record, but anyway highly unusual. In parts of England, Wales and Northern Ireland June 2007 rainfall totals were estimated to exceed a 200-year return period. As can be noticed from Figure 3.20, the spatial distribution of rain was very uneven, with north of England heavily affected, while Scotland or London were largely spared. Downpours were also exceptionally intense: the 24-hour rainfall in Winestead Booster in June had an estimated probability of occurrence of just 0.2%, while the 24-hour rainfall at Pershore College in July – only 0.1% (Hanna et al. 2008, Marsh and Hannaford 2007, Prior and Beswick 2008).

Local floods due to heavy rainfall already started on 27 May in England. In mid-June more extensive flooding occurred in Northern Ireland and north of England, while the area flooded peaked during late June and July rainfalls. The spatial footprints of those events varied significantly, however. As can be seen in Figure 3.20, exceptionally high river flows affected most of Great Britain, as well as Northern Ireland. The total runoff in June and July was an estimated 122 mm in England and Wales, twice the previous maximum recorded in 1968 and 332% of long-term average. At some locations the runoff volume was more than 700% of average, with peak flows exceeding an estimated 200-year return period (Environment Agency 2007, Marsh and Hannaford 2007, Marsh 2008).

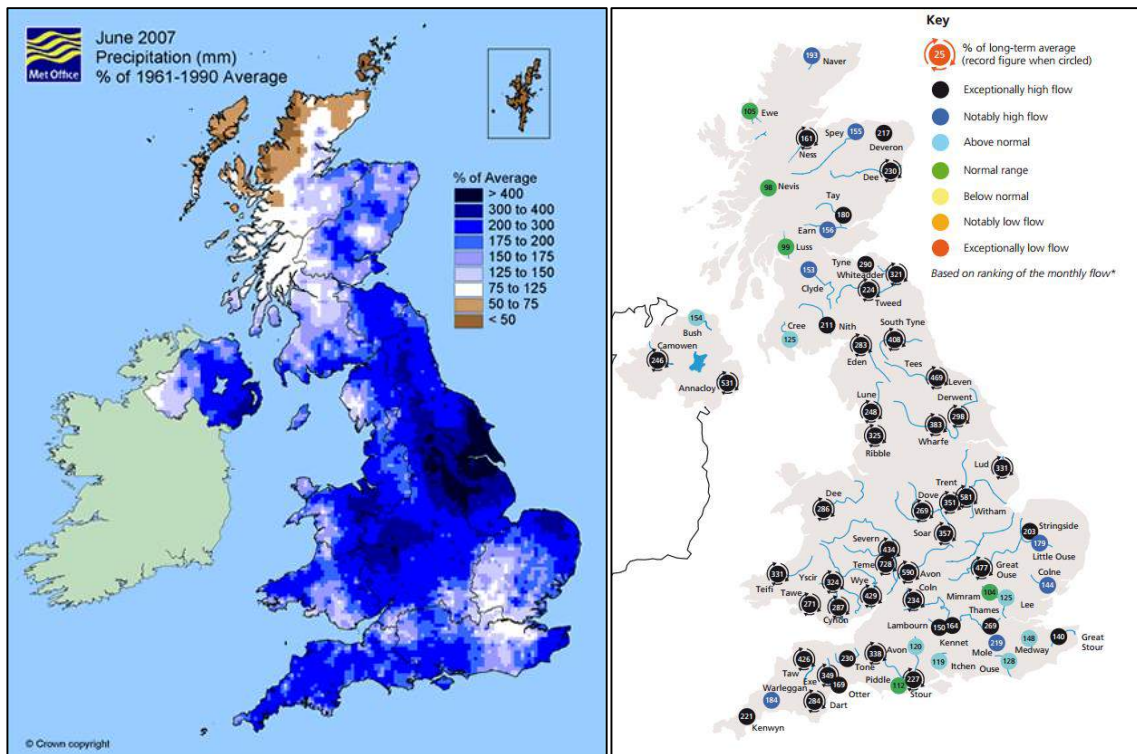


Figure 3.20. Left panel: precipitation in June 2007 as a percentage of 1961–1990 average (MetOffice 2012). Right panel: river runoff during June-July 2007 as a percentage of 1961–2006 average (Source: Centre for Ecology & Hydrology/NERC).

3.4.1.2 Impacts to Critical Infrastructure

The floods mostly affected England, where 13 persons were killed. Most of the fatalities were drownings, because people were trapped in buildings or cars, or because of failed attempts to get to safety by swimming across flooded rivers. Around 14 500 household were evacuated, a third of which were still displaced 10 months after the events (Milojevic et al. 2014). An official estimate (Chatterton et al. 2010) put direct and some indirect losses at £3 164m , though with large uncertainty bounds ($\pm 20\%$). The biggest damages were recorded in the housing sector (£1 200m), since about 48 000 houses were flooded, along with some 7 300 businesses (£740m). Damages to infrastructure and critical services came third at £693m (Table 1). It should be noted that out of 55 000 properties flooded, 19 000 were inundated from increased river discharges, while the remainder were affected by local accumulation of water from rainfall due to failure of drains, culverts, sewers and ditches to cope with the sheer amount of water (Environment Agency 2007).

Flood defences were largely overwhelmed during the flood, since they were usually designed to cope with a 1/75- or 1/100-years flood. 1 016 km of dikes were put under pressure (9% of national total), of which 525 km were overtopped. Out of 19 000 properties, 3 600 were flooded because dikes were overwhelmed. Flood defences were relatively resilient and well-maintained, since only two kilometres of dikes at nine locations failed structurally. Only at four locations failure occurred without overtopping. Impact of those failures was anticipated to be negligible. Total repairs costs of flood defences were £15m. Dams were also put under strain: dam at Ulley reservoir almost failed and 1 000 people were evacuated in precaution, while pumps had to be airlifted by the military to reduce load. Temporary flood defences were erected at many locations by local authorities, fire brigades, armed forces and citizens. Use of such emergency measures at Walham electricity substation effectively protected the site; supply of electricity to half a million people would have been lost otherwise (Chatterton et al. 2010, Environment Agency 2007, Neal et al. 2011, Pitt 2008).

Table 3.1. Estimated losses to important infrastructure and critical services during 2007 floods in England (adapted from Chatterton et al. 2010).

Sector		Estimated losses	
		Total (£ million)	% associated with direct damage
Utilities	Water and waste water	186	65
	Electricity	138	6
	Gas	<1	6
Communications	Roads	191	45
	Railways	36	29
	Telecommunication	<1	90
Services	Emergency services	8	10
	Environment Agency*	19	78
	Schools	49	76
	Community leisure centres	14	30
	Agriculture and food supply	50	15
Total		693	42

* responsible for upkeep of flood defences.

The biggest total losses were recorded in road traffic. £85m was spent on repairs almost exclusively by local government authorities, mainly on rural roads, bridges, street lighting and culverts. The most affected communities were Gloucestershire (£34m) and Sheffield (£15m). The Highways Agency, which is responsible for motorways, spent only £33 000 on additional repairs. This can be explained by much higher design standards of motorways compared to local roads. Six motorways had to close because of the flood and one of them (M1) was shut down for 40 hours. That incident alone cost an estimated £2.3m in delays of traffic (it was closed for precaution due to the imminent risk of Ulley dam failure). On the M5 motorway some 10 000 people were stranded overnight. Total cost of traffic disruption on motorways alone is estimated at £101m, though with large uncertainty bounds, ranging from £22m to £178m (Chatterton et al. 2010, Pitt 2008).

Railways were affected by water in 265 locations, of which 42 were significant damages. A vast majority (88%) of those incidents were caused by accumulation of rainfall, while the rest were caused by fluvial floods. 29% of losses in Table 1 are repair costs (£10.5m), while the remainder is the

estimated cost of delays (Chatterton et al. 2010). The Severn Valley Railway was closed for almost a year. Additionally, around 6 000 people had to stay overnight in rest centres, because they were not able to reach their homes due to rail network failure. Many railway stations had to close, including one in Banbury, flooded just nine years after previous such incident (Pitt 2008).



Figure 3.21. Flooded streets in Oxford (left) and Thatcham (right) (Source: Wikimedia images).

Only a small number of incidents related to telecommunication was recorded due to high resilience of this type of infrastructure in the sense that it can withstand extreme event and quickly recover afterward. This is the especially the case for mobile telephony.

Total losses are believed to be less than £1m, including repairs and cost of providing additional services during the floods (Chatterton et al. 2010).

Water supply and waste water treatment was severely affected during the floods. A total of 5 water treatment works and 322 sewage treatment works were flooded. Water treatment for 2.5m people was disrupted for an average of 2 days. Severn Trent’s Mythe Water Treatment Works were flooded, cutting off supply of mains water to 350 000 people for up to 16 days. Providing alternative sources of potable water (tankers, bottled water) cost an estimated £25m, while repair of the Works themselves cost nearly £30m (Chatterton et al. 2010, Pitt 2008).

In the electricity sector direct losses were fairly limited and totalled £9m. The worst disasters were avoided. Substation in Walham was protected by temporary defences set-up during the event, while Brinsworth substation and Above Ground Gas Installation at Guilthwaite were threatened by Ulley dam failure, which did not occur in the end. June floods caused power supply disruptions in Yorkshire and Lincolnshire, with 130 000 households being without electricity for an average 15 hours over five days. In Gloucestershire 12 000 households were cut off for an average 20 hours. Several thousand homes were also affected in other locations.

Among additional costs of the 2007 floods are spending on extra emergency services, which totalled £8m, including the deployment of 1 000 military personnel and some additional maintenance of rescue equipment. Almost a thousand schools were affected (£38m was spent on repairs), with 170 000 pupils losing two days of school on average. Local administration recorded damages to leisure centres, social housing and waste management systems (Chatterton et al. 2010). Finally,

42 000 ha of farmland was flooded with four-fifths of financial losses coming from damages to crops (Posthumus et al. 2009).

3.4.1.3 Conclusions

The 2007 floods have uncovered some deficiencies of flood protection in the UK. Most of the flooded properties and infrastructure were located in areas not protected by dikes. In other areas, many dikes were overtopped. The most significant impact on infrastructure was the breakdown of water and power systems. Additional flood defences that have been built around some power substations and water works saved many locations from sustaining more damages. Local roads were badly damaged due to low construction standards, while motorways proved resilient, though serious disruption of traffic on the latter was not avoided.

3.4.2 River floods, Central Europe, May and June 2013

Type of event	River flood
Date	May – June 2013
Location	Central Europe
Total damage	€ 12 billion
Fatalities	25
Affected critical infrastructure	
Type of damage to infrastructure	Road and rail closures, erosion of embankments and streets, damage to bridges, landslides blocking railways

Between the end of May and the beginning of June 2013, Central Europe was hit by a severe precipitation event which caused flooding over large areas of the Danube and Elbe catchments and their tributaries. Switzerland, Austria, Germany and the Czech Republic were affected. 25 fatalities were attributed to the event and the economic damage was estimated at about 12 billion Euros with most of the damage in Germany and Austria (Munich RE, 2014).

3.4.2.1 Meteorological and Hydrological Description

For the entire duration of the event an upper level low pressure system was located over Central and Eastern Europe. Its core moved from the Western Alps (29th of May) in a north-eastward direction. Warm and humid air masses from the Black Sea were transported anti-clockwise around the system into central Europe (Stein and Malitz, 2013). Several low pressure systems developed at the ground and contributed to the high precipitation amounts over Central Europe between the end of May and the beginning of June, with the precipitation maximum occurring between the 31st of May and the 3rd of June. Especially high precipitation amounts were associated with low “Frederik”. Frederik developed over the Adriatic Sea at the 29th of May and travelled in a north-westward direction (Figure 3.22). The north easterly flow at the western flanks of Frederik forced an ascent of the humid air at the Alps and the Ore mountains leading to extreme precipitation. Within 24 hours, rain amounts between 30 and 71 mm were observed on the northern slopes of the Alps with the highest values recorded for Aschau am Stein, which is located in Bavaria close to the Austrian Border. The highest

accumulated precipitation amounts measured for the period between the 31st of May 2013 12UTC and the 4th of June 12 UTC were also recorded for Aschau am Stein and exceeded 400 mm (Stein and Malitz, 2013). Between the 31st of May 00UTS and the 3rd of June 00UTC precipitation exceeded the climatological values for May in a large area including regions at the the German Austrian border, western parts of the Czech Republic and the German Ore Mountains (Figure 3.22). The high amounts of precipitation first led to immediate local problems such as flooding, erosion of streets and roads as well as mud slides. Over time the rain accumulated in rivers, resulting in river floods.

In addition to Frederik, a low called “Günther” developed over Eastern Europe, leading to high precipitation accumulations mainly over Belarus (Figure 3.22).

The heavy precipitation event of May and June 2013 in Central Europe was well predicted by the German Weather Service and warning was adequate (Stein and Malitz, 2013).

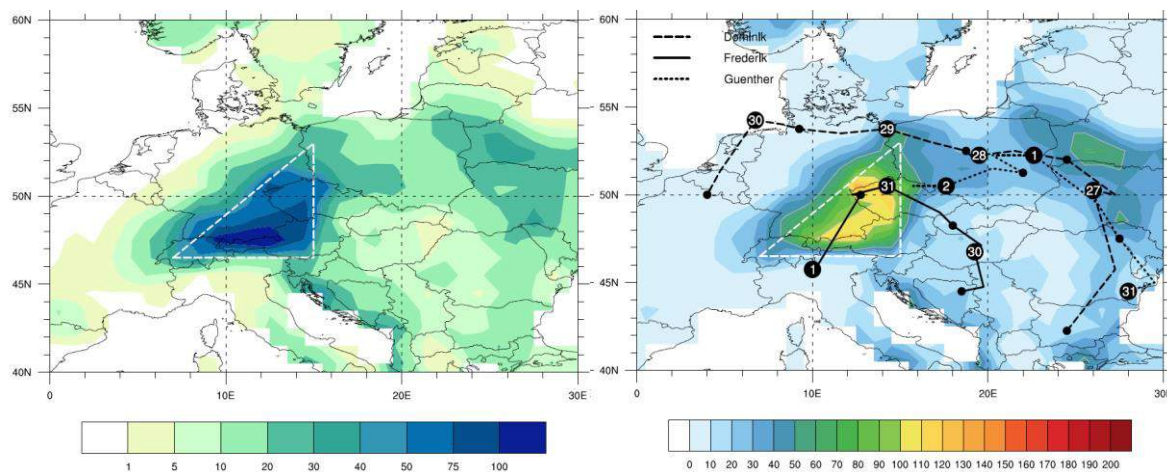


Figure 3.22. Left: GPCP precipitation accumulated over the 3 day core period of the heavy precipitation event from 31 May 2013, 00:00 UTC to 3 June 2013, 00:00 UTC. Right: fraction of total climatological May precipitation that fell in this 3 day period (shaded every 10 %) and tracks of the three consecutive cyclones (long-dashed: Dominik, solid: Frederik, short-dashed: Günther; derived from ECMWF analysis data) with 00:00 UTC labelled by day of May/June 2013 and small dots for 12:00 UTC positions. The white triangle highlights the core region affected by heavy precipitation. Taken from Grams et al. 2014.

Hydrological Preconditions

At the end of May, the soil was characterized by anomalously high saturation levels (Figure 3.23). Within Germany, 40% of the ground exhibited saturation levels exceeding all previous recordings since the start of the measurements in 1962 (not shown). It is believed that the high soil moisture has contributed to the extent of the flood as the soil’s storage capacity was exceeded. Moreover, evaporation of moisture over wet surfaces has been able to contribute to the amount of precipitable water (Grams et al. 2014).

3.4.2.2 Impacts to Critical Infrastructure

The event led to major disruptions in all affected countries. Roads and railroads were most affected. Many streets and several motorways had to be closed and repaired after the water masses receded. The Bavarian motorway A3, for example, had to be closed for 11 days. Railway tracks had to be closed in many places as well, due to flooding and subsurface erosion of the embankments. An example is the important high-speed rail links between Frankfurt and Berlin, and between Berlin and Hannover

(Figure 3.24). It had to be closed for repairs for several months after the event. In the Alps, mud slides blocked railway tracks and roads. In the Alps some minor electricity outages were reported, which were caused by mud slides damaging electricity lines. No major problems were reported regarding telecommunications.

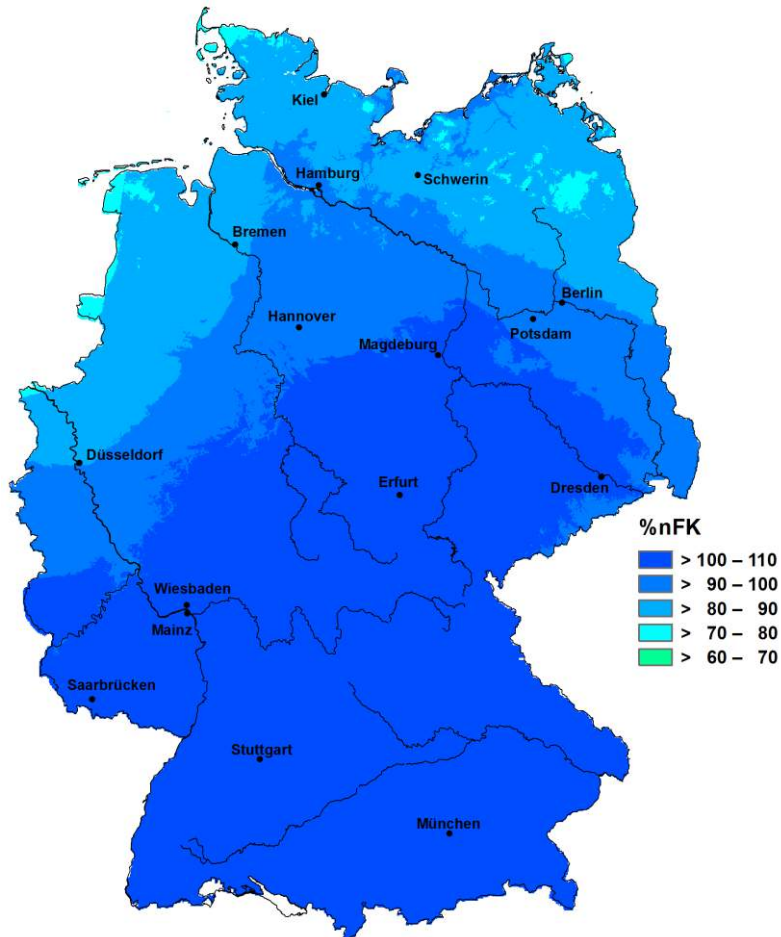


Figure 3.23. Soil moisture content usable for plants (nFK “nutzbare Feldkapazität”) in % (under winter grain on light soil) for the 31st of May 2013. Courtesy Deutscher Wetterdienst 2013.



Figure 3.24. Left: Railroad in Saxony-Anhalt is flooded (Focus, 2013). Right: Motorway junction in Deggendorf (Bavaria) is flooded after dyke breach (FAZ, 2013).

3.4.2.3 Conclusions

Severe precipitation in Central Europe falling on already saturated soil has led to severe flooding in Central Europe. Several countries including Germany, Austria, Switzerland and the Czech Republic were affected. Precipitation amounts and river discharges exceeded the 100-year return levels in many places (e.g. Blöschl et al. 2013, Merz et al. 2013, Schröter et al. 2014). The event caused severe damage to infrastructure, especially to roads and railways.

3.4.3 River flood, Dublin-Belfast railway, 21 August 2009

Type of event	River flood causing collapse of a bridge
Date	21 August 2009
Location	Dublin to Belfast Railway near Malahide, Ireland
Total damage	Unknown
Fatalities	0
Affected critical infrastructure	⚓
Type of damage to infrastructure	Collapse of bridge

On the 21st of August 2009, the Malahide Viaduct collapsed (Figure 3.25) as a result of bridge scour as a local passenger train passed over the bridge. The bridge which forms part of the Trans-European Transport Networks (TEN-T) was visually inspected three days before the collapse after reports of unusual water flows around one of the piers. The inspection did not identify any visible signs of scour. The local train driver reacted quickly and signalled that the line be closed preventing the high-speed Dublin-Belfast train from crossing the bridge.



Figure 3.25. Malahide Viaduct, Dublin

3.4.3.1 Meteorological Description

Heavy rainfall in the days preceding the failure caused river flooding. The high flows caused scour and undermining of one of the bridge piers.

3.4.3.2 Conclusions

The line was closed for 3 months whilst rebuilding occurred.

3.5 Thunderstorm gusts

3.5.1 Convective windstorm, Northrhine-Westphalia (Germany), 9 June 2014

Type of event	Convective windstorm
Date	9 June 2014
Location	North Rhine-Westphalia, Germany
Total damage	€ 880 million
Victims	6 fatalities
Affected critical infrastructure	
Type of damage to infrastructure	Railways and motorways blocked by fallen trees and other objects. Railway overhead lines damaged.

During the period of 7 – 10 June 2014, numerous severe thunderstorms affected parts of western and central Europe. The most severe storms occurred on 9 June 2014, when severe storms swept across northern France, Belgium and northwestern Germany. After several isolated supercell storms produced damaging hail up to 9 cm in diameter near Paris, a large mesoscale convective system (MCS) with a so-called “bow-echo” developed on the borders of the Netherlands, Belgium and Germany. This system tracked east-northeastwards and produced a swath of damaging wind gusts across the densely populated Ruhrgebiet region. A 40 m/s (144 km/h) wind gust was measured at Dusseldorf airport as the storm system passed. 6 people perished according to Brönstrup (2014) and most of the long distance railway lines and highways around the city were closed. According to Munich Re, overall losses caused by the storm reached 880 million Euros (Munich Re, 2014).

3.5.1.1 Meteorological description

The synoptic scale weather pattern featured conditions typical for severe weather outbreaks in this part of Europe. The major feature was a deep trough over the eastern Atlantic at the mid- to upper troposphere. Strong southerly to southwesterly flow was present on the forward flank of the trough (Figure 1), transporting a plume of air with a strongly decreasing temperature with height (lapse rates) from Iberia towards France and Germany. At the same time, close to the surface, a very warm and moist airmass was present with high dew point temperatures above 18 degrees ahead of the wavy frontal boundary. The combination of the moist air mass along with steep lapse rates created a highly unstable situation in the region. The European (ECMWF) and American (GFS) model forecasts simulations predicted that the convective available potential energy (CAPE) would exceed 3000 J/kg (Figure 3.26), a value that can be considered extreme in Europe. At the same time, combination of 5 m/s of easterly to northeasterly surface flow and 20 m/s southwesterly flow aloft created strong vertical wind shear, a well-known prerequisite for organised severe thunderstorms. An area where the prerequisites CAPE and strong wind shear were both available can be seen to stretch from France across the Benelux into northwest Germany (Figure 3.27).

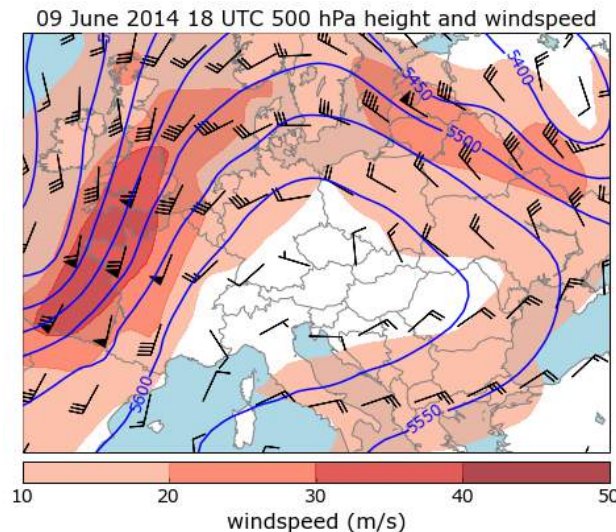


Figure 3.26. 18 UTC ERA Interim reanalysis of 500 hPa height and windspeed. Note the strong southerly to southwesterly flow stretching from Spain towards the North Sea.

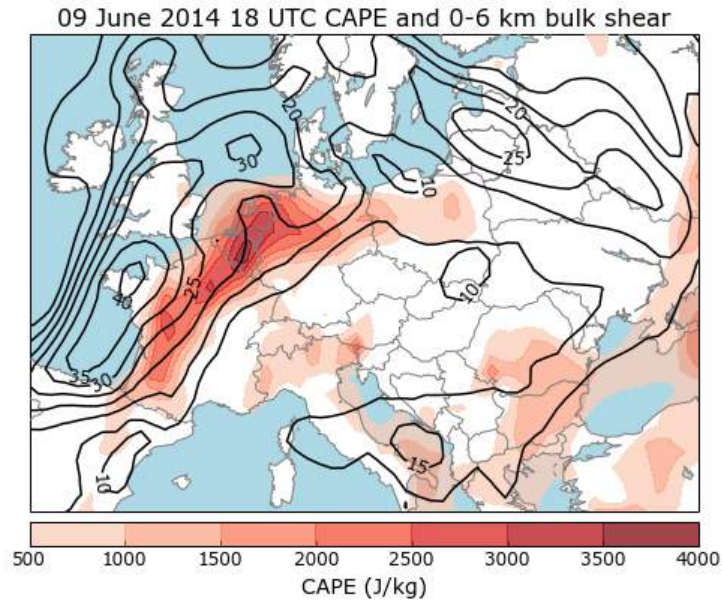


Figure 3.27. 18 UTC ERA Interim reanalysis of CAPE (J/kg) and bulk wind shear between 10 m and 6 km winds (m/s). Significant overlap of high CAPE values and strong wind shear were present in a wide swath from southern France to northern Germany.

The thunderstorm system that produced severe wind gusts formed as a cluster of non-severe elevated showers and thunderstorms over northern France around 16 UTC, progressing northeastwards. Explosive development commenced as the system reached the convergence zone over southeastern Belgium at 17 UTC. The system considerably grew in size and quickly attained a character of linear Mesoscale Convective System (MCS), or a “squall line”. Even though the radar reflectivity and lightning activity were very high the system initially did not produce much severe weather. However, upon reaching the border with Germany, its southern half began a rapid transformation into a bow-echo, which accelerated forward. The resulting bow-shaped radar echo was apparent by 18:30 UTC. By that time, the system began producing the first damaging wind gusts. It reached the Dusseldorf area as it attained its maximum intensity around 19 UTC. Most of the severe wind reports by voluntary observers in the European Severe Weather Database come from the period from 18:30 till 20:00 UTC (Figure 3.28). Afterwards, system weakened with bow echo structure becoming disorganised and moving towards the more stable environment. The last severe wind report arrived just after 22:30. In total, 68 severe wind reports were collected from Northwestern Germany between 17 and 23 UTC, most of them from Ruhrgebiet.

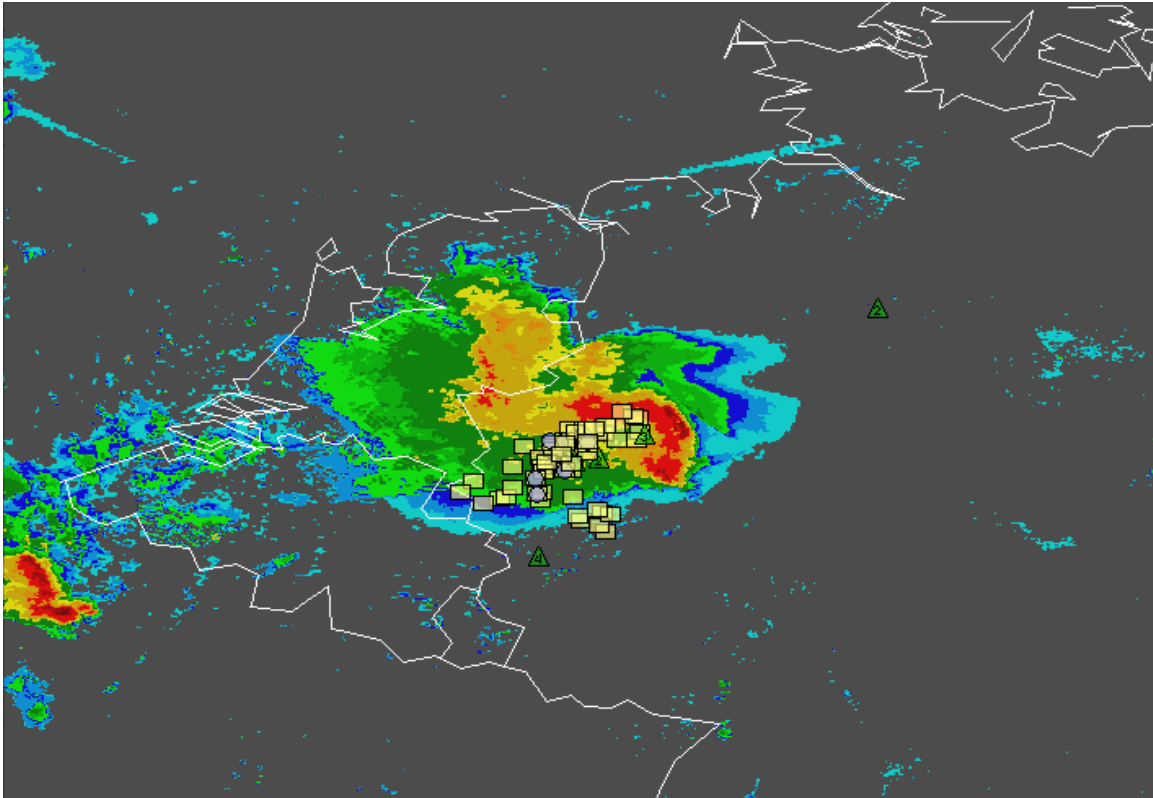


Figure 3.28. Radar image depicting the mature “bow-echo” convective system and severe weather reports collected between 17 and 20 UTC. The yellow squares correspond to severe wind gusts, green triangles to large hail and blue circles to heavy rain. The reports show a swath of severe weather in the wake of the convective system. Sources: ESSL, Deutscher Wetterdienst.

3.5.1.2 Impacts to critical Infrastructure

Most of the damage in the area was caused by uprooted or broken trees. It was estimated that up to 80000 trees were damaged or uprooted during the height of the storm (Tagesschau, 2014). Many of them fell onto roads and railway tracks. Several motorways were blocked by the fallen trees. Even more damage was done to the dense railroad network in this region. Fallen trees brought down overhead wires and blocked the tracks in many locations, crippling the rail connections in the region in the following days. Stations such as Essen or Dortmund were virtually cut off after the storm. Furthermore, many trains were stranded on their way. According to Deutsche Bahn report (Deutsche Bahn, 2014), 2200 km of overhead lines were damaged or destroyed due to the fallen trees and a third of the rail network in North Rhine Westphalia had to be shut down. Deutsche Bahn also informed that the storm inflicted more damage to the rail network than the Kyrill windstorm in 2007, worth of 8 million Euros to the infrastructure. One of the reasons for this may be that Kyrill occurred outside of the vegetation period, when deciduous forests are less susceptible to the severe winds. Public transportation was severely affected.



Figure 3.29. An example of a damage to the railway overhead power lines (catenary) due to the fallen tree after the convective windstorm of 9 June 2014. Photo: Rainer Klute.

3.5.1.3 *Conclusions*

A damaging convective windstorm occurred over North Rhine-Westphalia on 9 June 2014, with significant impact on the dense railroad infrastructure. Because of the active vegetation period, trees were especially susceptible to the severe winds. The main impact was tied to the trees falling on the railway power lines and blocking the tracks. Because of the widespread nature of the event, infrastructure was not restored completely for a long time, affecting many commuters. This case stresses out that convective windstorms, often occurring outside the regular season of winter time windstorms may have very similar if not even worse impact on the traffic infrastructure, albeit usually being more local in nature.

3.6 Tornado

3.6.1 Tornado outbreak, South Poland, 15 August 2008

Type of event	tornado
Date	15 August 2008
Location	South Poland, particularly near Czestochowa
Total damage	unknown
Victims	3 fatalities
Affected critical infrastructure	
Type of damage to infrastructure	Lamp posts blown down, signs bent over, cars thrown, safety barriers damaged

A widespread severe weather outbreak occurred on this day, spanning from northern Italy through Austria, and the Czech and Slovak Republic towards northern Poland. 8 people were killed by severe weather, 3 in Poland, 2 in Slovakia and Italy and 1 in Austria. Severe weather included damaging hail up to 8 cm in diameter, flash flooding and convective windstorms. But by far most well-known aspect of this episode was a tornado outbreak in Poland, one of the most prominent outbreaks in Europe in recent history. 10 tornadoes were reported to the European Severe Weather Database (Figure 3.30), of which 4 tornadoes were rated as F3 and one tornado as F2 on the Fujita scale of tornado ratings. Very serious damage occurred with whole forests flattened and several buildings being severely damaged or destroyed.

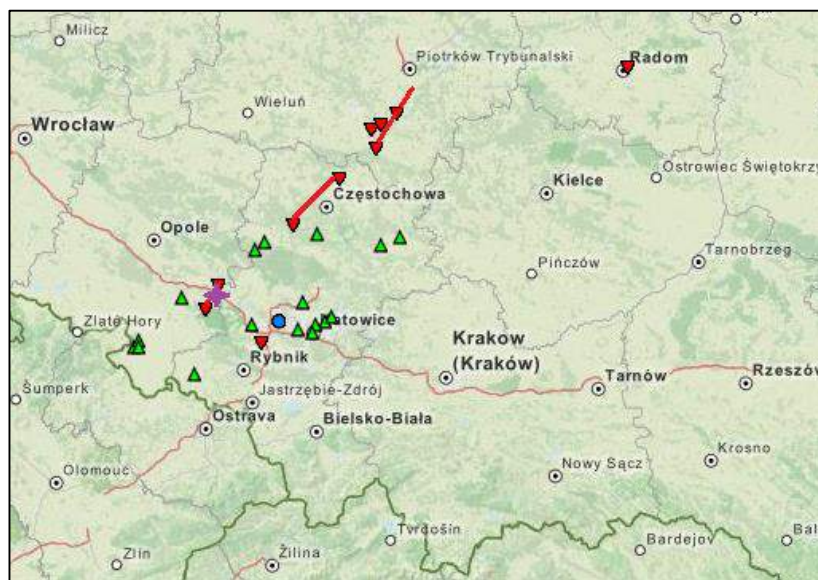


Figure 3.30. Plot of reports from the European Severe Weather Database (green triangles represent large hail, red triangles tornado and blue circles heavy rain reports) for 15 August 2008 over the area of interest (source: ESSL). A swath of tornadoes in the southwest to northeast direction is apparent from the picture. 3 main tornado tracks are plotted using the red line based on the report by Grochala (2012). Violet star marks the location of tornado impacting the highway.

3.6.1.1 Meteorological description

The synoptic scale situation was characterised by a deep mid- to upper tropospheric trough over Western Europe with an unseasonably strong southerly flow at its forward flank (Figure 3.31). Base of the trough rotated quickly from Southwestern France towards northern Italy during the day. Southerly surface wind advected warm and very moist airmass from the Mediterranean all the way to Poland ahead of the wavy frontal boundary with several separate low pressure centres. Furthermore, strong flow above managed to advect a plume of steep mid-tropospheric lapse rates from N Africa to this region. In a relatively large area, from northern Italy up to central Poland, conditions seemed very conducive for severe convection, with substantial degree of instability and also strong vertical wind shear. Figure 3.32 shows that the best overlap of high CAPE and strong 0-6 km shear existed over the northern Adriatics and southern Poland.

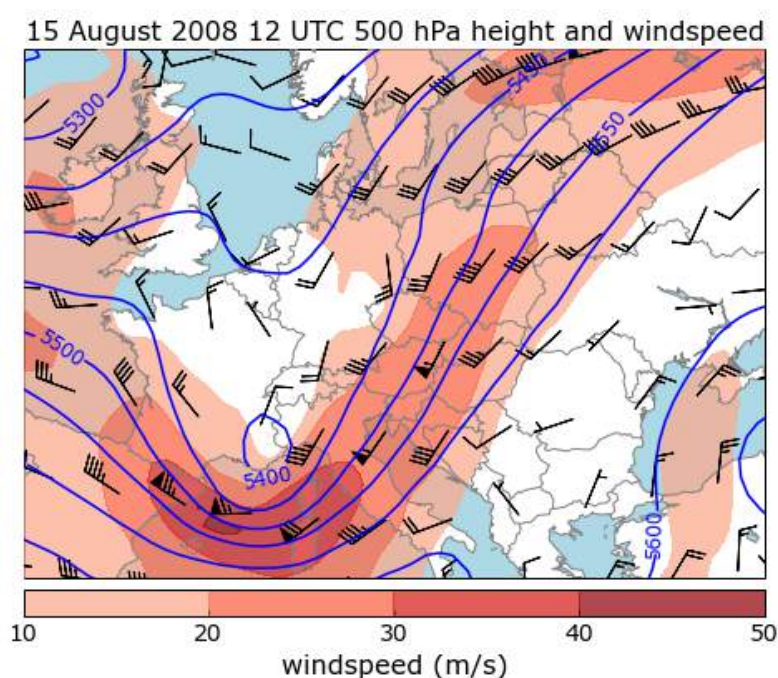


Figure 3.31. 12 UTC ERA Interim reanalysis of 500 hPa height and windspeed. Note the deep trough centered over southeastern France along with strong flow at the southern and eastern flank of the trough.

Although the conditions were conducive for severe convection over a very large area, tornadoes occurred only over southern Poland. One of the reasons for that may be the timing of the frontal wave and shallow surface low passage. Between 14 – 15 UTC, at the time of the convective initiation over the region, region was situated to the north of the surface low, with easterly to southeasterly surface flow, enhancing the degree of low level shear and storm-relative helicity. Moreover, airmass was characterised by low temperature – dewpoint depressions, with temperature readings around 25 and dewpoint readings around 20 deg C. Thus, cloud bases were rather low, which is another factor deemed necessary for tornado occurrence (Grünwald and Brooks, 2011)).

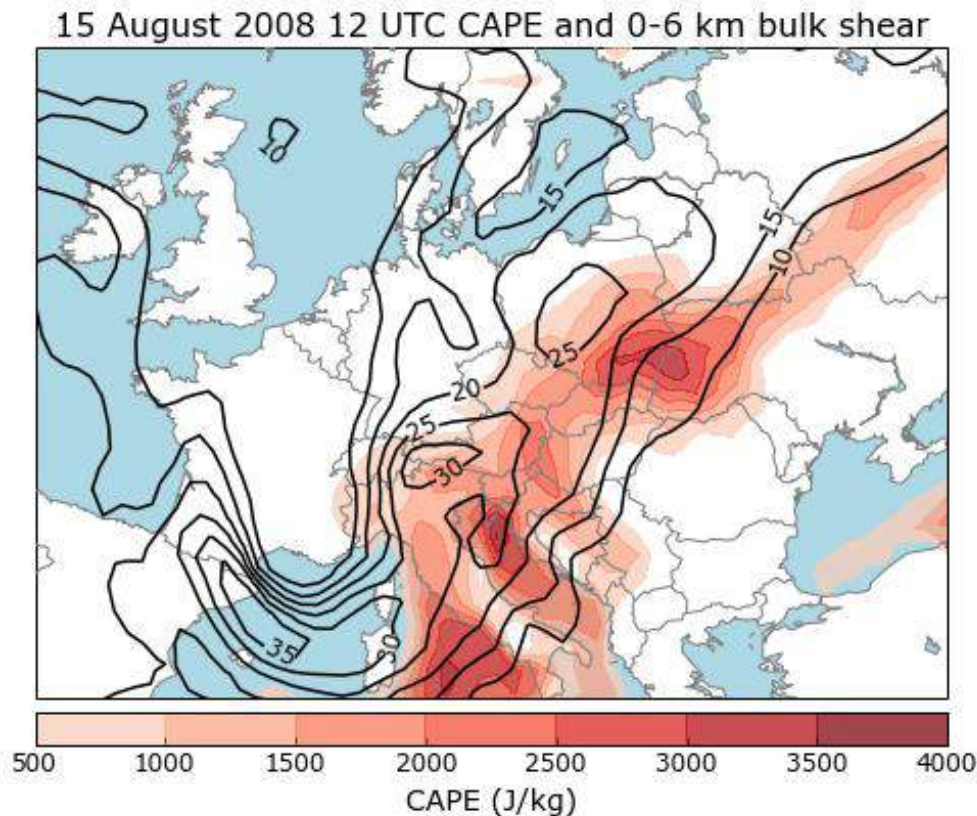


Figure 3.32. 12 UTC ERA Interim reanalysis of CAPE and bulk wind shear between 10 m and 6 km. Significant overlap of CAPE and strong shear existed from the Tyrrhennian Sea all the way towards eastern Poland, suggestive of potentially widespread severe weather outbreak.

All tornadoes occurred with a discrete supercell thunderstorm that formed over the far northern Czech Republic as a cluster of cells after 13 UTC and moved into Poland. The first and most damaging tornado occurred around 15 UTC. It cut a 20 km long path across southern Poland, from the village Dolnica to Dabrowka. At one point, it crossed highway A4 (E40) which we discuss below. Not far from the highway, in the village Balcarzowice, the tornado inflicted the most serious damage, attaining a rating of F3. Trees were uprooted or even debarked, numerous brick structures were badly damaged or destroyed, and 15 people were injured. The supercell thunderstorm continued producing more tornadoes as it moved northeastward. Another serious F3 tornado with a path length of 15 km occurred just 30 minutes later, southeast of Czectochowa, killing 2 people and destroying numerous houses as well. The last tornado was reported in Poland on this day occurred with the same storm at 17:30 UTC. After this time, the supercell merged with the other storms, formed a squall-line and ceased to produce tornadoes.

3.6.1.2 Impacts to critical infrastructure

According to the reports (Nto.pl, 2008), a 2 km stretch of the A4 motorway was affected by the tornado. Several cars and even trucks were thrown and rolled away from the motorway, some of them hitting and damaging the safety barriers in the middle. A bus with passengers was overturned, injuring around 30 people. Even though the tornado did not damage the asphalt surface of the motorway itself, it brought down the lamp posts situated at its center. Subsequently, traffic was blocked in both lanes for several hours. A study by Chmielewski, Nowak and Walkowiak (2013) investigated the damage inflicted by this tornado. They found that several traffic signs along the motorway were bent at ground

level. According to their calculations, the lower boundary of wind speeds necessary for such damage would be 71 m/s at the height of 2.3 meters. If we take into the consideration the damage assessment of F3 in the village located close to the motorway, then according to Feuerstein et al. (2011), the windspeed at 10m at that location would be around 80 m/s.



Figure 3.33. Damage to the light poles on the A4 motorway. A minivan thrown by the tornado can be seen in the back of the photo. Source: wiadomosci.gazeta.pl (2008)

3.6.1.3 Conclusions

This case documents a rather rare event of tornado impacting a highway in the southern Poland during the famous tornado outbreak of 15 August 2008. Compared to the ordinary windstorms, tornadoes have higher damage potential, but they usually impact only a smaller part of the traffic infrastructure. In our case, lamp posts were downed on the highway and cars were thrown either outside of the highway or impacted the safety barriers, damaging them. We speculate that in case of the strongest tornadoes (reaching F5 category), even parts of the asphalt surface could be peeled off the motorway surface.

3.7 Hail

3.7.1 Hail, Stuttgart (Germany), 15 August 1972

Type of event	Hailstorm
Date	15 August 1972
Location	Stuttgart and Fellbach, Germany
Total damage	At least DM 100 000 000 In today's value at least € 140 000 000
Victims	6 fatalities
Affected critical infrastructure	Road connections Rail connections (urban) Underground
Type of damage to infrastructure	Blocked roads, railways, underground lines for up to 6 days

On 15 August 1972, severe storms caused serious damage in several places in southwestern Germany (Figure 3.34). In the afternoon the city of Stuttgart, a town of more than 600 000 inhabitants, was hit by a severe hailstorm. Exceptionally large amounts of hail blocked the land transport system in parts for up to 6 days. The hailstorm caused damage of “hundreds of millions DM”. 6 people died in the severe storm. It is an extreme example of how underground infrastructure and underpasses can be affected by hail, in addition to the blockage of streets and urban railways. The description below details the accounts summarized in Stuttgarter Zeitung (2013) and the report on SWR television on 15 August 2006 (SWR, 2006).

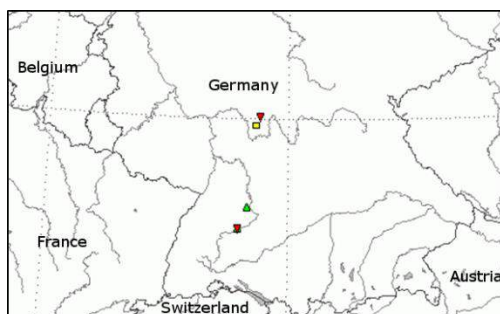


Figure 3.34. Reports from the European Severe Weather Database ESWD for the 15th August 1972 (green triangle: hail, yellow box: severe wind gusts, red triangle: tornado) as of 10 December 2014. The isolated green triangle marks the location of Stuttgart.

3.7.1.1 Meteorological Description

An mid/upper level low was on the 15th August 1972 situated over France (Figure 3.35) and was slowly moving eastward. While hot air was present in an upper ridge over central Europe, the air was cooler over France. Over Southwest Germany, ahead of the upper-level low, a low pressure system present and rising motion took place.

The maximum temperature in Stuttgart reached 24 °C on that day while further west in the Rhine valley only 20 °C were reached, but further east over Bavaria up to 31 °C, suggesting the presence of

a temperature boundary. Rich moisture was present according to widespread precipitation amounts of more than 30 mm on that day in Southwest and central Germany. Mountain stations reported strong wind gusts (up to 27 m/s on mount Brocken) on that day, which suggest that wind shear was strong in the lowest levels of the troposphere.

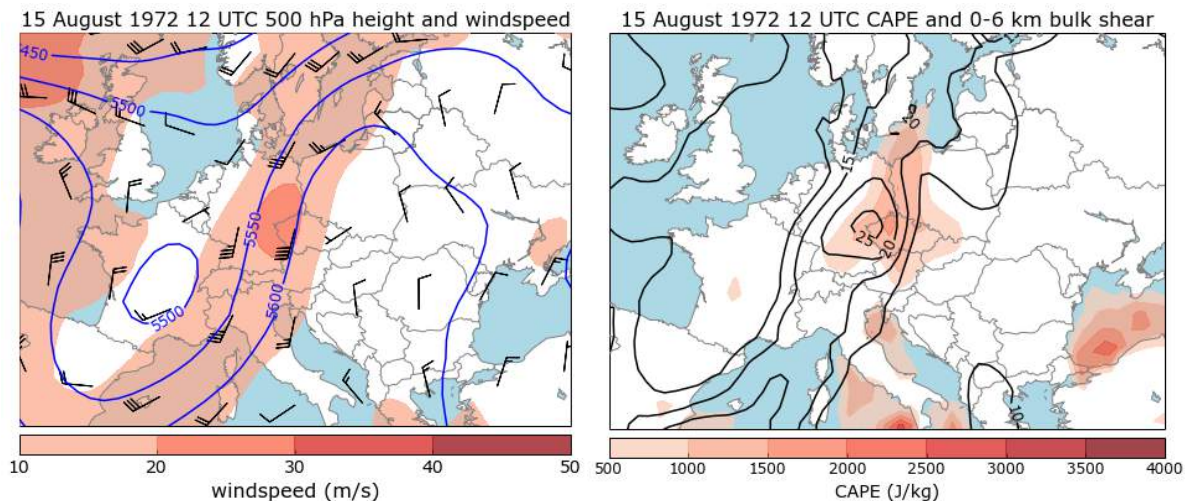


Figure 3.35. Weather pattern at 15 August 1972 at 12 UTC per NCEP/NCAR reanalysis data. Left: 500 hPa geopotential height and sea level pressure. Right: 850 hPa temperature and geopotential height. Source: ERA-Interim.

3.7.1.2 Impacts to Critical Infrastructure

The total damage was described by “hundreds of millions of German Marks” (*Stuttgarter Zeitung, 2013*), in today’s values an amount of hundreds of millions of EUR.

Streets and urban railways

Many streets and some urban railways in the Stuttgart area were impassable because of piles of hail, accumulating up to “man size”. Photos in newspapers illustrate that hail accumulates to incredible heights, even hiding some cars. It should be emphasized that the accumulation was not on a flat natural surface, but in inner town streets where hail was added from the surrounding roofs and probably also washed up from higher terrain. Nevertheless, blockages were widespread in the city, also because of failure of water pumps in street underpasses. The hail clogged rain gullies, resulting in a mush of water and ice in low lying places. This mush caused life-threatening situations in the underpasses, where people had to be rescued from the roofs of their cars, out of the icy cold pap. It took the maintenance services 6 days to clean up all hail accumulations in the city. The hail and water mixture intruded underground stations and pedestrian underpasses, forcing closures. The fire brigade reports that their material was also affected by the icy flooding. A rescue car with scuba diving gear for search action could not reach the area of the flooded underpasses. No detailed reports of telecommunication or power supply failures are available, but according to the amount of damage, also caused by severe wind gusts, such will likely have occurred in places.

3.7.1.3 Conclusions

The extreme hail event of Stuttgart on the 15th August 1972 shows that not only streets and urban railway lines, but also underpasses and underground systems can be highly affected by exceptionally large amounts of hail.

In total 6 people died in that event, 4 in cellars of buildings, when a mixture of hail and water clogged the drainage and water flooded the low lying parts of buildings with no escape routes open. In a recent newspaper interview the mayor of Stuttgart states that the city nowadays is better prepared for such an event. Weather warnings have improved, as well as emergency preparedness and communication. But the mayor says, that a remaining risk cannot be avoided.

In general it seems that typically cases of large hail amounts tend to block streets for a short while. According to the ESWD, cases of hail accumulations of 20 or 30 cm can be found nearly each year in Europe. Very large hail with diametres of more than 5 cm can affect critical infrastructure mainly by damaging roofs, the exterior shell of buildings, and especially glass fronts. As glass becomes frequently used in architecture, and such buildings are vulnerable to the impact of very large hail, cascading effects might become an increasing issue. These can be triggered if very large hail penetrates the outer shell and causes rain water to enter the structure, possibly reaching sensible areas of infrastructure.

3.8 Lightning

3.8.1 Lightning, Jistebnik (Czech Republic), 2009

Type of event	Lightning
Date	29 June 2009
Location	Jistebnik, Czech Republic
Total damage	unknown
Victims	none
Affected critical infrastructure	
Type of damage to infrastructure	Railway signaling system in station was struck by lightning

This situation was part of a long lasting period of thunderstorm activity over the Czech Republic. Many of the thunderstorms were slow moving and producing excessive precipitation. Just a few days earlier, on 24 June, major flash flooding event also occurred over the northeastern part of the Czech Republic, causing major damage and claiming 10 lives. However, on this particular day, no severe weather occurred in the area.

3.8.1.1 Meteorological description

The weather situation was influenced by the presence of a shallow mid and upper tropospheric low centered over southeastern Europe, with rather weak easterly to northeasterly flow over the region of interest (Figure 3.36, left). Surface observations from the day reveal the presence of a warm and humid airmass with 2 m dewpoints ranging between 18 and 20 °C. 12 UTC sounding from Prostejov, located in close proximity to the area of discussion, reveals a rather moist profile throughout the troposphere with relatively low CAPE over 500 J/kg and weak vertical wind shear. This is confirmed also by the ERA Interim reanalysis for 12 UTC (Figure 3.36, right), showing marginal CAPE values and 0-6 km wind shear below 10 m/s. Thus, conditions were not supportive of organized severe thunderstorms on that day.

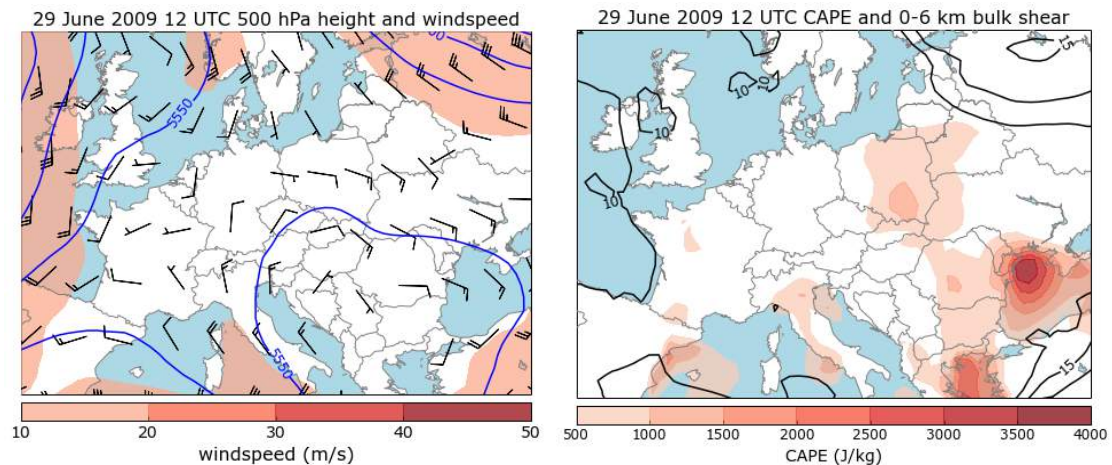


Figure 3.36. Left: 12 UTC ERA-Interim reanalysis of 500 hPa height and windspeed. Only weak easterly to northeasterly flow was present over the region. Right: CAPE and bulk wind shear between 10 m and 6 km. Marginal CAPE values and weak vertical wind shear (below 10 m/s) can be found over northeastern Czech Republic.

Widespread thunderstorm activity occurred over the region, mostly in a form of a multicellular cluster, slowly propagating from southern Poland to the southwest. The highest thunderstorm activity in the area of interest was noted between 14 and 15 UTC, based on the radar observations (not shown). However, we should note, that the thunderstorms did not produce any severe wind gusts, flash flooding or significant hailfall.

3.8.1.2 Impacts to critical infrastructure

Around 14:30 UTC, lightning struck the tracks and the signaling system of the main railway line between Ostrava and Brno cities in the railway station Jistebník. Parts of the station signaling and shunt control system were burnt and thus dispatcher lost control of the station signaling system. After this event, rail traffic had to be stopped with several trains ending their journeys prematurely in other stations. It took several hours before trains were allowed on tracks, even though in limited form, as stations dispatchers had to communicate using phone about the train positions.

3.8.1.3 Conclusions

This case deals with the lightning damaging the railway station signaling system in northeast Czech Republic. One thing to be noted about this event is that thunderstorm was not severe. In fact, as lightning is a basic component for every thunderstorm, even a weak thunderstorm will have a chance to produce such damage. Furthermore, it is impossible to predict what objects will the lightning hit during the thunderstorm. Thus, warning or predicting of such damage occurrence would be extremely difficult and may only involve a general warning for thunderstorm activity.

3.9 Snow and snow storms

3.9.1 Heavy snowfall, Helsinki metropolitan area, 17 March 2005

Type of event	Heavy snowfall
Date	17 March 2005
Location	Helsinki metropolitan area, Finland
Total damage	almost 300 cars crashed high but unknown financial losses
Victims	3 people died, 60 persons injured
Affected critical infrastructure	
Type of damage to infrastructure	highways blocked by crashed cars

Wintertime weather conditions challenge the fluency and safety of transportation. For example, during snowy and icy conditions, braking distances can be fourfold compared to bare road conditions (Haavasoja and Pilli-Sihvola, 2010). Whenever a reduction of both visibility and road surface grip occurs simultaneously, there is a substantial risk for severe pile-ups on crowded highways. Such events have occurred e.g. in Austria and the Czech Republic in March 2008. In Finland severe crash events happened e.g. in March 2005, in March 2011 and in February 2012. The March 2005 event is presented here (based on the studies by Juga et al., 2012). In that event, a sudden heavy snowfall during the morning rush hours of 17 March triggered severe pile-ups on four main roads in the Helsinki metropolitan area (see figures Figure 3.37 and Figure 3.38).



Figure 3.37. Crashed cars on 17 March 2005 near Helsinki city (photo: Board of Inquiry for Traffic Accidents).

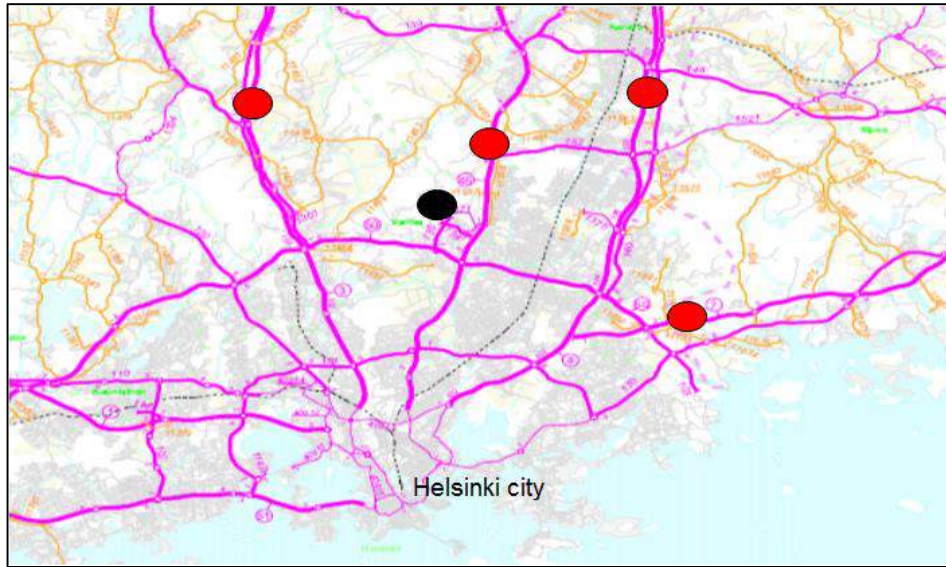


Figure 3.38. Major road network of the Helsinki metropolitan area (source: the Finnish Transport Agency). Red ovals show locations of the pile-ups, Helsinki airport (see weather observations in Table 1) is marked with a black oval.

3.9.1.1 Meteorological description

On 17 March 2005, a long period of dry and cold winter weather in Finland was finally ending as a low pressure was approaching southern Finland from the west (Figure 3.39). After a cold night, the morning temperatures were still 6-8 degrees below the freezing point. Light snowfall reached the Helsinki metropolitan area early in the morning, followed by a band of dense snowfall (Figure 3.40) before 08:00 Local Time (06 UTC). The visibility decreased and the minimum values dropped below 1000 m (Table 1).

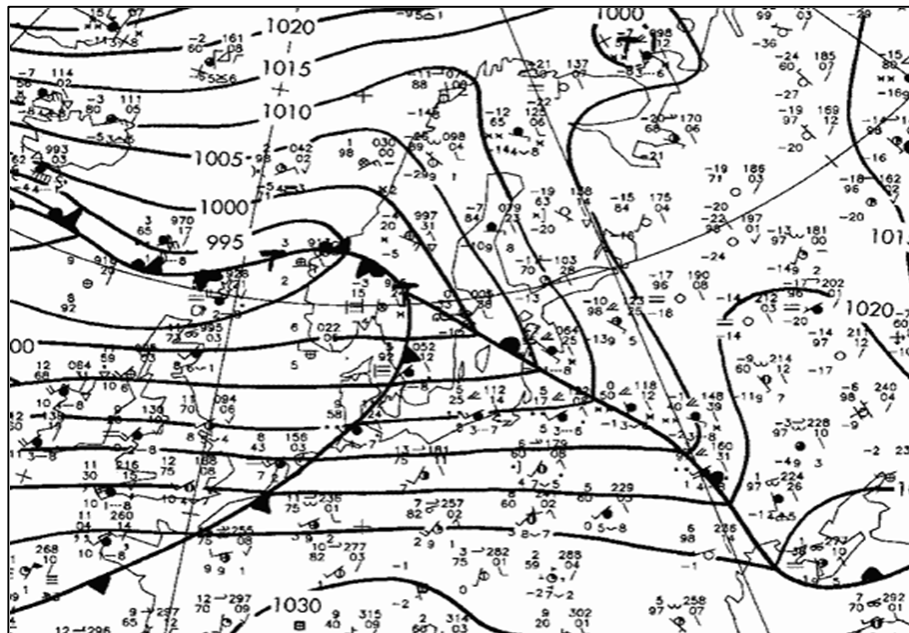


Figure 3.39. The weather situation in central and northern Europe on 17 March 2005 at 00 UTC (source Deutscher Wetterdienst (DWD)). The analysis shows pressure isobars (with 5 hPa intervals) and fronts; low pressure centres are marked by T. Synoptic weather observations are also plotted on the map.

The temperature was just slowly rising and the road surfaces were not salted (except for the western area) due to low morning temperatures. According to road maintenance guidelines, the contractors were not obliged to carry out salting in such low temperatures (although it was optional). The driving conditions rapidly worsened due to packed snow on the road surface and decreasing visibility due to drifting snow. The sharp leading edge of the snowfall area (Figure 3.40) probably took many of the drivers by surprise if they approached Helsinki from the northeast. Around 08:00 LT, severe pile-ups occurred on four highways leading to Helsinki city (locations in Figure 3.38). By the time of the crashes, some of the road weather stations reported low visibilities down to 600 m (which is consistent with the Helsinki airport observation, 700 m (Table 1). At the “windscreen level”, visibility was probably much poorer due to drifting snow, according to some comments from the drivers involved in the crashes.

In the pile-ups, almost 300 cars were crashed, 3 people died and 60 injured persons were taken to hospital. The traffic in the Helsinki region was badly jammed for the whole day. The removing of crashed cars and cleaning of the road sides took several days or even weeks. The investigation of the crashes, evaluation of the crashed vehicles, and the processing of compensations from traffic insurances took, of course, a substantially longer time. A similar event during dense snowfall happened again in the Helsinki region in February 2012 (Juga et al., 2014).

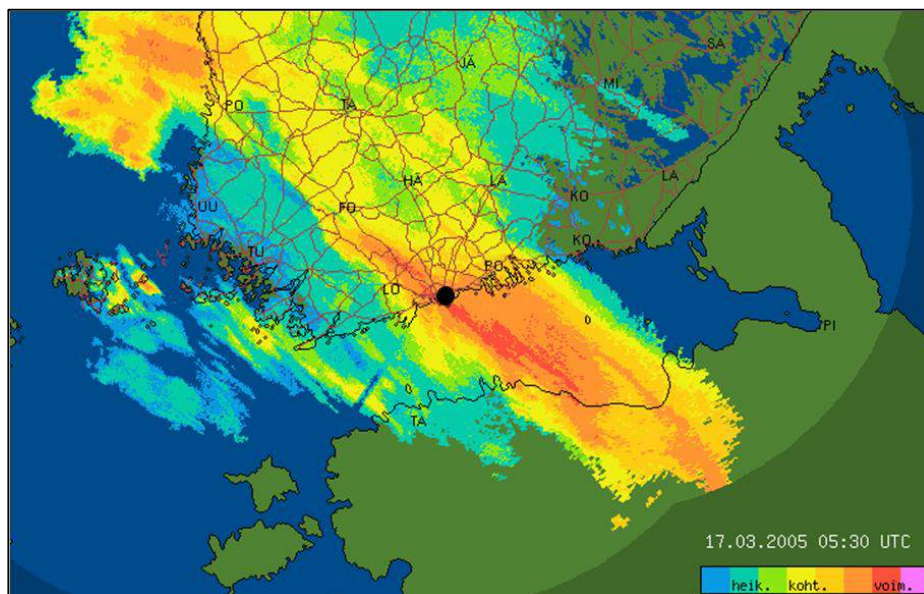


Figure 3.40. Radar image on 17 March 2005 at 07:30 LT (05:30 UTC), showing a southeast – northwest oriented precipitation band. The precipitation intensity is shown with different colours, red (and pink) indicating heavy precipitation. The location of Helsinki city is marked with a black dot.

Table 3.2. Weather observations at the Helsinki airport on 17 March 2005, ca 04-07 UTC. (Abbreviations for present weather: SN=snowfall; DRSN=drifting snow, FZRA=freezing rain, the minus sign in front of the symbol indicates weak precipitation).

Time (UTC)/ local time	Wind direction and speed (m/s)	Visibility (m)	Present weather	Temperature (deg. C)	Dew point temperature (deg. C)
04:01/06:01	E 6	2600	-SN	-7.2	-8.6
04:20/06:20	E 4	2200	-SN	-7.2	-8.4
04:50/06:50	E 5	1400	SN	-7.1	-8.3
05:20/07:20	ENE 6	1300	SN	-7.0	-8.1
05:50/07:50	ENE 5	1000	SN	-6.6	-7.7
06:03/08:03	E 5	700	SN	-6.2	-7.2
06:20/08:20	E 5	900	SN	-5.9	-6.9
06:50/08:50	E 5	1200	SN	-5.8	-6.9
07:05/09:05	ESE 5	2200	-SN, DRSN	-5.6	-6.7
07:20/09:20	E 6	3500	-SN, -FZRA	-5.6	-6.6

Milder air was streaming from the southwest towards southern Finland behind the main precipitation area, which moved further inland towards the northeast. However, a shallow layer of cold air still existed near the ground surface, where temperatures remained below 0 °C. Because of that, freezing rain occurred after the passage of the heavy snowfall. Some of the media blamed this as being the main reason for the occurrence of the crashes. However, based on weather observations (Table 1: freezing rain was observed at Helsinki airport at 09:20 LT) and a thorough analysis of radar data as well as images from road weather cameras, the conclusion was that freezing rain was mainly observed after the occurrence of the crashes, i.e. when the journalists arrived at the accident sites. So, the low visibility and decreased road surface friction due to dense snowfall were the main weather-related factors triggering the crashes. Although the snowfall was intense at the time of the crashes, i.e. around 08:00 LT (06 UTC), the total snow accumulation was just about 5 cm. Investigations later pointed out that too high driving speeds and too short distances between vehicles were also important reasons for the occurrence of the pile-ups.

in the previous evening Finnish Meteorological Institute (FMI) predicted some snowfall for the morning and issued a warning for poor driving conditions in the southernmost Finland. The TV-meteorologist also pointed out that it might be slippery during the morning rush hours. However, the event was to some extent underestimated, and a warning for very poor driving conditions was issued only after the occurrence of the crashes.

3.9.1.2 Impacts to critical infrastructure

The impacts of the dense snowfall during the morning rush hours were widespread. Pile-ups on four main roads disrupted traffic very badly in the Helsinki metropolitan area (Figure 3.38). In addition to

the casualties, a lot of people got stuck in the jams and could not reach their workplaces. Transport of goods was also disturbed, and, although the air-traffic was running quite normally at the Helsinki airport, people had difficulties to reach the airport due to the jams. There were many actors working under pressure after the occurrence of the crashes: the Police, Rescue Service, the Road Administration and maintenance contractors etc. The crashed vehicles had to be moved away from the roadways and the road surfaces had to be maintained to get the traffic running again. The investigation of the accidents started immediately and lasted for several months. One big task was the evaluation of the crashed vehicles and the payment of compensations by vehicle insurances to the crash event participants. This was a costly event, although an estimate of the total monetary costs is not available.

3.9.1.3 Conclusions

This case showed that hazardous winter weather can have large impacts on transportation and infrastructure. The most probable important reasons for the crashes were: a sudden worsening of weather, dense snowfall with poor visibility, and simultaneously, pre-existing packed snow on the road surface and related low friction, too high driving speeds and too short distances between vehicles. There are several means to prevent such accidents in the future: More efficient combined use of weather observations and radar data, development of road weather forecasting models and improvement of warning practices; provision of real-time weather information and warnings into vehicles; and finally, usage of weather-controlled speed limits and displays.

3.9.2 Snow storm, South and central Finland, 23-24 November 2008

Type of event	Snow storm (blizzard)
Date	23-24 November 2008
Location	South and central Finland
Total damage	41000 households without power 73 % higher number of traffic accidents
Victims	112 injured and 1 killed in traffic accidents
Affected critical infrastructure	
Type of damage to infrastructure	roads blocked by fallen trees, traffic disrupted by snow accumulation and poor visibility, blackouts in electricity supply

A blizzard can have large negative impacts on society, affecting e.g. all transport means, electricity supply, and possibly causing also damage to buildings. In the EU FP7 project EWENT, a blizzard was defined in the following way: daily mean temperature $\leq 0^{\circ}\text{C}$, 24h snow accumulation ≥ 10 cm and maximum wind gust (3 second) speed ≥ 17 m/s. So, during a blizzard, low temperature, heavy snowfall and strong wind are combined. Here the blizzard which came in over Finland from the south on 23 November 2008 is investigated, based on the studies by Rauhala and Juga, 2010. The weather hazard had large impacts especially in southern and central Finland.

3.9.2.1 Meteorological description

The first half of November 2008 was mild in southern and central Finland with daytime temperatures rising up to 10 °C at some places. Around 20 November a period of colder weather started, with temperatures falling below 0°C even in the southernmost part of the country. On 22 November, a low pressure system formed over Eastern Europe, moving northwards and deepening rapidly. On 23 November the low pressure centre was situated over Estonia, the air pressure being as low as 955 hPa in the centre of the low (see Figure 3.41). Cold northerly winds increased in Finland and the temperature stayed around -3 °C even in southern Finland for the whole day. Heavy snowfall started in South-eastern Finland in the morning, spreading towards the northwest during the day, so that it reached the west coast of Finland later in the afternoon. During the snowfall, rare wintertime lightning was observed at some places. The total 24h snow accumulation was large, being locally above 30 cm in the South-eastern coastal area (Figure 3.42), and elsewhere in southern and central Finland the snow accumulation was generally between 10 and 25 cm. The wind became strong and the maximum gusts rose to 27 m/s in Tampere airport in southern Finland, where the gust speed stayed over 20 m/s for more than 5 hours. So, this case clearly fulfils the blizzard criteria defined in the EWENT project (see section 1).

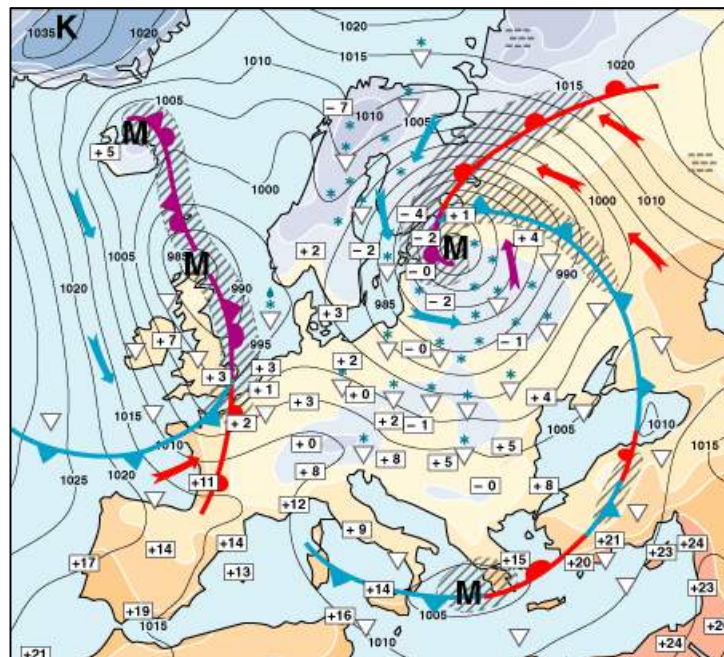


Figure 3.41. Weather situation in Europe on 23 November 2008 at 12 UTC (14:00 LT). The analysis shows pressure isobars (with 5 hPa intervals) and fronts; low pressure centres are marked with M and high pressure centres with K (analysis by FMI). The numbers represent the temperatures in °C.

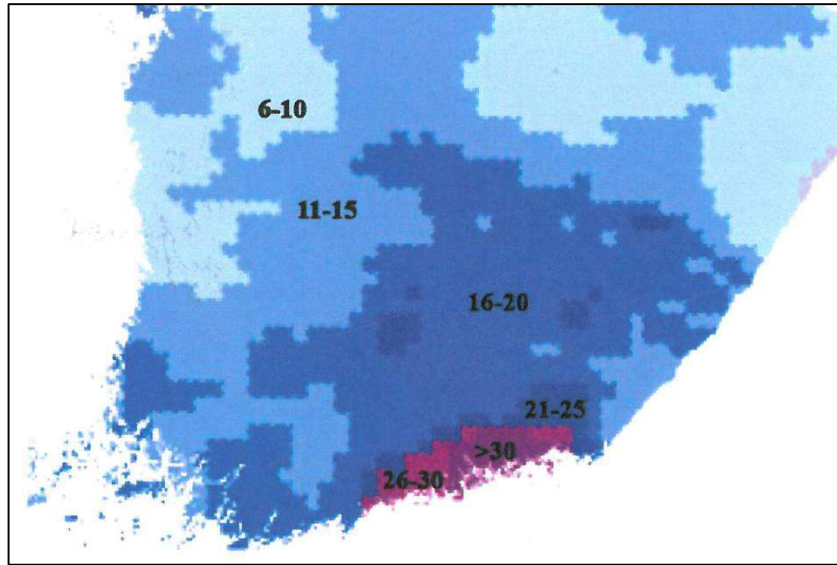


Figure 3.42. Snow accumulation (cm) in southern and central Finland based on radar measurements during the period 23 November 2008 06 UTC (08 LT) – 24 November 2008 05 UTC (07 LT). From Rauhala and Juga (2010).

The weather forecasts and warnings in this case were quite successful. The Finnish Meteorological Institute issued a warning for very bad driving conditions in southern and eastern part of the country, and a warning for poor driving conditions in western Finland. There was also a warning for gusty winds in the inland areas, and a storm warning for the sea areas.

3.9.2.2 Impacts on critical infrastructure

The strong gusty wind and heavy snowfall caused plenty of power failures, leaving 41000 households without electricity at least for some time. Also some building damage occurred, e.g. detached roofs due to wind gusts. All transportation means encountered problems and the number of traffic accidents in southern and central Finland rose by 73% compared to the average (normal) situation. In the worst affected areas at the south coast (including Helsinki city region), the number of traffic accidents on Sunday 23th was fourfold compared to normal. In total, one person died and 112 persons were injured in southern and central Finland during 23-24 November. Due to the gusty wind, a lot of trees fell on the roads; there were 20 accidents of a car crashing into a tree blocking the road, mostly because the driver did not in slippery road conditions and poor visibility see the fallen tree early enough. The maintenance contractors were operating under pressure, removing the fallen trees and snow from the roadways. The energy operators also had to remove the fallen trees from the power transmission lines and repair the possible damages.

3.9.2.3 Conclusions

During a blizzard, the situation can get so hazardous that the transportation and energy sectors may encounter big problems in spite of the fact that the weather event might have been successfully predicted and warned for. If the event occurs during the weekend (as was the case here), the operators must have extra personnel on alert, starting to work on the case when needed. On the other hand, the general public should avoid unnecessary movement outside during the worst weather conditions and prefer working from home if it is possible. The national weather services can formulate general

safety rules for the public or call-to-action statements, which can be included in the storm warning messages during the most severe events (for more information, see Rauhala and Juga, 2010).

3.9.3 Heavy snow loading, Finland, 31 October – 1 November 2001

Type of event	heavy snow loading combined with high wind speeds
Date	31 October– 1November, 2001
Location	Southern Ostrobothnia, Central Finland and Pirkanmaa, Finland
Total damage	177 000 houses were left without electricity
Victims	none
Affected critical infrastructure	
Type of damage to infrastructure	over 20 000 trees fallen onto power transmission lines

Heavy snow loading occasionally causes forest damage in cold climates. Damaged trees may further inflict disturbances in power transmission by bending or falling over power transmission lines. Moreover, snow, rime and ice accumulation on power lines itself causes problems in power transmission and most severe snow-load events with ice accretion may seriously damage even power transmission line towers and lead to great economic losses (e.g. Lahti et al. 1997; Zhou et al. 2012).

In November 2001 two storms, named as “Pry” and “Janika”, caused widespread damage in Finnish forests. The forest damage associated with Pry storm was not caused only because of high wind speeds but also due to a heavy wet snow loading that occurred just before the storm in central parts of Finland (Figure 3.43). It is impossible to totally distinguish between the damage caused by the heavy snow load and the subsequent storm but admittedly the combined effect of these two phenomena exacerbated the damage.



Figure 3.43. The area that suffered the most severe forest damage associated with the Pry storm (adapted from Hoppula 2005).

3.9.3.1 Meteorological description

The accumulation of snow on tree branches is most efficient when the temperature at the time of precipitation is just above 0 °C and then falls below freezing. According to Solantie (1994), snowfalls of 20–40 cm under temperatures near the freezing point produce low to moderate and snowfalls of about 60 cm very high risk for snow damage in forests. In general, wet snow accretion on electric wires has been considered to be most hazardous when associated with light winds (e.g. Kuroiwa 1965) because strong winds easily blow off any substantial accumulation of snow. Wind speed exceeding 9 m s⁻¹ is also expected to dislodge most of the snow from tree crowns (Solantie 1994).

The meteorological conditions leading to heavy snow loading associated with the Pyy storm have been studied in detail by Hoppula (2005). The situation started to evolve on October 29. A weak ridge of high pressure prevailed in Finland while a large low pressure area was approaching from the west. Temperature dropped couple of degrees Celsius below freezing on the evening of October 29 in southern and central Finland with the exception of the southernmost coastal regions. Winds were generally weak and widespread freezing fog and low level stratus clouds were formed since

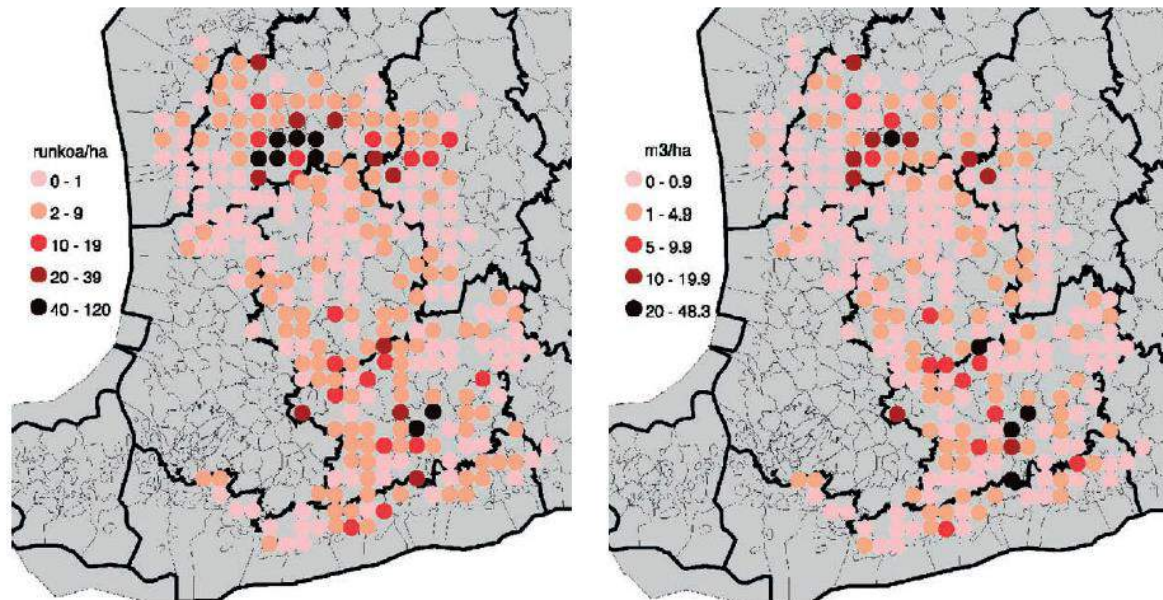


Figure 3.44. The average number of destroyed trunks per hectare (left) and volume stock of destroyed wood in square metres per hectare (right) in November 2001. The maps show the combined damage caused by the storms Pyy and Janika (adapted from Ihalainen and Ahola 2003). In the area shown in Fig. 1, approximately 70–90% of the total damage was associated with the Pyy storm (Hoppula 2005), whereas in southern Finland the damage was mainly caused by the Janika storm.

relative humidity reached 100% in atmospheric boundary layer. Atmospheric sounding profile from Jyväskylä airport, situated in the eastern part of the hatched area in Figure 3.43, on the late evening of October 29 is shown in Figure 3.45. Moisture was condensed into freezing fog and stratus clouds below the shallow inversion in the boundary layer. Weather conditions were thus favourable for riming and Hoppula (2005) estimated that, for instance in Seinäjoki about 150 km west-north-westwards from Jyväskylä, approximately 3 mm of rime was accumulated during the night.

On October 30, a centre of low pressure moved over the Åland Islands and the Gulf of Finland to the east (Fig. 4.4.4). Precipitation related to the occluded front of the low pressure system started during the early hours of October 30 in the western coast of Finland. The form of precipitation was at first locally freezing rain but on the afternoon of October 30, a heavy fall of wet snow and sleet was experienced over the hatched area in Figure 3.43. Temperature in the area varied between 0 and 0.5 °C on the afternoon. Winds were weak or moderate and heavy wet snow was effectively attached to the tree branches covered by rime. During the following night, temperature dropped again slightly below freezing and the snow load was frozen and attached tightly to the tree branches and crowns.

The low pressure that was situated north of the British Isles on October 30 (Figure 3.46), deepened and moved over southern Scandinavia and the Gulf of Finland within the next two days (Figure 3.47 - Figure 3.48). Related to this low, it started to snow again by afternoon of October 31 in the hatched damage area of Figure 3.43. Like on the previous day, temperature in the area rose just above 0 °C during the snowfall. The snowfall was most intense during the evening of October 31 and until the morning of November 1, over 30 cm of heavy, wet snow had fallen on many locations.

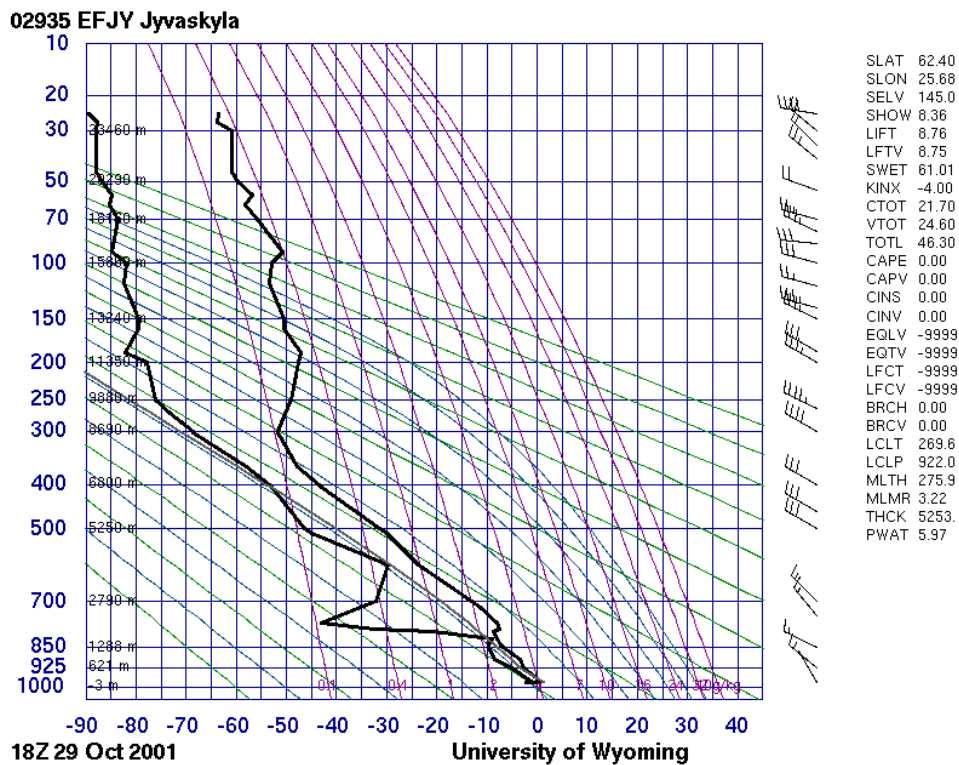


Figure 3.45.. Atmospheric sounding profile at Jyväskylä airport on 18 UTC October 29, 2001 showing the vertical temperature and dew point temperature profiles. Wind barbs in the right display the wind direction and speed (in knots) at a given pressure level. Wind barbs point in the direction "from" which the wind is blowing. Each short barb represents 5 knots, each long barb 10 knots. Data source: University of Wyoming.

The total precipitation between October 30 and November 2, as estimated by the weather radar network over the damaged area is shown in Figure 3.49. The precipitation sum was largely between 30 and 50 mm and most of this had accumulated between October 31 and November 1 as wet snow. On November 1, the snowfall gradually weakened and ended during afternoon. At the same time, strong northern winds emerged and temperature dropped rapidly below freezing. Highest observed

10-minute average wind speeds were 28 m s^{-1} on the western coast of Finland and in general $14\text{--}18 \text{ m s}^{-1}$ at inland stations. The wind was rather gusty because of a strong low level jet at the height of $1\text{--}1.3 \text{ km}$ at which height the wind speed exceeded 30 m s^{-1} .

During this episode, trees were mainly damaged on October 31 and November 1. At first, damage was caused solely due to heavy snow loads, but on later stage, because of combined effect of snow load and wind.

3.9.3.2 Impacts to Critical Infrastructure

Damaged trees fallen, leaned or bended over power transmission lines caused a lot of blackouts, particularly in the regions of Southern Ostrobothnia, Central Finland and Pirkanmaa but also in the north-eastern parts of Satakunta. Following the Pory storm, over 20,000 trunks fallen over power lines had been cleared away (Hoppula 2005). At most damaged sites, over 100 trunks had fallen over electric wires between the two adjacent power poles. A total of 177,000 houses were left without electricity after the Pory and longest blackouts lasted five days (Hoppula 2005). Power companies had also received over 25,000 phone calls concerning the blackouts.

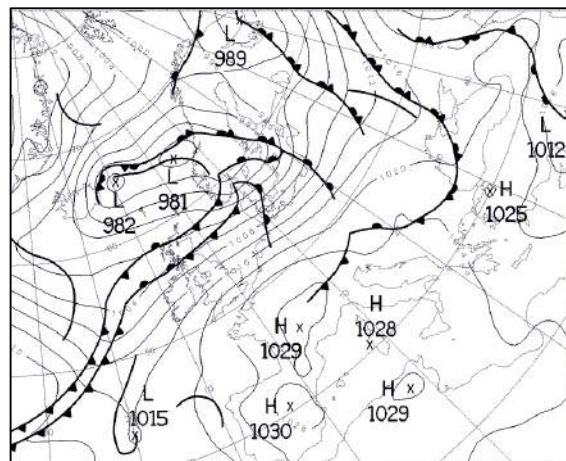


Figure 3.46. Surface weather analyse by the UK MetOffice for 00 UTC October 30, 2001.

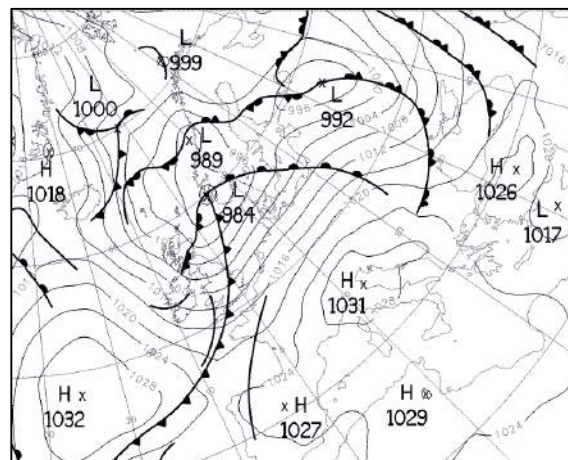


Figure 3.47. Surface weather analyse by the UK MetOffice for 00 UTC October 31, 2001.

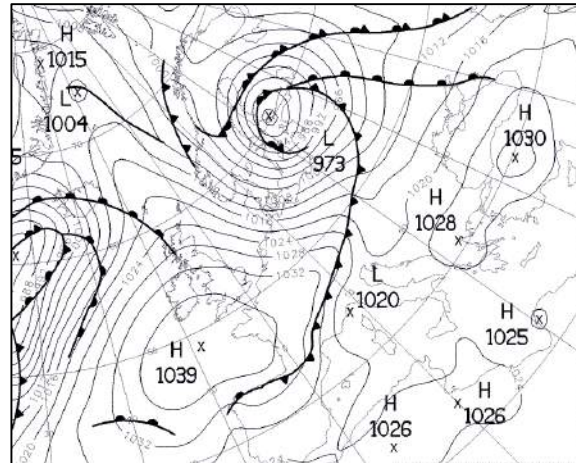


Figure 3.48. Surface weather analyse by the UK MetOffice for 00 UTC November 1, 2001.

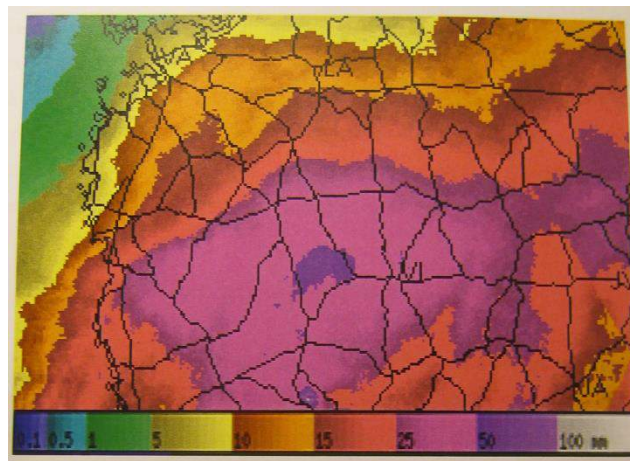


Figure 3.49. Total precipitation sum (mm) between October 30 and November 2, 2001, as estimated based on the weather radar network (adapted from Hoppula 2005).

The damage related to the Pory storm was largely caused by heavy snow loads but it is impossible to totally distinguish between snow and wind induced damages. The most severe damages were restricted to the areas which experienced first the heavy snow loading although the storm was more widespread (Figure 3.43, Figure 3.44). In many sources the damages are also combined with those caused by the Janika storm two weeks later largely on the same areas and it was more devastating storm than Pory. These two storms cut down 7.3 million cubic meters of wood in Finland (Metsätuhotyöryhmä 2003) and 90,000 trunks were fallen over power transmission lines (Ihalainen and Ahola 2003). Repair costs for power companies totalled approximately 11 M€ and forest damage caused equal loss for forest owners (Ihalainen and Ahola 2003); however, the total damage caused to electric supply companies was mainly due to the Janika storm.

3.9.3.3 Conclusions

Heavy snow loading occurred in the regions of Southern Ostrobothnia, Central Finland and Pirkanmaa before the Pory storm on 1 November 2001. The snow loads and the subsequent storm caused widespread forest damage which in turn damaged the power lines through fallen trees.

Weather conditions for accretion of snow on the trees were very favourable during this case. Firstly, the trees were covered by rime before the snowfall which enhanced the efficiency of snow to lodge on the tree branches. Secondly, temperature remained between 0 and 0.5 °C during the snowfall but it dropped slightly below the freezing point between the two snowfall episodes so that the wet snow fallen during the first episode froze and attached tightly to the tree crowns. In general, wet snow is most efficiently attached to trees when temperature at times drops for short periods slightly below 0 °C during the snowfall (Hoppula 2005). Thirdly, the temperature dropped again below 0 °C after the second and more intense snowfall episode and at the same time, wind speed increased substantially. This probably increased the damage because when frozen, the snow loads are less effectively dislodged from the tree crowns by wind and strong winds associated with heavy frozen snow loads thus tend to break the tree stems (Valinger and Lundqvist 1992). Hence, it can be concluded that both the storm exacerbated the snow-induced damages and the snow loads exacerbated the wind-induced damages. Based on the experiences from the Pury storm, Hoppula (2005) concluded that wet snow hazards inflict forest damage when temperature during the event is between 0 and 0.5 °C, wind speed between 3 and 6 m s⁻¹ and precipitation exceeds 25 mm.

Inspired by the damages, several actions were conducted during the following year. Already in November 2001, the Ministry of Trade and Industry of Finland nominated an official receiver to inspect the functionality of electric supply under harsh natural conditions (Forstén 2002). One consequence of this inspection was that, as suggested by the official receiver, customers in Finland are nowadays allowed by the law to receive compensation from power cuts lasting over 12 hours.

3.10 Freezing rain

3.10.1 Freezing rain, Slovenia, 31 January – 3 February 2014

Type of event	Freezing rain
Date	31 January - 3 February 2014
Location	Slovenia, in particular Notranjska region
Total damage	€ 430 million (estimate)
Victims	2 fatalities, and several persons injured
Affected critical infrastructure	
Type of damage to infrastructure	ice and falling trees broke down the power lines living about 250 000 people without electric power for days, rail transportation was stop, many roads were closed, cities and villages were cut off, vehicles were covered by thick ice, telecom installations were also damaged and water supply disrupted, about 500 000 ha of forest damaged

Freezing rain causes accumulation of ice on the surface and infrastructure. Light freezing rain and drizzle produce slippery surfaces, hampering the transportation while more intense freezing rain may lead to multiple failures of infrastructure. Such cases were registered for example in UK on 23–24 January, in Moscow on 25 December 2010, or in Slovenia from 31 January to 4 February 2014.. In this study we present the recent case from Slovenia; as there are only very few studies available about the consequences of this particular case, most of the information are from the media reports.

Due to highly unfavourable weather conditions, blizzard and freezing rain started hitting Slovenia on 31 January 2014 and continued during 1-2 February 2014, resulting in a large scale disaster. Many regions have been affected but mostly the Notranjska region in the south-western part of the country. The state of emergency was proclaimed for the whole country on 2 February 2014. The severe blizzard also affected Croatia and Serbia.

3.10.1.1 Meteorological Description

In most situations, freezing rain occurs ahead of a warm front as warm, above-freezing air overrides a shallow layer of below-freezing air near the surface. Freezing rain is a common phenomenon, but its occurrence on such a large scale is very rare.

The weather pattern around Slovenia was very unsettled for several days around late-January / early-February 2014. A low pressure system over the Central Mediterranean caused very rainy and snowy conditions south of the Alps from 30 January onward. The lingering area of low pressure pumped warmer air northward towards Central- and Eastern Europe. In Western Europe, colder air was still prevalent and a fairly stationary front stretched in between these different air masses (Figure 3.50).

February 2nd 2014 12UTC

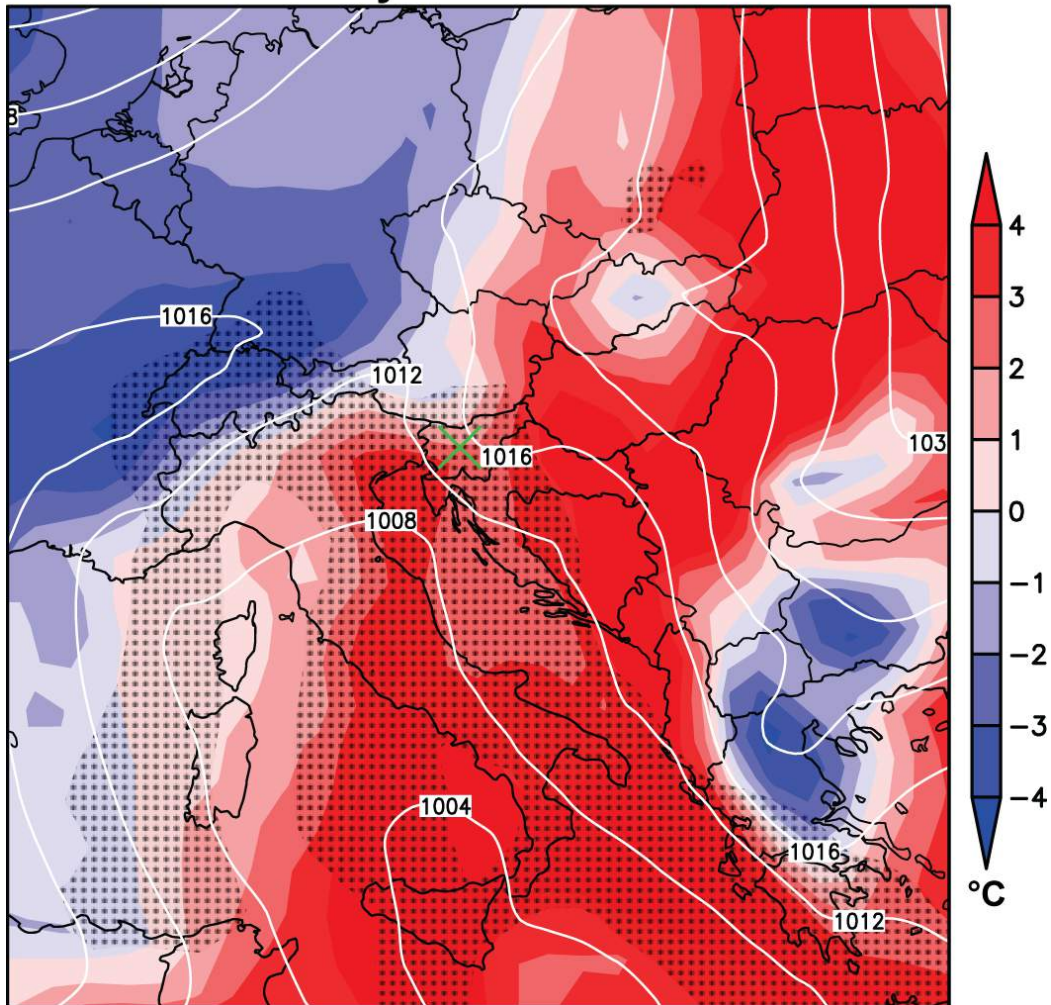


Figure 3.50. ERA-Interim 850 hPa temperature (shaded), mean sea level pressure (white contours), six-hour precipitation of at least 1mm (stippled) on February 2nd 2014 at 12 UTC. The large green X denotes the location of the capital of Slovenia, Ljubljana.

Slovenia was located near the frontal area where warm air was being pushed from the southeast. The ERA-Interim reanalysis simulated precipitation in the area though it does not distinguish between freezing rain and other precipitation. However, the conditions were supportive of freezing rain in Slovenia since warmer air from S-SW spread over colder surface air from easterly flow. The Primorska, Notranjska and Koroška regions were already affected by freezing rain on 31 January 2014.

On 1 and 2 February 2014, snow and freezing rain gripped almost all of Slovenia covering the country and its capital, Ljubljana entirely in ice.

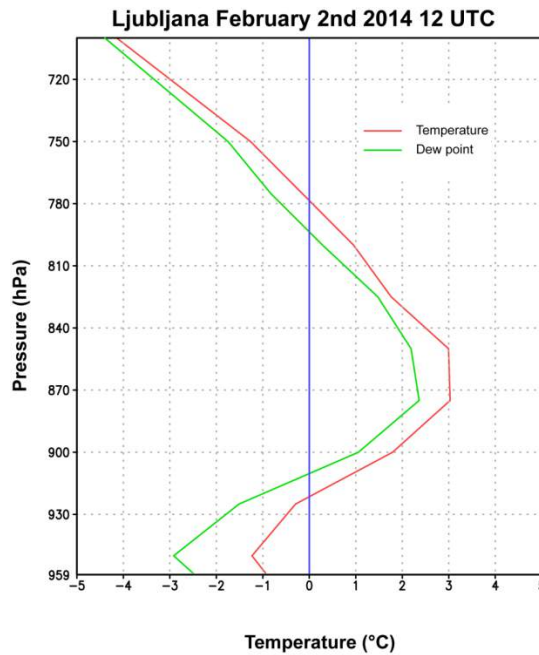


Figure 3.51. Vertical profile of temperature and dew point over Ljubljana on February 2nd 2014 at 12 UTC as simulated by ERA-Interim.

The 850 hPa level is approximately at a height of 1.5 km. At that level the temperatures were above freezing but on the ground the temperatures were still around 0 °C or slightly below. This setup created a typical vertical profile of freezing rain events as shown in Figure 3.51.

According to the ERA-Interim reanalysis, the warmer air aloft was approximately three degrees above freezing on February 2nd whilst the surface air was slightly below zero. Additionally the sounding station in Zagreb showed a similar vertical temperature indicative of freezing rain potential on February 2nd 2014 (not shown). The Ljubljana airport reported freezing rain throughout the day on February 2nd with the most intense phases being around 10 UTC and between 14-16 UTC based on METAR-observations. The extreme weather situation persisted for unusually long time, 4 days.

3.10.1.2 Impacts to Critical Infrastructure

The extreme weather conditions caused massive damages to infrastructure. The ice brought down power lines, fell trees, and froze vehicles in place. In the first few days of February, snow and freezing rain caused serious damage in the entire area of the City of Ljubljana as well.

3.10.1.3 Impacts to energy and telecommunication infrastructure

Freezing rain, snow and falling trees caused extensive power outages with more than 80,000 client sites affected, leaving around 250,000 people without electric power. The falling trees, sleet and snow have damaged or completely destroyed 30 kilometers of electricity lines, and another 174 kilometers or nine percent were in addition inoperative.

On 2 February 2014, the Republic of Slovenia requested assistance through the European Union’s Civil Protection Mechanism with a request for 100 power generators (100 - 300 kVA) in order to provide electricity to the affected population. As of 5 February, there were still 50,000 people without electric

power, some for the 5th consecutive day. The situation was the worst in Postojna, city located in the SW part of the country, with all electrical lines damaged (Figure 3.52). Austria, Germany and the Czech Republic sent in emergency generators, the army deployed 100 soldiers to assist the civil defence units in the Postojna region and help those in need.

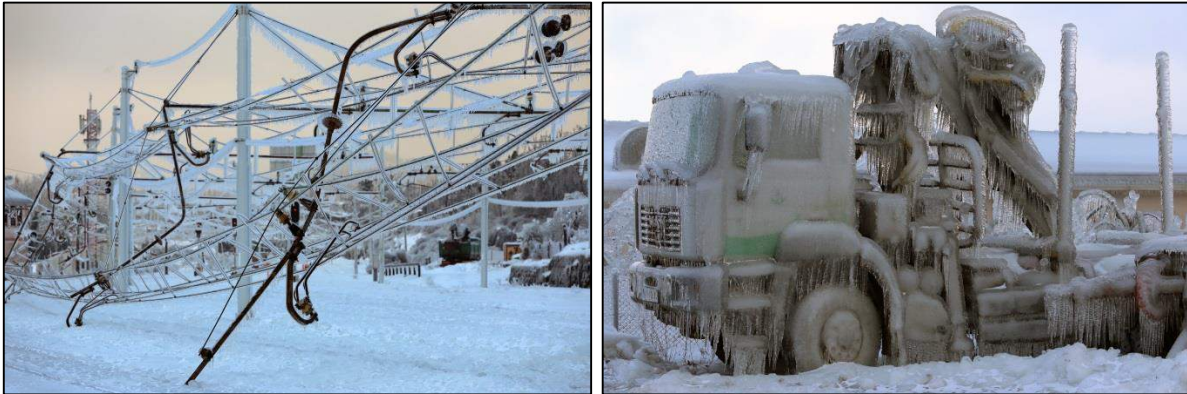


Figure 3.52. Ice-damaged rail infrastructure at the Postojna railway station; ice covered truck in Postojna (photos by D. Rozman).

The ice storm severely damaged the telecommunication installations and disrupted the water supply.

Infrastructure of traffic and transportation

Railways traffic was stopped in some parts of the country. Road traffic was also heavily disrupted, as many of the roads were inaccessible due to conditions and fallen trees. In Ljubljana roads were closed for several days. Towns and villages were cut off as roads and rail lines became impassable.

Economic impacts

The biggest loss to Slovenia was undoubtedly the natural disaster suffered by the forests. Roughly half of Slovenia's total forest, 500 000 ha or 5.155 million m³ of wood have been damaged, trees were broken as they could not support the weight of the ice. This represents the amount of wood normally felled in a year. The broken trees had to be cut down or trimmed as soon as possible. 93% of forest roads were closed.

Some companies and factories closed down for several days. Also schools and kindergartens were closed for several days. Families who spent some days in the blackout were without heating, water, food and means of communication. Falling trees and branches also wrought major damage at Ljubljana ZOO, where several fences were damaged.

Two people died and several others were injured. The available first estimates of the costs of damages of extreme weather conditions are diverse and unofficial. However, a rough estimate raises the costs for recondition the power system infrastructure to 47 million euro (SINFO, February 2014), of which 37 million euro constitutes the damage to the electricity distribution system and 10 million euro to the transmission system. The damage in railway infrastructure were estimated to 20 million euros not including the damage the transport companies, and in state roads infrastructure to 9 million euro (SINFO, February 2014). Losses to the economy were estimated to approximately 42 million euros. The total estimated damage was around 430 million euro (Pristov et al. 2014).

3.10.1.4 Conclusions

Although the freezing rain is not a rare event, the case from Slovenia from January-February 2014 is one of the most severe freezing precipitation events recorded in Europe over a relatively large area for such a long period. This devastating freezing rain event caused so significant damages on the critical infrastructure, that the local government declared a state of emergency and requested international assistance to mitigate the consequences.

3.11 Wildfire

3.11.1 Wildfire event in Västmanland, Sweden, 31 July 2014 - 11 September 2014

Type of event	wildfires
Date	31 July 2014 - 11 September 2014
Location	Municipalities Fagersta, Norberg, Sala and Surahammar in Västmanland, Sweden
Total damage	burned area circa 150 km ²
Victims	1 fatality
Affected critical infrastructure	
Type of damage to infrastructure	approximately 1 200 people were evacuated, around 25 houses and outbuildings were burned down or damaged, several roads and railways were blocked, boat traffic in nearby lakes and canals was closed off because of water intake for airborne firefighting, and even the airspace over the fire area was closed off from all the other airplanes than those taking part in the extinction operations.

The wildfire in Västmanland, Sweden, in 2014 is a conflagration, i.e. a great wildfire that broke out on 31 July 2014 in north-eastern part of the Surahammar Municipality, near the border of the Sala Municipality in Västmanland, Sweden. The fire affected directly four Swedish municipalities: Fagersta, Norberg, Sala and Surahammar (**Error! Reference source not found.**). The fire started from a sparkle from a forestry machine. Preceding extremely warm and very dry conditions in the area enabled the fire to blaze up and spread rapidly. Fire was considered to be under control on 11 August 2014, but the extinction activities ended officially on 11 September 2014. Approximately 13 800 hectares of forest were burned, mostly in Sala. It was the largest wildfire in Sweden or even northern Europe since at least the 1950s. It has been estimated that the conflagration was one the most serious natural hazards in Sweden in modern times.

Around 1 200 people were evacuated from their homes during the first week of the fire. Around 25 buildings were burned down or damaged; half of them were houses and the other half outbuildings. One person died and two persons were badly injured during the fire (Nature World News, 2014). The economic consequences will fall particularly upon the forest sector.

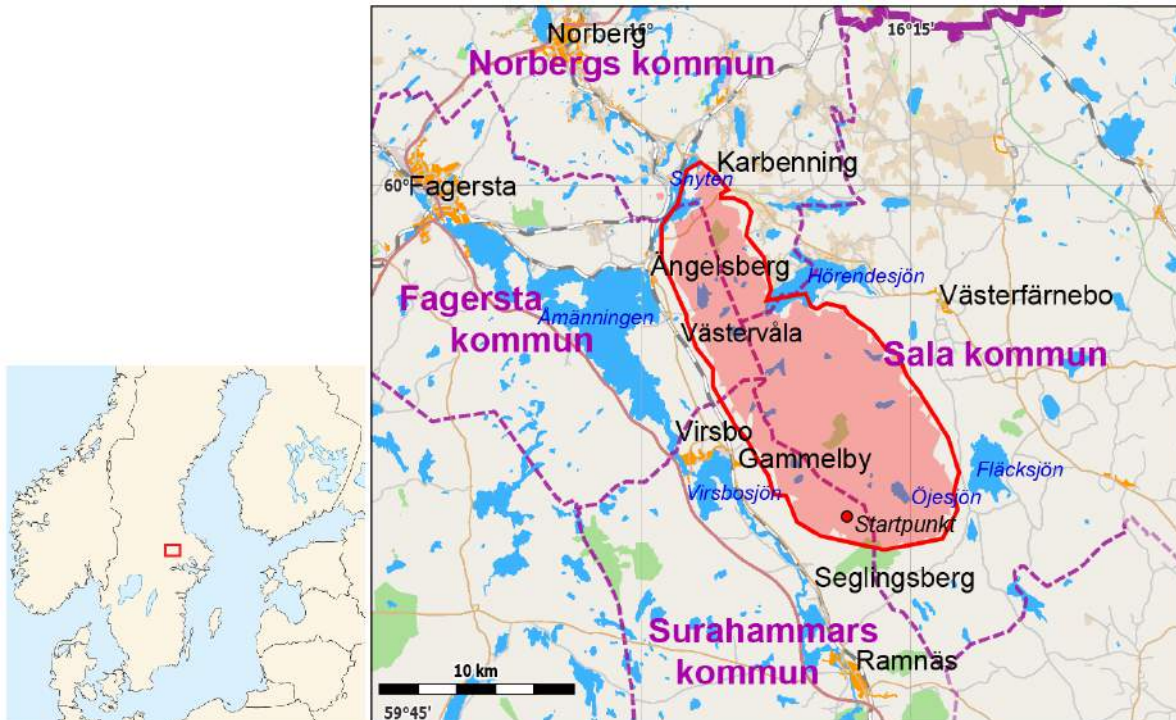


Figure 3.53. Location of the wildfire in Västmanland, Sweden (left) and the affected area on 13th August 2014 (right). The starting point of the fire is shown with a red circle ("Startpunkt") in the map on right (map taken from http://sv.wikipedia.org/wiki/Skogsbranden_i_Västmanland_2014)

3.11.1.1 Meteorological Description

Spring 2014 was exceptionally warm in Sweden and started approximately one month earlier than usual. Considering the whole country, it was the second or third warmest spring during the records (SMHI, 2014a). Especially March was very mild; monthly mean temperature exceeded the long-term average in places by over 5 degrees and the month became in many places record warm. Precipitation during spring was generally somewhat higher than on average.

SMHI (2014b) reported that June 2014 was more than one degree colder than on average in the Västmanland area. The rainfall amount was close to the long-term average. However, July 2014 in Sweden was very warm, in places even record-warm, and dry as well. In the Västmanland area July was over 3.5°C warmer than average, and the precipitation sum less than half of the average (**Error! Reference source not found.**). In the latter half of July, temperature exceeded 30°C on several days in Västmanland (SMHI, 2014c). Thus, the preceding very warm and dry conditions made the surroundings easily flammable. The fire was started by a spark from a forestry machine performing ground preparation in a logging area. During the emergency call it was estimated that 30 times 30 meters area was on fire. In the evening that day the fire area was 60 hectares. According to the forest fire danger maps produced by European Forest Fire Information System (EFFIS) at Joint Research Centre (JRC) the fire danger in large areas in southern and middle Sweden was considered "high" on 31 July (**Error! Reference source not found.**).

In the beginning of August, temperature rose even higher: on 4 August temperature peaked over 34°C in Västmanland. At the same time wind strengthened and the fire was rapidly spreading out during

that and the next day (SMHI, 2014d, e). Fire danger was still “high” in the area, even though not over as vast area as in the beginning of the fire (**Error! Reference source not found.**). Situation got better towards 6 August as the wind settled. It was considered that the fire was under control on 11 August but the post-fire extinguishing operations still took another month. Difficult terrain in the wooded area complicated the rescue operations.

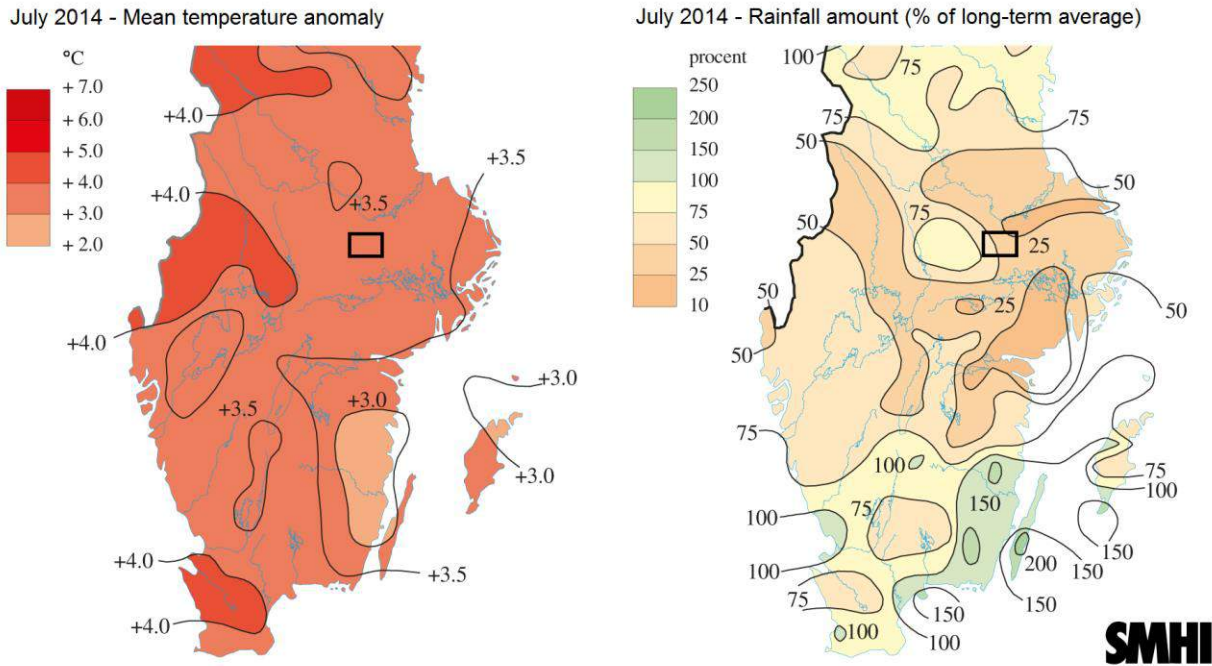


Figure 3.54. Anomalies of monthly mean temperature (°C) and precipitation sum (%) in southern part of Sweden in July 2014. The fire area is shown with the black square (SMHI 2014c).

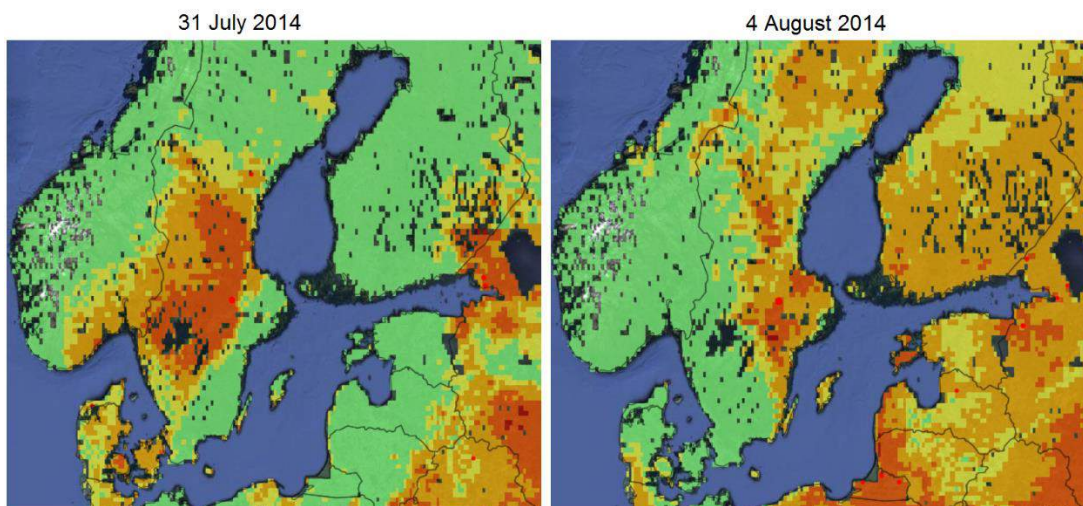


Figure 3.55. Fire danger forecasts for 31 July (left) and 4 August (right) 2014 by European Forest Fire Information System (EFFIS) at Joint Research Centre (JRC). Color codes for the fire danger level are: green=very low, yellow=low, orange=moderate, red=high, dark red=very high. The bright red dots are the so-called “hotspots”, i.e., active fires detected by remote sensing instruments. Also the Västmanland fire is labeled as one.

3.11.1.2 *Impacts to Critical Infrastructure*

Impacts to traffic and transport

Several roads in the area were partly or fully closed during the fire. All the road blocks were dissolved by 13 August, except one in the northern part of the fire area which held until 22 August. Traffic on railways was also disturbed as several rail sections were blocked having effects especially on supply of goods. The whole railway network was in use again on 20 August. Boat traffic in nearby lakes and canals was closed off for some days because of water intake for airborne firefighting. Even the airspace over the fire area was closed off from all the other aircrafts than those taking part in the extinction or surveillance operations.

Economic impacts

One sector having heavy consequences of the fire is the forest sector. First estimates made after the fire revealed that total of 13 800 hectares (138 km²) of forest was burned down or damaged. This would mean a reduction of the net value during logging by tens of millions of Euros. The largest forest owners in the fire area are AB Karl Hedin (5 000 ha), Bergvik Skog Väst AB (2 000 ha), Mellanskog from the Sveaskog koncern (1 500 ha), and Västerås diocese (1 000 ha). All timber that still has some value (in a form or another) will be salvaged from the fire area. It will require a significant contribution from the forest work sector and most probably there will be lack of suitable operators in the area. Large amount of the damaged timber left behind is fully suitable for energy production as fuel wood. This will count as oversupply to the markets, dump the prices and probably impair the position of the other fuel wood suppliers in the area (Danske Bank, 2014).

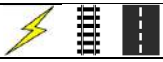
The Swedish state will pay (or have paid) compensation to the municipalities through the Swedish Civil Contingencies Agency according to a particular law concerning protection from a natural hazard. However, the municipalities have to take care for an excess, which has been estimated to range in the four directly affected municipalities between over 20 000 EUR in Norberg Municipality and around 80 000 EUR in Sala Municipality. Total costs of the direct rescue operations, the firefighting personnel and rescue helicopters being the largest expenses, have been estimated to be around 550 000 EUR per day. The Swedish state invested additional 32.5 million EUR for the Swedish Civil Contingencies Agency to be distributed further to the municipalities, 27 million EUR for direct firefighting, and 5.5 million EUR for surveillance and other rescue services.

3.11.1.3 *Conclusions*

As summers in the north are fairly short and typically moist, conflagrations occur only seldom. In addition, the efficient fire prevention, warning and suppression systems have helped to keep the wildfires small and under control, leading to only minor consequences. Keeping that in mind, the Västmanland fire 2014 is a significant case as it reminds us that these kinds of serious conflagrations are fully possible also in the northern Europe.

3.12 Coastal Flood

3.12.1 Storm surge with coastal flood, France, February 2010

Type of event	Coastal flood
Date	27–28 February 2010
Location	Vendée and Charente-Maritime departments, France
Total damage	€2.5 billion (official estimate, including windstorm damages)
Victims	41 flood-related fatalities
Affected critical infrastructure	
Type of damage to infrastructure	direct damage and destruction by floodwater and strong wind, cessation of services. Flood defences damaged.

Winter storm Xynthia passed through Europe between 27 February and 1 March 2010, causing many damages in the Western part of the continent. 59 fatalities were recorded, of which 47 in France. It was the biggest storm in that country since the Lothar and Martin storms in December 1999. Most of the fatalities and damage was associated with a storm surge that hit the western coast of France on the night of 28 February.

3.12.1.1 Meteorological and hydrological description

The storm developed in unusually low latitudes, near the Tropic of Cancer, off the coast of Madeira and the Canary Islands. It moved northeast reaching the Iberian Peninsula on the morning of 27 February. The storm caused heavy rainfall and strong winds affected northern Portugal and Spain before moving to the Bay of Biscay. It reached the coast of France around midnight on 28 February. The storm itself was not particularly strong: it reached a minimum air pressure of 969 hPa, with a 20 hPa drop in 24 hours (in 1999, the pressure dipped 32 hPa in 24 hours). Maximum speed of wind gusts (Figure 3.56) in the coastal zone was 161 km/h in Scillé, lower than in 1999 and 2009. Sustained wind speeds were 10 on the Beaufort wind speed scale (25–28 m/s). The storm moved through coastal departments of Vendée and Charente-Maritime to central France and then to Belgium, Germany, Netherlands, Denmark and finally Norway (Kolen et al. 2010, Meteo France 2010, Bertin et al. 2012, Maurer et al. 2012, Pineau-Guillou et al. 2012).

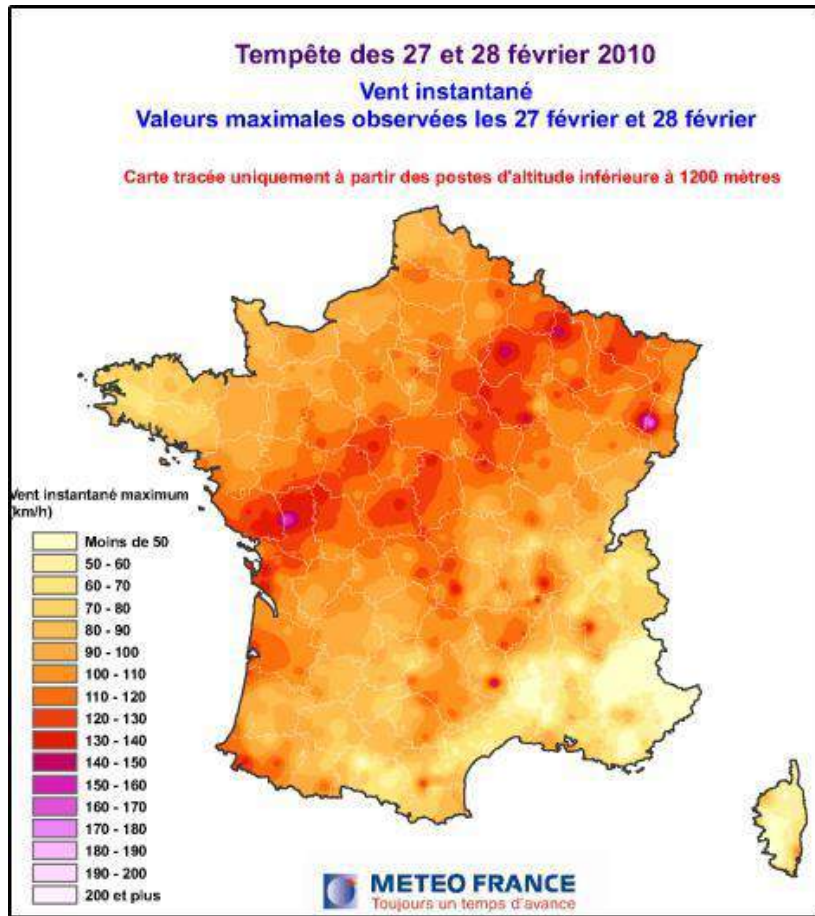


Figure 3.56. Maximum wind gust speeds during the Xynthia storm in km/h (Meteo France 2010).

The storm coincided with a high spring tide, causing water levels to rise steeply. Maximum levels were recorded between 2 and 3 a.m. on 28 February. The highest water surge (i.e. the measured water level minus the modelled tide height) was observed at La Pallice, the harbour of La Rochelle (station no. 4 in Figure 3.57). It reached 1.53 m, which is estimated to exceed a 100-year return period. In Saint-Nazaire (no. 2), which laid directly in the path of the storm, the surge peaked at 1.16 m, which corresponds to a 20–50 year return period. Further from the storm the surge was less severe, with a 10–20 year return period in Verdon (no. 5) and 5–10 year in Concarneau (no. 1). However, the total observed water level had much lower probability of occurrence because of the synchronisation of the surge with the tide. In stations no. 2, 3 and 4 in Figure 3.57, the return period of measured water levels was higher than 100 years, while in stations 5 and 6 it was about 20–50 years. It should be noted that during the events there was very little rainfall and river discharges were close to average, so they did not exacerbate the consequences. Additionally, exceptionally high water levels were also observed at some locations along the English Channel, particularly in Dieppe, but no flood was recorded there (Bertin et al. 2012, Pineau-Guillou et al. 2012, Breilh et al. 2013).

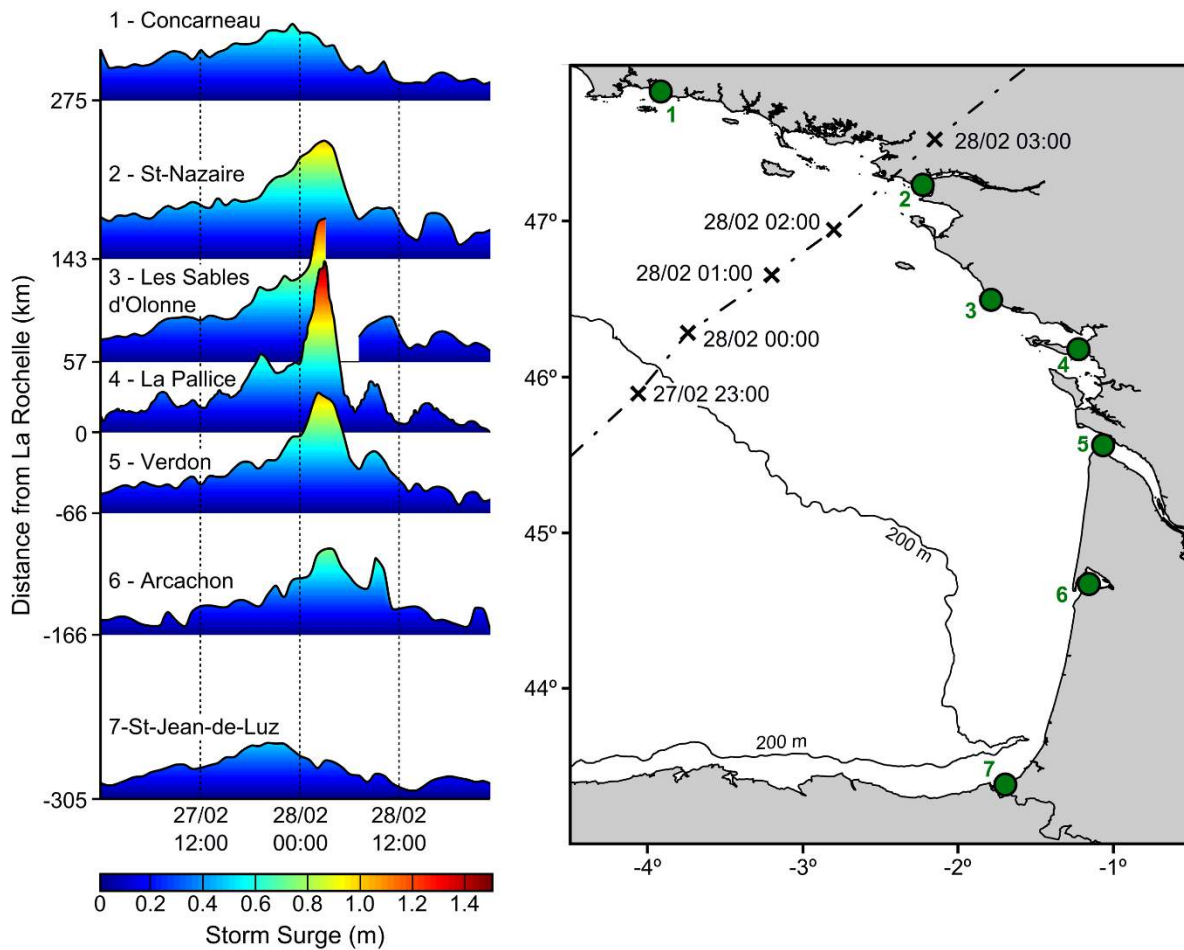


Figure 3.57. Water level anomalies (observed water levels minus the tide) at selected tide gauges along the coast (Bertin et al. 2012).

3.12.1.2 Impacts to Critical Infrastructure

Because of the surge 41 persons drowned, with further 2 persons killed by waves while camping on a pier in Loire-Atlantique department. 3 persons died because of the windstorm in the Pyrenees and another one in central France. 29 deaths occurred in Vendée department, all of them in la Faute-sur-Mer commune which had only 828 citizens in the beginning of 2010. The other 12 deaths were recorded in the Charente-Maritime department in six different communes around La Rochelle. 682 houses were destroyed completely, while 10 000 people had to be evacuated (Anziani 2010, Lumbroso and Vinet 2011, Vinet al. 2012, Kolen et al. 2013, Insee 2014). An official estimate put the value of flood- and wind-induced damages at €2.5 billion (Anziani 2010), while according to a more detailed study the insured losses totalled €1.48 billion (FFSA / GEMA 2011). The number of claims and their values are presented in

Table 3.3.

Table 3.3. Number of insurance claims and total value of claims in millions of € related to Xynthia storm. Source: FFSA / GEMA 2011.

Type of asset	Flood damages		Windstorm damages		Total	
	Number of claims	Value of claims	Number of claims	Value of claims	Number of claims	Value of claims
Houses	19 000	450	339 500	430	358 500	880
Cars	10 500	60	22 500	35	33 000	95
Businesses	5 500	235	73 000	270	78 500	505
Total	35 000	745	435 000	735	470 000	1 480

As can be noted from Table 2, the number of people affected by flood was much smaller than by windstorm, but the value of damages was almost the same, because the flood had bigger impacts on the assets it affected. Storm surge caused €745m of damages, including €470m in Charente-Maritime department and €195m in Vendée. Losses from windstorm added €85m and €50m, respectively (FFSA / GEMA 2011).

The critical infrastructure most severely affected by the storm surge was flood defences. They largely failed during the storm and vastly contributed to the death toll: 37 out of 41 victims lived in areas protected by flood defences. A significant part of the defences were merely coastal dunes, but in many locations dikes and seawalls failed as well. They were both overtopped and breached. The most significant was the breach of dunes near la Faute-sur-Mer, which resulted in a devastating flooding of the village (Fig. 5). In total, 120 out of 224 km of dikes required repair after the storm in Charente-Maritime department along with 75 out of 103 km of defences in Vendée. A strengthening of 120 km of dune coast and 45 km of rocky coast eroded during the storm was required. Along the English Channel, though no flooding inland occurred, the coastline defences were damaged: after-storm replenishments to dunes in Normandy alone cost €4m. In Gironde department, located south of Charente-Maritime, seven breaches of dikes were recorded (Anziani 2010, Vinet et al. 2012, Kolen et al. 2010, 2013).

Most of the French coastal flood defences, which total around 1 300 km were built in the 19th century. The owner responsible for its upkeep is frequently unknown. The design standard of the dikes is anticipated to provide protection only for events with a return period of less than 100 years. Moreover, the defences in the area in question were not fully repaired after the 1999 storm surges (Bersani et al. 2010, Kolen et al. 2010).

Many damages to roads were recorded, since many communal and even departmental roads are located atop of dunes and embankments. Those were eroded during the storm, destroying the roads (Figure 3.58). That includes several locations far from the main flooded zone, such as Moutiers-en-Retz, more than 100 km north, where dune erosion undercut a departmental road. Many roads were flooded cutting off affected villages. Several bridges had to be closed during the storm, restricting access to Ré and Oléron islands. All over the country, traffic disruptions occurred because of falling trees blocking the roads (Bersani et al. 2010, Pedreros et al. 2010, Maurer et al. 2012).



Figure 3.58. Damaged parking in La Rochelle (source: Wikipedia).

A railway from La Rochelle to Rochefort, which runs along the coast, was severely damaged because of the flood. 3 km of tracks had to be replaced, while the railway was unavailable for service for almost two months (until 23 April). Falling trees caused delays to traffic in many locations in the country, but particularly in the coastal zone. High wind speeds also caused cancellation or delays of hundreds of flights during the event. Damages were also recorded to harbours, especially in the old harbour in La Rochelle. Many small boats were destroyed in ports (Maurer et al. 2012, Kolen et al. 2013)

Power grids largely failed along the path of the storm due to high velocity of wind, with around one million people being without electricity on 28 February. This includes 320 000 people in two coastal regions affected by the flood. The power was brought to almost all customers within two days. The blackout is regarded as a contributing factor to the death toll: most of the one-storey houses in the flooded area had electric roller shutters, which could not be opened when the power was cut, trapping people inside the houses (Maurer et al. 2012, Vinet et al. 2012, Kolen et al. 2013).

Finally, large area of agricultural land was flooded: 45 000 ha in Charente-Maritime department and 11 000 ha in Vendée. Insurers received 1 700 claims totalling €26m, with additional €112m of claims resulting from wind damage. Agricultural land was affected by saltwater, reducing its productivity. Fishing boats and oyster farms were also severely damaged, especially on Île de Ré (FFSA / GEMA 2011, Maurer et al. 2012, Kolen et al. 2013).

3.12.1.3 Conclusions

The Xynthia storm resulted in many casualties, most of which can be linked to flood defence infrastructure failure, which were inadequately maintained. Road and rail infrastructure were all damaged, mainly because they were located on embankments and dunes which served as flood protection, but often failed to withstand storm surge water. Power grid failure, a result of the windstorm, contributed to a number of deaths.

4. Synthesis of stakeholder interviews and past cases

4.1 Stakeholder interviews

The RAIN project partners have carried out 25 interviews with stakeholders during October and November 2014, either in person or by telephone. The stakeholders we selected from the network of contacts of the RAIN partners contributing to the Hazard Identification Work Package. In addition to the 25 interviews, data was gathered from three additional stakeholders by distributing a questionnaire by e-mail. From here on, we mean to include those as well, when we refer to ‘interviews’.

The interviews were carried out with the aim to answer the following questions¹:

1. Which sectors of CI are impacted by extreme weather?
2. Which extreme weather phenomena impact which sectors?
3. What ways do these impacts take place exactly?
4. In what ways have operators presently prepared for extreme weather?

The majority (21) of 28 interviewed stakeholders (75%) were operators or managers of critical infrastructure, including road or railway management, electrical power or telecommunications. A further 7 stakeholders (25%) are involved in emergency management. Table 4.1 lists the interviewed organizations.

To carry out the interviews, the RAIN partners used a guideline for a semi-structured interview, which is listed Appendix B. This chapter presents the results per hazard type group. However, the first section starts out with a quantitative analysis of all interview responses and per infrastructure type.

<p>Railway management</p> <ul style="list-style-type: none"> • Croatian Railways • Irish Rail • Deutsche Bahn • ÖBB Infrastruktur AG (Austria) • Finrail Oy (Finland) 	<p>Road management</p> <ul style="list-style-type: none"> • Trafikverket (Sweden) • Norwegian Public Roads Administration • City of Helsinki, Public Works Department (Finland) • Centre for Economic Development, Transport and the Environment, Southeast Finland • Bundesamt für Straßenwesen, Federal Road Research Institute (Germany)
<p>Telecommunications</p> <ul style="list-style-type: none"> • Ericsson GSc (Romania, responsible for Europe) • KPN (Netherlands) • Elisa Corporation (Finland) 	<p>Electrical power</p> <ul style="list-style-type: none"> • Wien Energie GmbH (Austria) • Fingrid Oyj (Finland) • Vattenfall (Germany)

¹ The interview also included a sizeable number of questions relating to arrangements of stakeholders with weather services. The analyses of the responses to these questions are topic of a forthcoming RAIN report.

Multiple types of critical infrastructure	Emergency services
<ul style="list-style-type: none"> Department for Infrastructure and Environment (Netherlands): rail, road, aviation, shipping BVG (Berlin public transport company): metropolitan public transport Rijkswaterstaat West-Nederland Zuid, district Noord (Netherlands): roads, inland waterways, flood defences 	<ul style="list-style-type: none"> South Savo rescue service (Finland) Helsinki City Fire Department (Finland) National Police Board of Finland Rescue Service (Finland) Austrian Red Cross, Regional Association of Lower Austria Regional Association of Fire Brigades in Lower Austria FU Berlin on behalf of Berlin Fire Brigade (Germany)

Table 4.1. Stakeholders interviewed for the assessment of extreme weather impacts.

4.2 Impact of the various extreme weather phenomena

The stakeholders have been asked which types of extreme weather affects the type critical infrastructure they manage. They were also asked to subjectively assess if failure of the CI to the extent extreme weather event could do so, would cause a high impact to society. The results of this query are summarized in Fig. 4.1.

The figure shows that **wind storms, heavy rainfall and river floods**, as well as **snow(-storms) and freezing precipitation** constitute the five phenomena that the stakeholders most often identified as affecting their CI. Each of these phenomena was judged to be a threat by more than 19 stakeholders (68 %). The list of the phenomena with a high impact to society is led by **river floods, snow (storms) and coastal floods**.

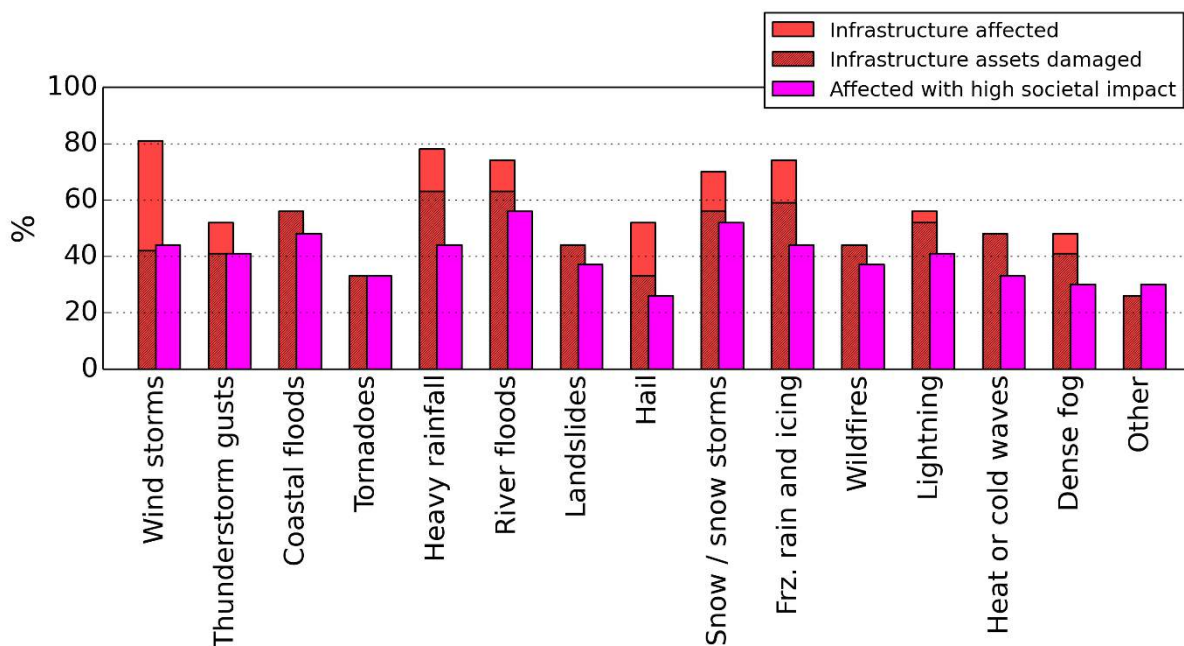


Figure 4.1.

The ratio between the two percentages enables us to differentiate between phenomena that (almost) always when they affect CI cause a great societal impact and those that do not. Any type of floods or tornadoes are judged to always have a great impact, whereas hail or wind storms may do not always cause a great societal impact when they harm CI.

An analysis of these results per CI sector shows which sectors are most vulnerable and to which (hydro-)meteorological phenomena. These results are summarized in Figure 4.2.

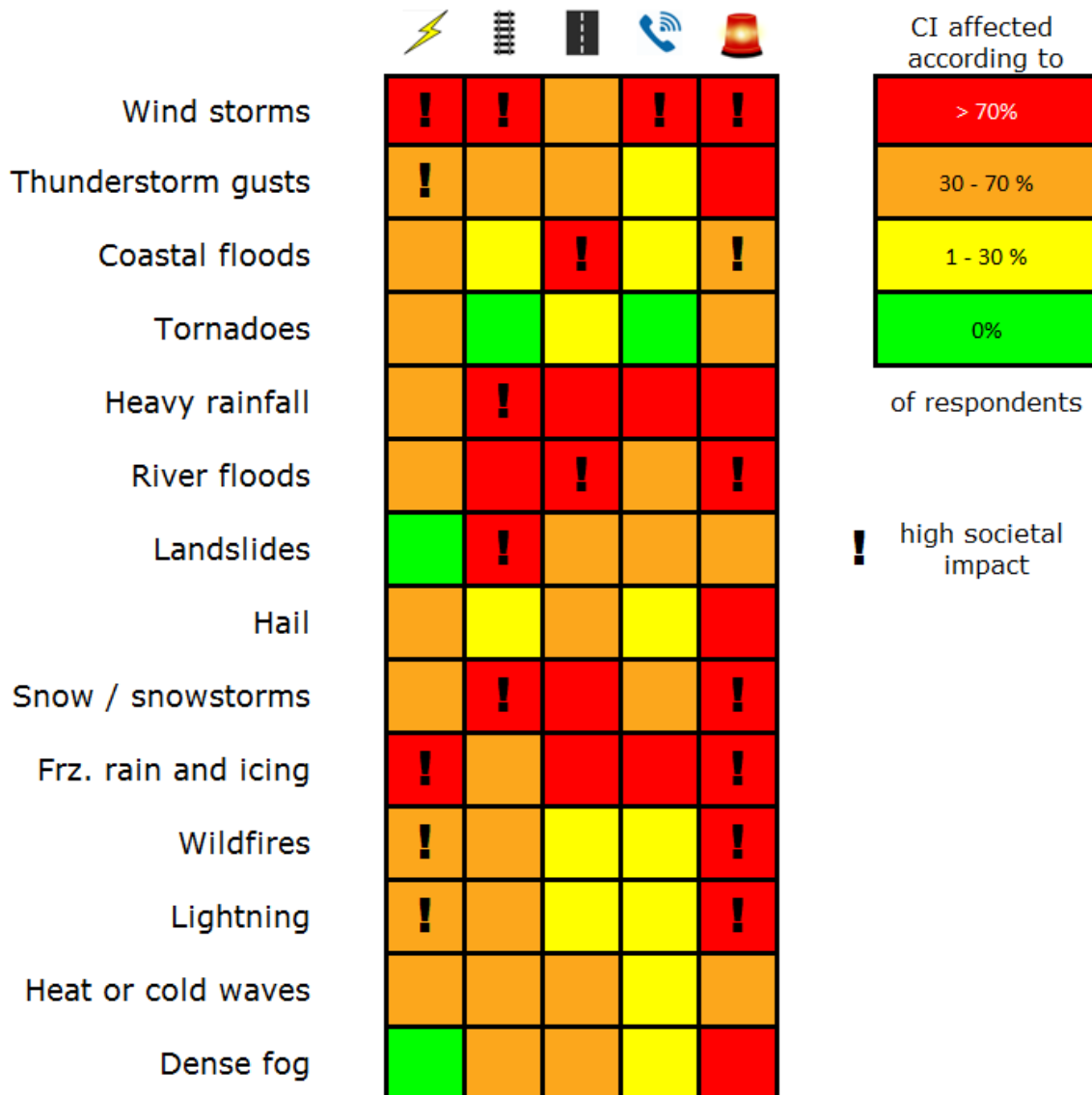


Figure 4.2. Matrix showing the fraction of interviewed stakeholders indicating that a particular sector

Electrical power delivery is affected by **freezing precipitation**, and by **windstorms**, according to all stakeholders from this sector. To a lesser extent heat or cold waves, wildfires, snowfall, heavy rain, floods, thunderstorm winds, tornadoes and hail were indicated as phenomena affecting power supply. Outages caused by freezing precipitation, by windstorms, wildfires, lightning or by thunderstorm gusts were judged to be capable of having a high societal impact.

Railways are vulnerable to many extreme weather hazards. According to the interviewed stakeholders, the most important phenomena are **landslides, snowfall, heavy rain, river floods, windstorms and lightning**. To a lesser extent, thunderstorm wind, wildfires, heat and cold waves and dense fog also affect rail transportation. Windstorms, heavy rainfall, landslides and snow (storms) were judged to potentially impact society to a great extent.

Like railways, roads are highly vulnerable to many of the extreme weather phenomena. Most important are **snowfall, freezing precipitation, heavy rain** (even without large-scale flooding), and **coastal and river floods**. However also windstorms, hail, thunderstorm winds, landslides, heat and cold spells as well as dense fog affect rail systems, according to 30 – 70 % of the interviewed stakeholders from this sector. The impacts of coastal and river floods were identified by most respondents of causing high societal impact.

Telecommunication systems are affected by **wind storms, heavy rainfall and freezing precipitation** according to the highest number of respondents from this sector. River floods, landslides and (snow storms) were also mentioned by an important (30-70%) share of those interviews. There was a great consensus that wind storms have a potential of causing great disruptions to telecommunication systems.

The stakeholder interviews were also held with emergency services and managers. This group was to a high degree (>70%) convinced that any of the hazards could affect or require emergency services. Only coastal floods, landslides, tornadoes and heat or cold waves were each mentioned by more than 30% of those interviewed. Coastal flooding was judged to potentially have a high societal impact.

4.3 Impact of wind storms

4.3.1 Affected sectors

26 out of 28 (93%) of the stakeholders state that the function of their infrastructure is somehow affected by windstorms. In the following the impacts of windstorms, the consequences of the resulting damages and preventive measures are summarized separately for the different types of infrastructure, as well as for emergency operators.

4.3.2 Impacts

The main damages of windstorms to the electricity sector are caused by trees, which fall on power lines after being blown down by extreme wind gusts. Usually, trees affect rather smaller regional power lines. Here it is difficult to keep the lines clean from vegetation during the growing periods, simply because of the large amount of line kilometres. These lines are especially endangered in autumn, when the trees still wear their leaves. The leaves on the trees increase the aerodynamic drag and thus increase the probability of wind damage. Shallow root trees are stronger affected than trees with taproots, because they are less stable. Major power lines are less threatened by falling trees. Here the main problem is the direct effect of extreme wind, which damages the lines. The impact increases if strong wind is combined with icing of the power lines. This can lead to “dancing” lines. The

lines can start oscillation, which may cause them to fall or to touch neighbouring lines causing them to short-circuit.

The consequences of failures within the grid are blackouts, which can affect large areas and high numbers of customers. If wind turbines are shut down, additional electricity needs to be purchased from other operators of neighbouring countries. Compensation payments for customers and repairs of the damages need to be covered and may cause additional costs.

Windstorms can cause trees to fall onto roads, which leads to disruptions of the traffic. The traffic on bridges, especially on motorways, is directly affected by strong winds, because speed reductions may become necessary. Like road transportation, train service can be affected by trees on the railways and by blackouts caused by the storm. Strong winds can also damage or destroy catenary wires.

The main impact of windstorms on telecommunication and data grids is caused by disruption of the power supply. Batteries or generators can provide power to important parts of the telecommunication infrastructure for a limited time period in case of blackouts. However, if the batteries are depleted, a loss of communication or connectivity is the consequence. In regions where telecommunication lines are over ground, they can be damaged by strong wind speeds.

Emergency operators are mostly affected by blocked roads due to fallen trees. In case of an emergency a delay of the rescue service is possible due to resulting traffic jams and a general increase in the needs for help due to the storm. Problems can occur with home nursing, because patients cannot be reached.

4.3.3 Preventive and response measures

Wind turbines need to be stopped if wind speeds are too high. This way, damage can be prevented, since wind power plants are designed stable enough to withstand high wind speeds. Power lines in endangered areas are disconnected from the grid. Additional power plants can be started which can provide additional resources, in order to compensate voltage drops due to disconnection of damaged part of the power grid. Fingrid Oyj uses shared IT-systems based on a commercial agreement and involve the weather service in case of an emergency management. Vattenfall also has a close contact to weather service. In Germany 4 regional load dispatch centres constantly monitor weather and weather warnings. They contact the German weather service if necessary.

In extreme cases roads need to be closed, in order to prevent accidents with cars, especially with trucks or trailers. In the Netherlands this is for example done by the Governmental Department for Infrastructure and Environment. Also in the Netherlands, Rijkswaterstaat performs maintenance and reconstruction of all damages directly after the event. Extra personnel is deployed for monitoring and traffic control in case of a windstorm event. They cooperate closely with the weather service. In Germany weather warnings are provided by the weather service to agencies in charge of highway maintenance. BaST also receives climate projections in order to create suitable building regulations for the construction of streets, bridges and tunnels. In Finland CETD also provides warnings for road users regarding strong winds.

In case of an approaching windstorm no technical measures are taken. Preventive measures are reduction of speed limits, closures of tracks and evacuations of stations. DB reduces speed limits to 80 km/h in case of a storm warning. They use an internal warning system which includes warnings from

the German weather service. DB is part of a program which investigates climate change, with the aim to take climate change into account when planning new infrastructure.

To be prepared for windstorms, Elisa Corporation has a real-time cooperation with weather forecast organisations. Additionally, phone warnings are delivered to clients before, during and after the event.

Many emergency services have developed pre-designed procedures to enhance preparedness, for example an increase of the standby personnel. In case of strong wind warnings, major public events may be cancelled. After windstorms the fire brigades (Berlin) are responsible for removing trees from the roads and to clear accidents. A shared IT-system (FEWIS) was developed in cooperation with the German weather service to provide customized weather warnings. FEWIS is operationally used by the fire brigades. In case of the Austrian Red Cross, weather warnings are distributed via central warning units in the individual provinces.

4.4 Impact of thunderstorm gusts

4.4.1 Affected sectors

Of the 26 of the critical infrastructure operators (93%) who stated that windstorms as affecting their operations and 16 (57%) stated that this also applies to thunderstorm-related gusts. The difference is can probably be explained by the fact that thunderstorm gusts or so-called convectively driven windstorms, are typically smaller areas. Furthermore, in some regions in Western Europe, thunderstorm gust often occur in concert with large-scale windstorms and the distinction is not made by CI operators. The intensity and impact of thunderstorm-related winds may be high wherever they occur.

4.4.2 Impacts

A reason for the relatively high impact of thunderstorm-related winds is their occurrence during the warm half of the year, when deciduous forests have leaves and are more susceptible to the wind damage than in the cool season in which most other windstorms occur. Type of impacts are very similar to that of other windstorms, and are typically rails and roads blocked by trees, such as in the 2014 Northrhine-Westphalia case described in Section 3.5.1. These trees and large branches that are also responsible to most damage to power lines. In some cases, wind itself may bring down the power lines, even including the high tension power lines, as was the case of 1 March 2008 (Pistotnik et al, 2014). As many thousands of households may be left without electricity as a result, the risk for a high societal impact exists.

4.4.3 Preventive and response measures

No particular responses or preventive measures for thunderstorm-related wind gusts were mentioned by those interviewed, besides arrangements with weather services for providing tailored warnings, which 19 of 28 (68%) of stakeholders have made.

4.5 Impact of heavy precipitation and consequential phenomena

One has to distinguish between the direct effects of heavy precipitation and secondary effects such as river floods (see Section 0), landslides and mudslides, which can be caused by precipitation.

4.5.1 Affected sectors

All interviewed stakeholders except one energy company and one telecommunication company (i.e. 26 out of 28; 93%) state that they are in some way affected by severe precipitation or its consequences (flooding, mudslides). The telecommunications company claiming not to be affected is one that claims to be resilient to all forms of extreme weather, in the sense that their system has a high level of redundancy and, at worst, impacts are local.

Heavy precipitation especially affects road, rail and emergency services. In the Netherlands, the risk of river flooding is seen as the most essential problem, while land and mudslides do not play an important role. Thresholds relevant for the stakeholders begin at 20mm/hour. Below that level, only minor effects or a risk for aquaplaning is expected.

4.5.2 Impacts

The following consequences of heavy precipitation were mentioned by the infrastructure operators:

Heavy precipitation

- Extreme local precipitation can cause dysfunctions in transmission substations.
- Heavy precipitation can erode streets.
- Erosion on rail embankments
- Tunnels can be flooded
- Streets and highways can be flooded
- Railroads can be flooded
- Risk of aquaplaning

River Flooding

- Erosion on bridges crossing rivers
- Debris can lead to damages of pillars of bridges over rivers
- Flooding of streets
- Flooding of railroads

Landslide/Mudslides

- Streets can be blocked and damaged
- Railroads can be blocked and damaged

4.5.3 Preventive and response measures

Drainage systems for railroads, roads, tunnels and motorways are in place. They are inspected on a regular basis. Additional inspection may take place if a warning for heavy precipitation is issued. To prepare for the challenges associated with climate change, research is conducted to determine which design for drainage systems will be adequate in the future.

4.6 Impact of river floods

4.6.1 Affected sectors

River floods were considered a relevant hazard by 23 out of 28 (82%) of the interviewed stakeholders. This source of hazard can affect all analysed sectors – road, rail, power grids, telecommunications, emergency services and flood defences.

4.6.2 Impacts

Roads and railways are particularly vulnerable, according to stakeholders. Flooding of those assets can cause surface damage, erosion and instability of slopes and stop the flow of traffic on them. Pillars of bridges could be damaged by debris in the water during a flood. Damage can occur also to power grid substations and flood defence structures.

4.6.3 Preventive and response measures

A majority of stakeholders (19 of 28; 68%) have made some sort of arrangement with weather services. Nine of them receive forecasts of river floods, usually with a forecast duration of 2 days or more. The stakeholders that did not have special arrangements with weather services used publicly available forecasts and warnings. Most of the stakeholders have developed emergency plans. These include measures such as deployment of temporary flood defences, additional personnel, evacuations, dispatch of warnings, closure of roads and railways, use of backup power generators, and cooperation with emergency services. According to the stakeholders, prevention is mostly done by a proper design of infrastructure, which takes into account the flood probability of occurrence and intensity, as well as climate change. Other methods mentioned include installing an independent secondary power supply.

4.6.4 Conclusions

The stakeholders mostly mentioned flood damage to roads and railways. Experience from past cases show that this is the infrastructure particularly vulnerable in terms of both direct and indirect damage. Even if a flooded road/railway did not require much repair after a flood, the disruption of traffic caused by incapacitation of those assets was often substantial. Power grids are more resilient and very little damage can be expected to telecommunication systems.

4.7 Coastal floods

4.7.1 Affected sectors

Coastal floods were considered a relevant hazard by 16 out of 28 (57%) of interviewed stakeholders. The difference in numbers compared to river floods is mainly due to the fact that four interviewees were from Austria, which is landlocked. Stakeholders representing all analysed sectors – road, rail, power grids, telecommunications, emergency services and flood defences – mentioned this hazard.

4.7.2 Impacts

The stakeholders did not mention specific impacts of coastal floods, but they would be mostly similar to river floods, causing damage mainly to roads and railways, as well as various coastal protection infrastructure.

4.7.3 Preventive and response measures

A total of seven stakeholders have arranged the delivery of coastal flood forecasts. All but one receive at least a 2-day forecast. Other preventive or response measures were not mentioned specifically, but are likely to be similar to river floods.

4.7.4 Conclusions

Experiences from past events show that coastal floods with a potential to cause damage to infrastructure are less frequent than river floods. Flood defences are mostly affected, while roads and railways located very near the coast can also sustain substantial damage. Power grids and telecommunications are usually outside the extent of coastal floods, though storm surges typically occur together with windstorms, which incapacitate power grids leading to power outages also in flooded areas.

4.8 Impact of hail

4.8.1 Affected sectors

No fewer than 15 of 28 interviewed (54%) considered hail to have an impact on infrastructure, including two out of three electrical power companies and three out of seven road management companies.

4.8.2 Impacts

The impacts of hail include the destruction of photovoltaic systems by large stones, which is a problem for power companies. In addition, large hail may destroy railway electrical systems. Hail of all sizes causes a reduction of road traffic safety, and thereby road capacity. Regardless of hailstone size, large amounts of hail can block drainage systems and thereby aggravate flash flooding, an example of which is given in Section 3.7.1.

4.8.3 Preventive and response measures

No specific measures besides arrangements for weather services were mentioned.

4.9 Impact of snow (storms) and freezing precipitation

4.9.1 Affected sectors

Altogether 23 respondents (79.3%) considered snow and snowstorms as a relevant severe weather event, 23 (79.3%) respondents considered freezing rain and 14 (48.2%) cold and heat waves as relevant weather events.

4.9.2 Impacts

According to the respondents, the above mentioned severe winter events may impact all the critical infrastructure types considered here, including rail, road, energy transmission infrastructure, telecommunication and data grid, emergency management. Respondents from all the countries referred to damages on the above mentioned infrastructure types, however the effect of those varies.

Heavy snow and freezing rain may severely impact road, rail and air transportation: roads and rail tracks could be temporarily closed, the rate of road accidents may increase, delays and cancellations are expected. In addition, in order to maintain road usability, snow removal logistics needs to be considered, snow removal tools (snow ploughs, snow pushers) may also lead to some damages in road surfaces. Snow loading and accumulated ice on power lines or trees may cause failure and power outages. The list of the impacted infrastructure and the level of the damage are given in the table below.

Table 4.2. Types of impact on various sectors Intensity thresholds for wintry extreme weather suggested by stakeholders.

Type of infrastructure/services	Snow or snowstorm			Freezing rain			Cold or heat waves		
	Assets/part of infrastructure	Failure with high impact on society	Function	Assets/part of infrastructure	Failure with high impact on society	Function	Assets/part of infrastructure	Failure with high impact on society	Function
Road	*	*	*	*	*	*	*	*	*
Railways	*	*	*	*	*	*	*	*	*
Power transmission		*	*	*	*	*	*		*
Telecom and data grids	*	*		*	*	*	*		*
Emergency and Rescue	*	*	*	*	*	*	*	*	*
Number of respondents	10	10	18	11	7	18	8	3	11

4.9.3 Thresholds

17 respondents indicated the intensity of the snowfall and 12 respondents gave the intensity of freezing rain and low temperature with severe consequences. The responses range on a large scale even for the same type of infrastructure. The thresholds given by the respondents are listed in the table below.

Table 4.3. Intensity thresholds for wintry extreme weather suggested by interviewed stakeholders.

	Fresh snow on ground (cm/h)	Freezing rain (mm/h)	Freezing rain-total accumulation (mm)	Cold (°C)
Flow and road	40 cm/day 20 cm/day 5 cm/h 30 cm/d 10-20 cm/day an increase in snow depth of 35 cm in 14 days or 30 cm in 7 days provided that the snow depth is already originally >35 cm	5mm/h 20 mm/h 0.5 mm/h any amount	1 mm 5 mm 20 mm	-30 °C or -35 °C for longer periods in Finland
Rail	10 cm/h, 25 cm/day, 80 cm/day in Alpine area 30 cm/d 80 cm accumulated below 250m ASL	20 mm/h	20 mm	-20 °C -25 °C -10 °C -30 or -35 for longer periods in Finland
Power transmission	30 cm/d	20 mm/h	20 mm	-30 °C or -35 °C for longer periods in Finland
Telecom and data grids	100 cm/day	1 mm/h	1 mm 10 mm	
Emergency and Rescue	30 cm/d 20 cm/d	20 mm/h	20 mm	-30 °C or -35 °C for longer periods in Finland

4.9.4 Preventive and response measures

Regarding the preventive measures implemented, all the respondents have arrangements with weather services for providing warnings for all kind of extreme weather situations. Some of the respondents are using the publicly available warnings; others receive direct early warnings based on agreements about the information needed. About 85% of the respondents provided information about emergency plans in case of severe weather warnings. This includes in most of the cases protocols and pre-designed procedures, cooperation with local emergency authorities to ensure the preparedness, and action plans for the warned event, e.g. action plan for exceptional snow situation, heavy snow accumulation on roads, control of rail switch heaters prior to cold spells, warnings for speed reduction.

The measures implemented for winter severe phenomena, i.e. snow storms, freezing precipitation varies along the respondents. In fact, only few of the respondents mentioned any measures taken for winter events, mainly road, rail, aviation and water transportation infrastructure, and energy transmission infrastructure are enhanced. The measures taken include improved winter maintenance on roads, warnings for road users, priority for snow clearance from roads, reduction or closure of rail services, de-icing of aircrafts, ice-breaking on waterways varying according to the severity of icing, power lines are taken of the grid in case of icing or snow load or are run at overload to melt the accumulated freezing rain. Respondents desire for improved road weather models and forecasts, including higher scale and temporal resolution, as well as better monitored infrastructure.

4.9.5 Conclusions

The analysis of the interview responses confirms the significance of severe winter events and their consequences on critical infrastructure. Based on the responses given snow and snowstorms are the most relevant winter events, which is partly due to the higher frequency of snow events compared to the rest of winter events but also to the heavy disruption that snow might cause for example in transportation. However, at some point it was difficult to provide a hazard specific analysis, as it was difficult to separate to which hazard the questions/answers are related. Regarding the intensity of events that might lead to significant consequences in critical infrastructure, the thresholds provided by the respondents ranged on large scale even for the same infrastructure type and geographical area. Some of the thresholds fall in with those defined by us in earlier studied, while some of them require further revision. As for the extreme winter weather cases occurred during the past 25 years, it appears that only very few of the cases are precisely recalled, mostly only the hazard type is remembered without data and location that leads to the conclusion that most of the operators do not keep a track of past extreme event.

4.10 Impact of wildfires

4.10.1 Affected sectors

Altogether 12 respondents (43% of all respondents) consider wildfires a relevant weather phenomenon affecting CI. 6 of these respondents are emergency managers. In addition, two out of four railway companies remarked the function of their system, i.e. the rail traffic, must be halted in case of wildfires. One out of seven road managers and one out of four telecommunication providers also mentioned that their systems are affected. The respondents who stated this are spread throughout Europe.

4.10.2 Impacts

For the given options, the respondents indicated that the impacts fall most typically upon train and road traffic (7-8 respondents out of 12). Impacts on emergency management were considered notable by 7 respondents and impacts on power transmission was chosen by 6 respondents. Three respondents considered impacts on information flow important. Other impacts mentioned outside the fixed options were impacts on health care systems.

In more detail, wildfires on rail and road embankments can lead to disruptions in traffic flow. Tracks and roads may be temporarily closed preventing or complicating the traffic. Possible road blocks may, e.g., prevent or delay the operation of home care (home nursing and catering for aged and disabled) and daily needs of groceries and transportation of citizens. Even curfews are possible. Public and private property, such as buildings, houses and other constructions, and vehicles, may be destroyed or damaged in a fire. In case of a conflagration massive evacuations might be needed and masses of people can be injured (mainly traumas). Telecommunication system failures may cause delays for officials, such as delays on forwarding fire alarms to fire departments. Lack of mobile phone communication systems may cause delays for emergency calls of fires.

The only respondent giving intensity for an event that might lead to severe consequences was South Savo Rescue Service (FIN) (which, however, did not identify wildfires as relevant weather event in question 8, and is therefore not mentioned in the table above). According to them high flammability together with fire index over 5 would be considered as this kind of case. The fire index they are referring to most probably is the Finnish Forest Fire Index (ranges from 1 (very low) to 6 (very high)).

4.10.3 Preventive and response measures

Most respondents already have agreements or other arrangements with national weather services to obtain weather forecasts and relevant warnings. There are also warning systems for rescue officials and other operators. Pre-designed procedures to enhance preparedness and to ensure communications have been made. Emergency plans for warning cases are also common.

However, the respondents wish for better quantitative forecasts (especially of precipitation), earlier forecasts and warnings, and improved accuracy and timing of forecasts. They also desire better knowledge, plans and more training on dangerous weather events. More knowledge about the impacts of the dangerous weather events to daily life and infrastructure are needed.

Dedicated forecasts were the most common essential framework arrangement made with weather services that was mentioned by the respondents. Also memorandums of understanding, detailed working procedures and involvement of weather services in emergency management were general arrangements. Contracts and shared IT-systems were more uncommon. All agreements are non-commercial. Information exchange is done by telephone, IT-systems, email, telefax, and webpages.

4.10.4 Conclusions

Wildfires were only discussed briefly in the interviews. This can be interpreted as a sign of the low relevance of wildfires as a dangerous weather event; i.e., wildfires have traditionally not posed a major threat for the critical infrastructure. When occurring, the main consequences of wildfires are falling upon traffic, public and private property, and daily life of citizens. The analysis of the documented responses to the interviews was not straightforward. The compilation of this summary became therefore somewhat subjective.

4.11 Impact of tornadoes

4.11.1 Affected sectors

Tornadoes are, compared to the convective windstorms, less frequent and a probability of one occurring at one particular location is very small. This fact was reflected in the interviews – only 9 of the interviewees (32%) identified tornadoes as a factor potentially affecting critical infrastructure.

4.11.2 Impacts

Tornadoes were mentioned by the stakeholders only once in the context of the destruction of wind turbines. Most of the tornadoes are weak and their effect is similar to that of ordinary windstorms as

described above. In case of strong (F2 – F3) tornadoes, local severe damage can occur to power lines. The past case in Section 3.6.1 describes a case of a tornado impacting a road. The impact of tornadoes can be bigger in the low probability scenario of it hitting a facility handling chemical or radioactive goods (e.g. a nuclear power plant), which could have a large impact on surrounding critical infrastructure. Otherwise, the small size of tornadoes limits their overall impact.

4.11.3 Preventive and response measures

No specific measures were mentioned, besides the delivery of user-tailored forecasts by weather services.

4.12 Impact of lightning

4.12.1 Affected sectors

Lightning was considered a hazard to the critical infrastructure by 16 of 28 interviewees (57%). Lightning was mostly seen as a risk to the electrical systems and especially the railway (4 out of 5) and telecommunication (3 out of 4) operators indicate to be affected by this phenomenon.

4.12.2 Impacts

An indirect lightning strike may result in an overvoltage in the electrical circuits, disrupting the correct functioning. Furthermore, direct lightning strike can cause unrepairable damage to the many electrical systems deployed in the railway system. In case that signaling system (or the switch controlling system) fails, traffic may be severely disrupted as trains can proceed only at very low speeds, if at all. Telecommunication infrastructure is vulnerable to lightning strikes as well. The most important sections of power grids are, however, well-protected. Lightning is of relatively low relevance to road management.

4.12.3 Preventive and response measures

Many systems sensitive to lightning strikes have installed measures to prevent serious consequences when lightning strikes close to their systems. A railway operator indicates that it is impossible to fully ruled out that that electric installations be damaged or railway control centres can be out of order. Very high protection measures against lightning have been installed against them affecting the systems controlling storm surge barriers, where a malfunction could have high impacts. However, since lightning accompanies every thunderstorm, damage may occur even with relatively weak thunderstorms, which are not usually warned for.

5. Method Development for the detection of Extreme Weather Impact

5.1 Physical and statistical flood risk analysis methods

5.1.1 Introduction

This section describes briefly the possible methods to be used by TU Delft in WP2 of the RAIN project. The concept is to combine physical and statistical methods of river and coastal flooding analysis, so they could be used in a Monte Carlo analysis. The main sources of uncertainty will come from extreme weather events. These will be characterized through multivariate probability distributions that may be inferred from data or/and structured expert judgments. The document thus describes both, the range of possible physical models to use and the probabilistic techniques available for construction of multivariate probability distributions.

5.1.2 Physical methods

5.1.2.1 *Geographical Information Systems*

Geographical Information Systems (GIS) are commonly used in flood analyses. Unfortunately, for simulating hypothetical (probable) floods, their accuracy is limited, because they merely observe spatial relations between data. They can only represent a 'static' flooding, without taking into account the dynamics of the events. However, because this approach is much less computationally demanding, it can be applied on a much larger scale. They could also be used when data is scarce; for example, only marginal probability distributions are used, while information on bathymetry or type of soil is not needed. The quality of the results mainly depends on the resolution of digital elevation models (DEMs) used in such analyses. A few most important GIS methods are outlined below.

5.1.2.2 *Methods for calculating flood zones in coastal areas*

'Bathtub fill' method

This is the method usually applied when hazards posed by storm surges is assessed. It is a simple cut-off of a DEM at a certain elevation, which is a representation of a water level during storm surge of a given probability of occurrence (Figure 5.1). This may turn out to be an oversimplification of coastal floods, since the extent of inundation is largely dependent on the duration of the storm. Wave overtopping of dunes and other coastal structures also contributes to the flood. However, for smaller floodplains not protected by higher ground (dunes, dikes etc.), it is relatively accurate. Variations of the method use different assumptions of connectivity (i.e. the possibility for water to move between raster cells) with the source of flooding. GIS tools disregard connectivity at all, but with further work areas not connected (using 4 or 8 neighbouring raster cells) can be cleared out from the analysis, which is the desirable approach (Bates and De Roo 2000, Breilh et al. 2013, Poulter and Halpin 2008).

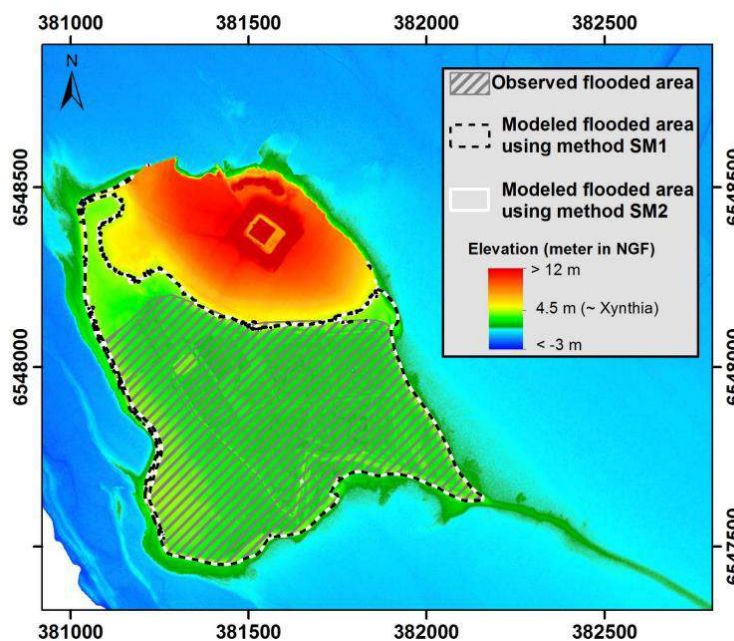


Figure 5.1. Example of a 'bathtub fill' approach (at different assumed water levels, SM1 and SM2) used in a case study in France (Breilh et al. 2013).

Surge overflowing method

This is a semi-dynamic method proposed to improve the accuracy of 'bathtub fill' simulations. By using the rectangular weir discharge equation it is possible to estimate the amount of water flowing over a dike or similar structure, under the condition that temporal data on water levels are known. The total volume of water estimated to have flown over the structure during an event can be then spread over a floodplain using GIS tools (Breilh et al. 2013).

5.1.2.3 *Methods for calculating flood zones in rivers*

Linear interpolation

This is the simplest method of reconstructing river floodplains. As with the previously described methods, two kinds of data are required: water levels at gauge stations and a DEM. Water levels of a certain probability of occurrence are interpolated between gauge stations (or, on occasion, extrapolated) in order to obtain them for the entire river under consideration. This level is intersected, perpendicularly to the river, with a DEM, creating a floodplain. The quality of this method is low, but easy to apply on a very large scale (Apel et al. 2009). However, no measurements are available on many smaller rivers, hence it is not applicable everywhere.

Regression

In order to overcome the problem of lack of data for many river catchments, the Norwegian Water Resources and Energy Directorate used an indirect method in their preliminary risk assessment. It is based on a regression between the catchment area, derived from GIS data, and water levels of certain probability of occurrence at different gauge stations. Since the relation between the two is not strong enough to allow a direct application of a regression line, a function was created that covers 98% of cases (Figure 5.2) This function was applied to all rivers and streams and the resulting water levels

were intersected, via buffering, with a DEM covering the whole country. The main drawback of this method is that it often severely overestimates the risk (NVE 2011).

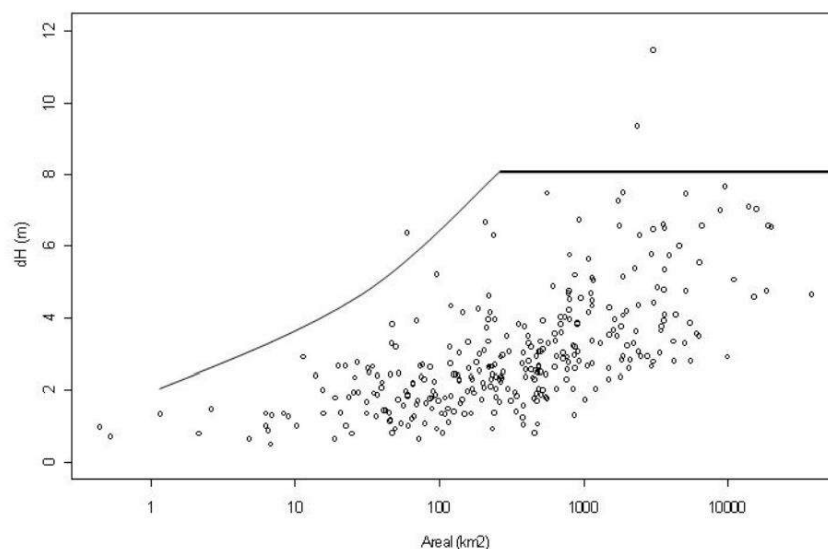


Figure 5.2. Relation between catchment area and water levels in Norway and the function (solid line) used for preliminary flood risk assessment (NVE 2011).

5.1.2.4 Hydraulic models

Hydraulic models are a more robust and accurate method than GIS, though requiring more types of data and computational power. They are applicable only for small-scale research and detailed calibration and validation of the results is expected. Many variations of them exist; they can be one-, two- or three-dimensional and use linear or non-linear flow equations. Calibration and validation is typically carried out by comparing the modelled water levels and extent of flood with gauge station records and aerial/satellite images taken during a flood event (Bates and De Roo 2000, Freer et al. 2013).

1D model

A one-dimensional (1D) model represents the rivers and channels as a linear object, therefore allowing movements of water along a single dimension. The dimensions of the river bed and surrounding floodplain are defined in cross-sections at certain points along the modelled river. The method utilizes de Saint-Venant non-linear differential equation to calculate discharges in a longitudinal profile at nodes. A 1D model is typically easy to set up and calibrate, does not require much data (bathymetry and topography is only given in cross-sections) and is accurate in calculating flows in the river bed. It is possible to calculate both dynamic and static ('steady state') floods using 1D models, providing as input ('boundary condition') water levels or discharges. However, the accuracy for calculating actual flooding is much lower and it is not applicable for areas of complex topography or coastal floods. 1D models are implemented in several packages, including American HEC-RAS, Dutch SOBEK 1D and Danish MIKE 11 (Ervin and MacLeod 1999, Horritt and Bates 2002, Hunter et al. 2007, Sobey 2001).

2D model

A two-dimensional (2D) model is an extension of 1D models allowing flows in perpendicular directions. The calculations are made utilizing a computational grid or mesh and can be rectangular, triangular or curvilinear with changing resolution. The mathematical core of these models is usually comprised of a 2D derivative of de Saint-Venant equations (variant known as ‘shallow water equations’), which provide depth-averaged flows of water. It allows the calculation of flood extents with higher accuracy, especially in areas of complicated topography and when detailed information on flow directions and velocities is needed. However, it is not possible to calculate accurately flows in small rivers within a reasonable resolution of a 2D model, unless a flexible mesh is supported by the software used. In effect, 2D models are mainly used for coastal areas. Examples of 2D implementations include SOBEK and Delft3D packages, MIKE21 or French TELEMAC (Bates and De Roo 2000, Horritt and Bates 2002, Hunter et al. 2007, Kim et al. 2014).

1D/2D model

1D and 2D models have certain drawbacks when it comes to simulating river floods, hence a hybrid model is often applied. Here, rivers are modelled as a 1D network, while the surrounding terrain is modelled in 2D. The two components exchange information between them at designated points (nodes), so when water levels in a river exceed a defined level, surplus water is sent to a 2D cell (Figure 5.3). Such a modelling option is available in SOBEK and MIKE FLOOD. It is typically the most efficient method of calculating river floods (Apel et al. 2009, KZGW 2010).

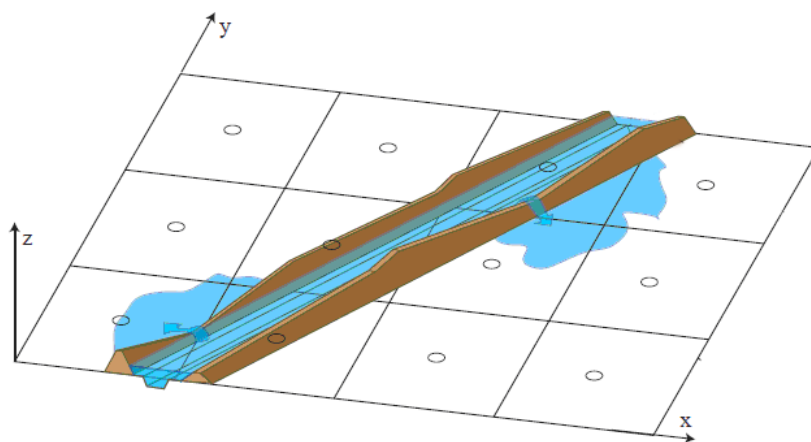


Figure 5.3. An example of a hybrid 1D/2D model (KZGW 2010).

Rainfall-runoff model

Rainfall-runoff (RR) models are a variant of the models presented above. Whereas the aforementioned models use hydrological data as boundary conditions, here rainfall is transformed inside the model into discharges. This approach is used mainly in mountainous areas threatened by flash floods, where there are typically no gauge stations, disastrous floods can appear even in the smallest creeks and knowledge of the event’s timeline is crucial for the analysis. Rainfall, flows and infiltration can be modelled for each 2D cell in some software packages (e.g., Delft3D) but it is very computationally demanding. In practice, a mixed 0D (zero-dimensional), 1D and 2D model is used (as implemented e.g., in SOBEK). A (sub-)catchment is simplified as a 0D node, which calculates the amount of water flowing into a stream based on, among others, rainfall, temperature, soil permeability, slope steepness and catchment area. Afterwards the simulation continues like in a standard 1D/2D model. RR models

require detailed data and are very case-sensitive, i.e. the results vary widely depending on constantly changing variables such as soil moisture or temperature, which have a minor impact on flood analysis for lowlands (Deltares 2014, Segond et al. 2007).

5.1.2.5 *Limit state functions*

In engineering, limit state functions are used to evaluate failure probability of structures and devices, including flood defences. The general equation is as follows:

Equation 5-1

$$Z = R - S$$

where R is the resistance of the structure in question and S is the load applied to it. The structure fails if $Z < 0$. Characteristics of both variables differ depending on what failure mechanism and structure is analysed (Naulin et al. 2012). Typically, both resistance and load are represented with a probability distribution since the former has a (sometimes considerable) degree of uncertainty, while the latter is a random variable conveniently represented as a probability distribution. As can be seen in Figure 5.4, failure occurs at the intersection of probabilities of load and resistance.

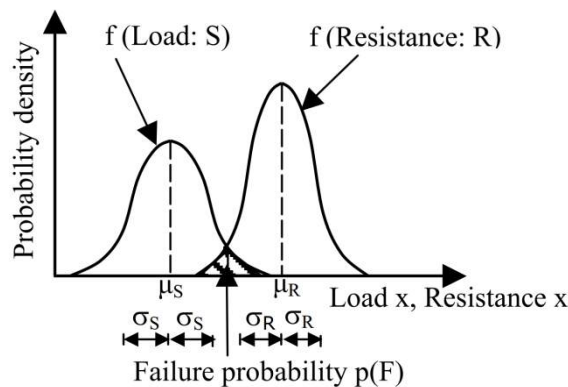


Figure 5.4. Failure probability as an outcome of load and resistance probability (Möllmann and Vermeer 2007)

Flood defences could fail due to a number of mechanisms, such as overtopping, piping, heave, seepage, erosion, instability etc. For some of them, several limit state functions have been developed. An example function for piping in a dike is as follows:

Equation 5-2

$$Z = L - m_c C(h - h_b - 0.3d)$$

where L is the piping length, C is erosion resistance, m_c is the model uncertainty factor associated with C , h is the water level (primary load), h_b is the landside water level and d is the thickness of aquitard at exit point. Parameters L , h_b and d could be measured and are deterministic or have a small uncertainty, whereas the erosion resistance is known only with a large uncertainty. Water level is probabilistic, therefore a failure probability can be obtained using a joint probability distribution (section 3.2/3.3) or by performing a Monte Carlo Simulation (see section 4) (Schweckendiek and Kanning 2009, Vorogushyn et al. 2009).

5.1.3 Statistical methods

5.1.3.1 Univariate probability distributions

A standard approach in flood research is to calculate the probability that an event (described by sea level, river discharge or rainfall) will exceed a certain value. Hydrological and meteorological events are usually assumed to be stationary random processes, thus following a certain probability distribution which does not change over time. In hydrology among the most commonly analysed distributions are Gumbel, gamma, lognormal and Weibull. Two-parameter Gumbel and Weibull distributions are part of the three-parameter generalised extreme value (GEV) distribution developed specifically for hydrological and meteorological research (Gumbel 1958). Figure 5.5 presents a comparison between observations (assigned to an empirical probability distribution) and its best approximation as a Gumbel distribution.

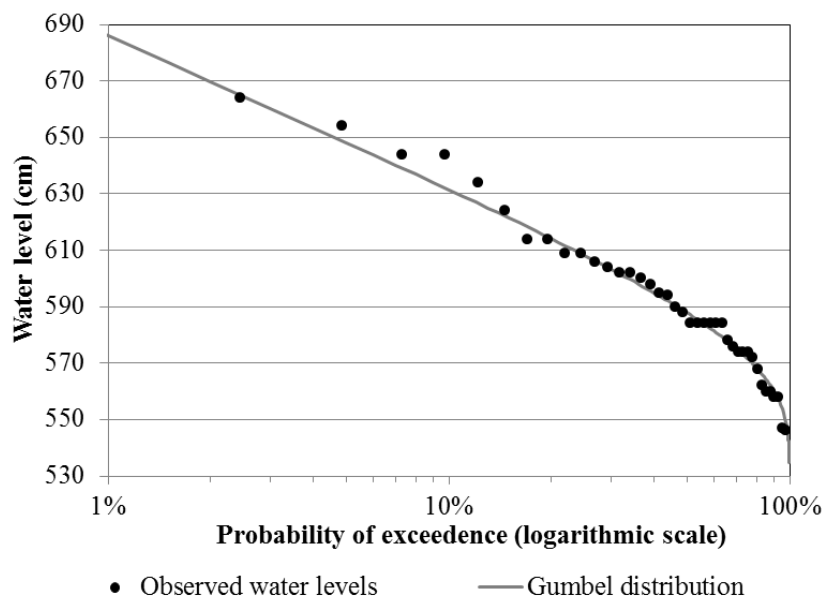


Figure 5.5. Empirical and theoretical (Gumbel) distribution of annual maximum water levels in Kołobrzeg (1901–1940). Adapted from Paprotny (2014).

Exceedance probabilities in flood research are usually considered in a yearly scale, therefore a 5% exceedance probability corresponds to an event that on average will exceed a certain value once in 20 years (alternatively called a 20-year return period). Probabilities of 1% and 0.5% are among the most commonly used in flood hazard mapping and designing flood defences (Table 5.1).

Variables such as annual maximum river discharges or sea levels can be represented as one of the several probability distributions. An example procedure for choosing a probability distribution for a certain one-dimensional data set is provided in appendix B (Anderson and Meerschaert 1998, Buishand 1989, Katz et al. 2002, Ozga-Zielińska et al. 1999).

Table 5.1. Examples of flood probabilities (per year) used in Europe.

Country	Probabilities used in flood hazard mapping	Probabilities used in flood defences design
Germany	1/20, 1/100, 1/300	
Italy	1/20–50, 1/100–200, 1/500	
Poland	1/10, 1/100, 1/500	1/10, 3/100, 1/50, 1/100, 1/200
Switzerland	1/30, 1/100, 1/300	
The Netherlands		1/250, 1/1250, 1/2000, 1/4000, 1/10000
United Kingdom	1/20, 1/100, 1/200, 1/1000	1/50–200

5.1.3.2 Bivariate and multivariate probability distributions

Bivariate probability distributions are an extension of the univariate sort described previously, which allows us to calculate a joint probability of two random variables. The simplest realisation is a bivariate normal distribution, though it does not fit well with meteorological and hydrological data analysed here. An example problem solved by bivariate probability distributions is the preparation of extreme weather scenarios, where the intensity of an event (rainfall or river discharge) is juxtaposed with the event’s duration. These variables have usually very asymmetric marginal distribution and used to be analysed by means of intensity-duration-frequency (IDF) nomograms. An alternative is to calculate the joint probability through copulas (Huibregtse et al. 2013, Schölzel and Friederich 2008).

Copulas are “multivariate distribution functions whose one-dimensional margins are uniform” (Nelsen 2006). They can have many shapes which depend mainly on the type of copula and the correlation between the variables. Spearman’s rank correlation coefficient can be used here, while the type of copula can be determined using for instance the Cramér-von Mises test. An important concept related with copulas is tail dependence: there can be upper or lower tail dependence, or no dependence at all. In Figure 5.6Figure 5.5 three different types of copulas are presented, with different tail dependences. Upper tail dependence can often be found in, for example, meteorological data, therefore Gumbel copula is usually suitable (Huibregtse et al. 2013, Schölzel and Friederich 2008).

Bivariate copulas can be extended into multivariate copulas, i.e. copulas combining three or more variables. An example application can be an analysis of relations between extreme water levels at several coastal tide gauges (Joe 2014).

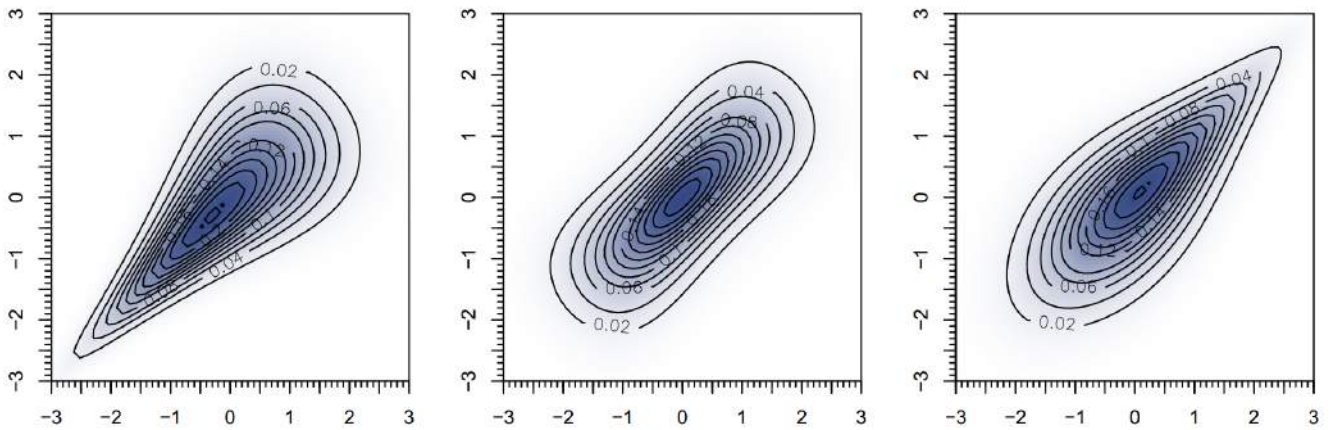


Figure 5.6. Probability density function for three example Archimedean copulas, Clayton (left, lower tail dependence), Frank (center, no tail dependence) and Gumbel (right, upper tail dependence) (Schölzel and Friederich 2008).

5.1.3.3 Monte Carlo simulation

Monte Carlo simulation is a method of combining probability distributions and physical models described previously. It generates a random value from given probability distribution(s) which can serve as input to a physical model. When this procedure is repeated an appropriate number of times, a probability distribution of the physical model’s result can be derived (Lemieux 2009). For instance, random data from a river discharge intensity and duration copula could be an input for limit state function analysis or flood risk analysis.

5.2 Windstorm impact identification methods

5.2.1 Introduction

Windstorms which are related to extra-tropical cyclones cause large amounts of damage within large areas of Europe in the winter seasons. In many studies extreme extra-tropical cyclones have been analyzed, both in the form of case studies as well as regarding their climatological characteristics (e.g. Pinto et al. 2007, Donat et al. 2010, Fink et al. 2009).

In order to objectively characterize the cyclone properties, different methods have been developed in order to identify the location of the cyclones and to track their movement in time and space within atmospheric model or reanalysis data, which were reviewed by Ulbrich et al. (2009). In many cases pressure fields or products derived thereof are used for the identification and tracking of cyclones (e.g. Murray and Simmonds 1991, Hoskins and Hodges, 2002).

Leckebusch et al. (2008) introduce a method, which is more impact oriented. Instead of focusing on the cyclone as a pressure system, the focus is on the wind field which is related to the cyclone and is responsible for the main damage caused by the storm systems. Basically, the method consists of two steps, first the identification and tracking of the extreme wind fields, and second the calculation of the intensity of the individual storm systems. The identification and tracking takes into account that damage (from an insurance perspective) occurs only, when a locally defined threshold wind speed is exceeded (Klawns and Ulbrich, 2003). This threshold is defined as the 98th percentile of the daily

maximum wind speeds and therefore depends on the local wind speed distribution. Thus, the approach reflects that the local infrastructure is already adapted to the existing wind climate. For each time step coherent areas of wind threshold exceedances are regarded as a wind cluster belonging to the same storm event. For each of those clusters the center of mass is calculated and regarded as the position of the wind field. The wind clusters are subsequently tracked in time by a nearest neighbor approach. Thus, the resulting tracks represent the temporal and spatial development of a storm.

A Storm Severity Index (SSI) is introduced, which is used to determine the intensity of each identified storm track (Leckebusch et al. 2008).

Equation 5-3

$$SSI = \sum_t^T \sum_k^K \left[\left(\max \left(0, \frac{v_{k,t}}{v_{perc,k}} - 1 \right) \right)^3 \times A_k \right]$$

t refers to the time, k refers to the grid boxes, v is the daily maximum wind speed and v_{perc} is the local percentile of the wind distribution used as the threshold. Thus the SSI is the sum of the normalized and cubed exceedances of the local 98th percentile of daily maximum wind speeds, weighted with the affected area A_k represented by the size of the individual grid boxes. The SSI is based on the assumption that (insured) damage usually occurs within the upper 2%-quantile of the local wind speed distribution (i.e. if the 98th percentile is exceeded). However, this includes major damages to critical infrastructure, as well as minor damages, which have no considerable impact on the society and economy. The aim of this work is to modify the SSI to include only the most extreme wind speeds relevant to critical infrastructure.

The regulations which determine the wind loads that critical infrastructure must be able to withstand are defined in structural design codes developed by the governments. Similar to the SSI-approach, these wind load thresholds depend on the local wind climate. Usually the 50-year return level of the wind speed is regarded as a suitable threshold. This wind speed return level corresponds to an occurrence probability of 0.02 per year and is much higher than the 98th percentile used for the standard SSI.

By combining the approach of using return levels of wind speeds and the tracking and identification of storm events via the 98th percentile of wind speeds we create a modified SSI which captures the intensity of the storm relevant for critical infrastructure. The tracking and identification of the storm event is conducted as in the standard approach by using clusters of coherent exceedances of the 98th percentile. However, for the subsequent calculation of the SSI we use the local 50-year return level of the wind speed v_{RL} .

Equation 5-4

$$SSI_{RL} = \sum_t^T \sum_k^K \left[\left(\max \left(0, \frac{v_{k,t}}{v_{RL,k}} - 1 \right) \right)^3 \times A_k \right]$$

The modified storm severity index SSI_{RL} thus represents the sum of the normalized and cubed exceedances of the local 50-year return-level of the wind speed distribution.

5.2.2 Estimation of return levels

The estimation of return level is based on the Fisher-Tipper theorem, which states that the distribution of maxima of samples of random variables can only converge to one of three possible distributions, namely the Gumbel distribution, the Fréchet distribution, or the Weibull distribution. Those three distribution families can be combined to the generalized extreme value (GEV) distribution

Equation 5-5

$$F(x; \mu; \sigma; \xi) = \exp \left\{ - \left[1 + \xi \left(\frac{x - \mu}{\sigma} \right) \right]^{-1/\xi} \right\},$$

where μ is called the location parameter, σ the shape and ξ the scale parameter.

A common approach is to use block maxima for fitting the GEV distribution. In our case we use the highest 6-hourly 10m wind speed of the extended winter season (October-March) at each individual grid point. Then we apply the R package “ismev” based on Coles (2001) to fit the underlying GEV distribution to the seasonal block maxima. As a first approach we apply the stationary case, where μ , σ and ξ are regarded as constant in time. This way we estimate the return level fields, which are subsequently used for calculating the SSI_{RL} .

For our analysis we use and compare different reanalysis products (see table 1). A reanalysis is a combination of model and observational data generated with the help of data assimilation techniques with the aim to produce a consistent dataset describing the atmospheric development of the previous decades.

Table 5.2: Reanalysis products used for the analysis.

Name	Period covered	Resolution of data	Citation
ERA-40	1957-2002	1.125°	Uppala et al. 2005
ERA interim	1979-today	0.7°	Simmons et al. 2007
NCEP-I	1948-today	1.875°	Kalnay et al. 1996
NCEP-II	1979-today	1.875°	Kanamitsu et al. 2002
JRA55	1958-2013	1.25°	Ebita et al. 2011

For the estimation of the 50-year return level the ERA-40, NCEP-I and JRA55 reanalysis datasets were chosen, because they have the longest overlapping period, which spans 45 years from 1958 to 2002. The estimated return-levels of the land area within the European region show a high spatial variability,

ranging from below 10 m/s in the Balkan region to more than 23 m/s in the northern parts of Great Britain (Figure 5.7a-c). In general the coastal areas along the North Sea and Atlantic Ocean show higher than for example the Mediterranean and Eastern European region due to the more direct exposure to windstorm arriving from the North Atlantic. Although the large scale features of the spatial pattern agree between the different reanalysis products, regional differences occur. The standard deviation between the return-levels of the ERA-40, NCEP-I and JRA55 reanalysis highlight these regions (Figure 5.7d). The largest disagreement occurs in western Scandinavia with standard deviations of 7.65 m/s, resulting from very low return-level in the ERA-40 data. Another area of disagreeing values is the eastern part of Spain and North Africa, where ERA-40 show rather low and JRA55 shows relatively high return-levels.

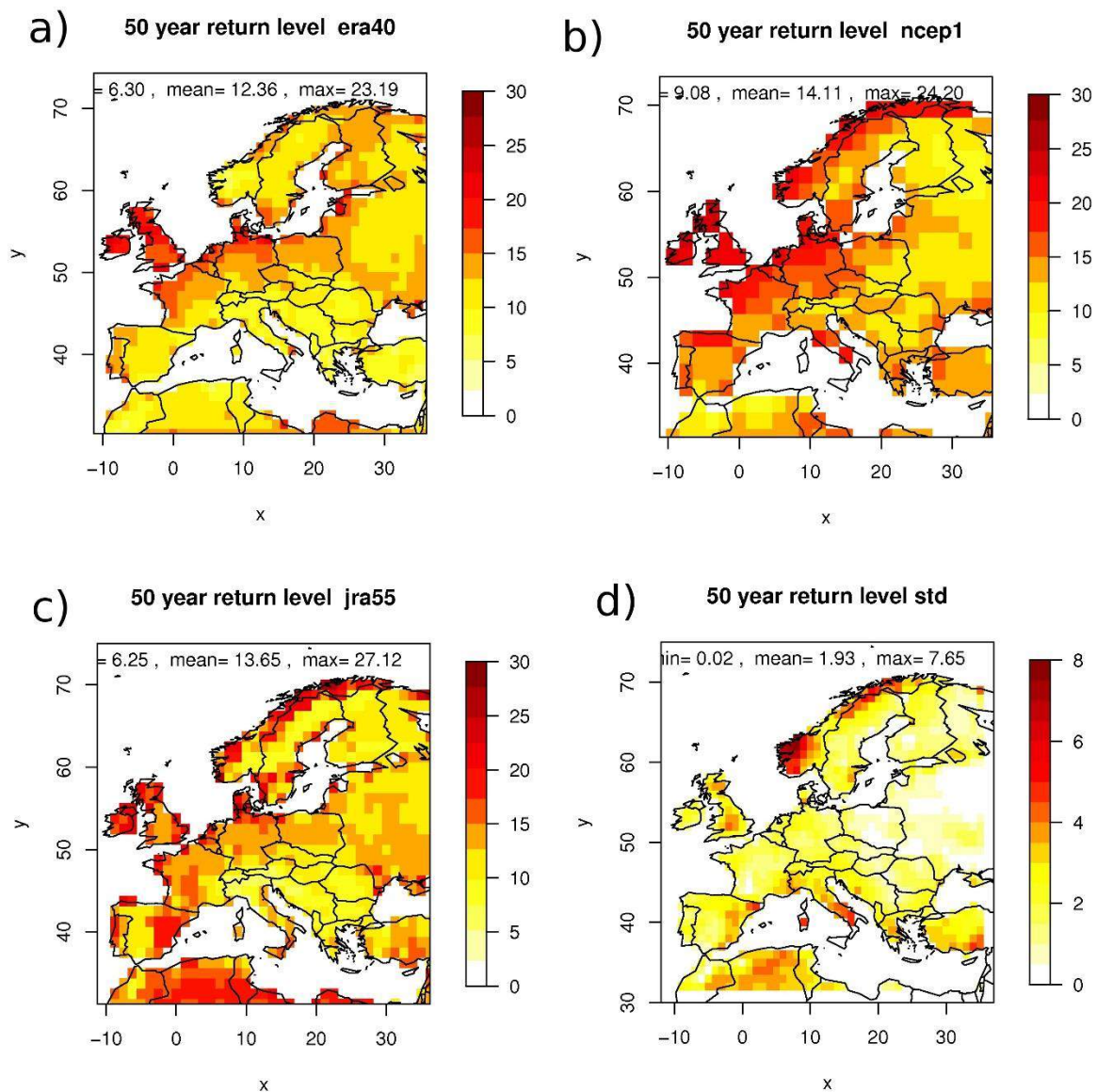


Figure 5.7: 50-year return levels of 6-hourly 10m wind speeds from different reanalysis datasets, estimated from maximum seasonal (ONDJFM) wind speeds using the GEV approach (a-c). Standard deviation of the three return level fields (d).

There are many reasons which can contribute to the cause of those disagreements between the different reanalysis datasets. Firstly, different models, resolutions and parameterizations are applied to create the datasets. The 10m wind speeds may for example depend strongly on the parameterization of the boundary layer processes. Although wind speed observations are not assimilated directly into the models, the use of different observational datasets could also influence the resulting 10m wind speed in the different reanalyses. However, the average standard deviation between the three reanalyses is 1.93 m/s, which is very low compared to the uncertainty related to the estimation of the return-level itself. This suggests that it is possible to use the different return level estimates for the modified SSI and compare the results.

As an example, the temporal development of maximum ONDJFM wind speeds is displayed for the different reanalyses for the grid point "Berlin" (13.4°E,52.5°N). The seasonal maxima show a strong interannual variability. All reanalyses except for NCEP-II are on a similar level varying between approximately 9 and 16 m/s. Only NCEP-II show values which are much higher ranging from about 16 to 24 m/s. The 5-year running means of the seasonal maxima show relatively good correlations between the different reanalyses (Table 2). Despite the large bias of NCEP-II, the correlations with the other reanalyses are good, for example 0.98 with NCEP-II. Thus, care should be taken when evaluating the results achieved with the NCEP-II dataset.

lon 13.4° lat 52.5°

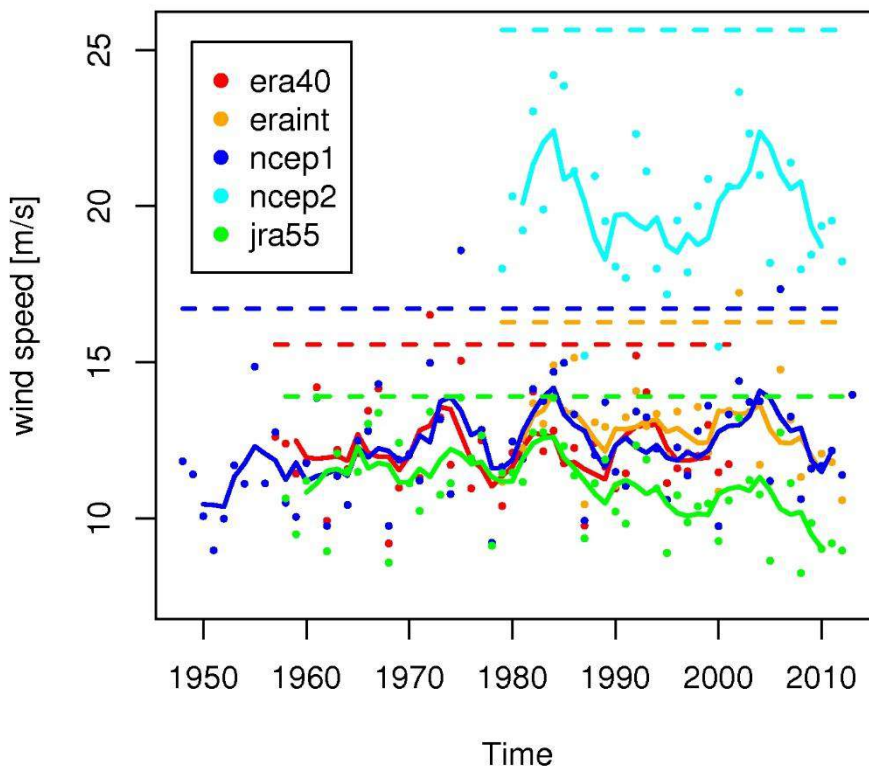


Figure 5.8: Time series of local seasonal (ONDJFM) 10m wind maxima at the grid point "Berlin" for different reanalysis datasets. Seasonal wind maxima (points), 5-year running mean of seasonal wind maxima (solid lines) and the 50-year return level, estimated with the GEV approach for the period of the individual reanalysis dataset (dashed lines).

Table 5.3: Correlations of overlapping periods of 5-year running means of ONDJFM maximum wind speeds at the grid point "Berlin" between different reanalysis datasets.

	ERA-40	ERA-interim	NCEP-I	NCEP-II	JRA55
ERA-40	1.00				
ERA-interim	0.40	1.00			
NCEP-I	0.46	0.67	1.00		
NCEP-II	0.31	0.65	0.98	1.00	
JRA55	0.30	0.73	0.38	0.65	1.00

5.2.3 Towards the application of the modified Storm Severity Index

As described above the windstorms are now tracked by identifying coherent areas of winds speeds exceeding the local 98th percentile. As an example the track of windstorm “Kyrill” is displayed (Figure 5.9). Kyrill affected the European region around the 18th January 2007. Here the track of the wind field is shown as it was derived from the ERA interim data. It shows the passage of the storm arriving from the North Atlantic, crossing Central Europe and dissipating further eastward. The large area enclosed by the blue contour located over Central Europe resembles the cluster of exceedances of the 98th percentile at this specific time step. The respective time step is also marked on the track. The green contours show areas, where the 50-year return levels were exceeded at the same time step. Exceedances occurred within southern Germany and in the border region of Germany, the Czech Republic and Poland.

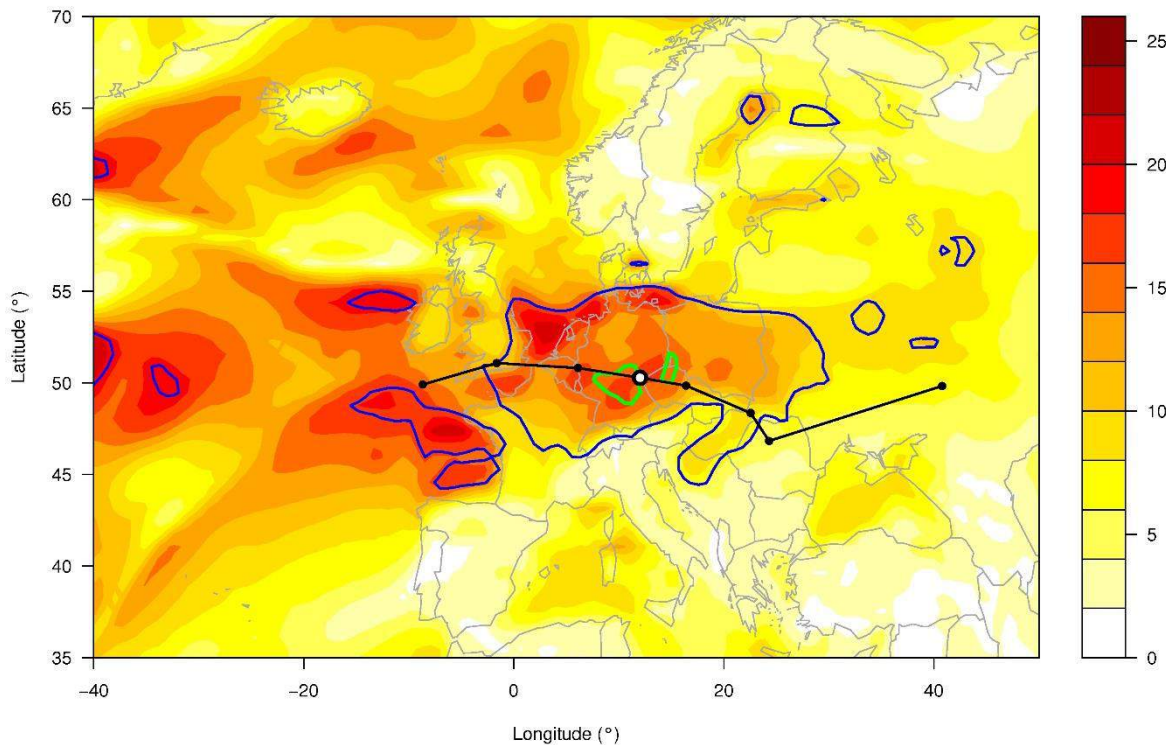


Figure 5.9: Track of windstorm “Kyrill” from 18.01.2007, 0 UTC until 19.01.2007, 18 UTC (solid black line, markers placed at 6-hourly increments) based on ERA interim data. ERA interim 10m wind field in m/s at 18.01.2007, 18 UTC (colors). The contours show the area where the wind speed exceeds the local 98th percentile (blue) and the local 50-year return level of wind speeds (green).

5.2.4 Outlook

As a next step the tracking of wind fields will be extended to the whole time series of the different reanalysis products and the SSI as well as the SSI_{RL} values for the identified systems will be calculated. Those can then be compared and analyzed regarding their climatological characteristics.

Furthermore, the GEV method allows to directly infer the uncertainties of the estimated return levels, for example by using a profile likelihood approach. These uncertainties can be interpreted as confidence intervals, adding a lower and upper bound to the return-level. Our aim is, to propagate these uncertainties into the calculation of the modified storm severity index SSI_{RL} . This way the uncertainty of the SSI_{RL} values due to the parameter estimation of the GEV method can be quantified.

After finishing the evaluation of the recent climate with the help of the reanalysis data, the aim is to extend the analysis to future climate projections, e.g. the CMIP5 simulations performed for the last IPCC report.

5.3 Hazardous precipitation identification methods

5.3.1 Introduction

Rainfall is highly variable in terms of spatial extent, duration and intensity. Both small scale and large-scale events can pose a risk on infrastructure. In addition, both short duration rain spells of high intensity and long lasting rainfall of moderate intensity, which can accumulate to damaging amounts of water, have to be considered.

To take these characteristics of rainfall into account, the identification tool for heavy precipitation identifies events of various duration and spatial extent. All events exceeding a predetermined critical threshold are identified.

5.3.2 Calculation of critical thresholds

Drainage systems for components of critical infrastructure networks are usually designed to be able to cope with a certain amount of water per time unit. This amount is also called the “design rainfall”. It can be assumed that only precipitation, which exceeds the design rainfall, can be harmful for the infrastructure component. In this study we therefore set out to identify heavy precipitation events which exceed the design rainfall.

The design rainfall is often specified by national or international laws and regulations. It is based on the climatological values of precipitation in a certain region and it is specified in terms of return levels for a given return period (i.e. the amount of rain per time unit only exceeded every n years). The return levels can be estimated using a Peak Over Threshold (POT) method or by fitting a Generalized Extreme Value distribution to the data set. For the RAIN project the POT method is applied using the “extremes” package of the statistical software R. The return levels differ for events with different durations and different return periods. Hydrologists describe the relationship between the intensity, the duration and the frequency of precipitation at a given place with intensity-duration-frequency (IDF) curves. Empirical equations exist to describe this relationship and to fit the IDF curves (e.g. WMO 2009). An

example is shown in Figure 5.10. The lines indicate the amount of precipitation that can be expected for different durations and return periods in mm/hour for a grid box over Slovenia using the observational E-OBS data set (Haylock et al. 2008). With increasing duration the intensity (amount of rainfall per time unit) of the events decreases, while the total amount of water associated with an event increases with duration. Per definition events with a low return frequency (i.e. high return period) are associated with higher intensities than events with higher return frequencies.

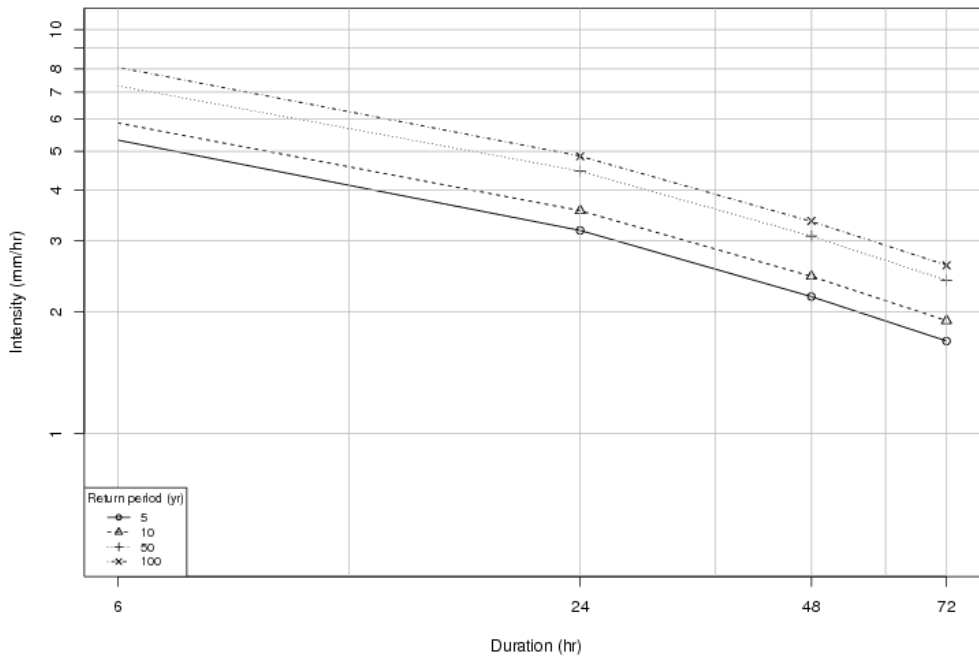


Figure 5.10. Intensity duration frequency curve for a grid point over Slovenia. Based on the E-OBS data set.

For the RAIN project IDF curves will be fitted for each grid point in each analysed data set. Thus, individual threshold are determined for each location, duration and return level which are relevant for the project. A map of the 5-year return level for 24 hour rainfall over Europe based on the gridded observational E-OBS data set is shown as an example in Figure 5.11. In general, return levels are higher over elevated regions such as the Alps as precipitation is often triggered by orographic lifting. Especially high return levels are also present at the western Norwegian coast. The general flow as well as the passage of mid-latitude cyclones are mostly directed from west to east. The western coasts of the continents and the western flanks of mountainous regions are therefore especially prone to precipitation, which is reflected in the return levels. In the Mediterranean region cyclones coming from the sea can transport humid air masses. Here, the regions bordering on the coast show the highest return levels.

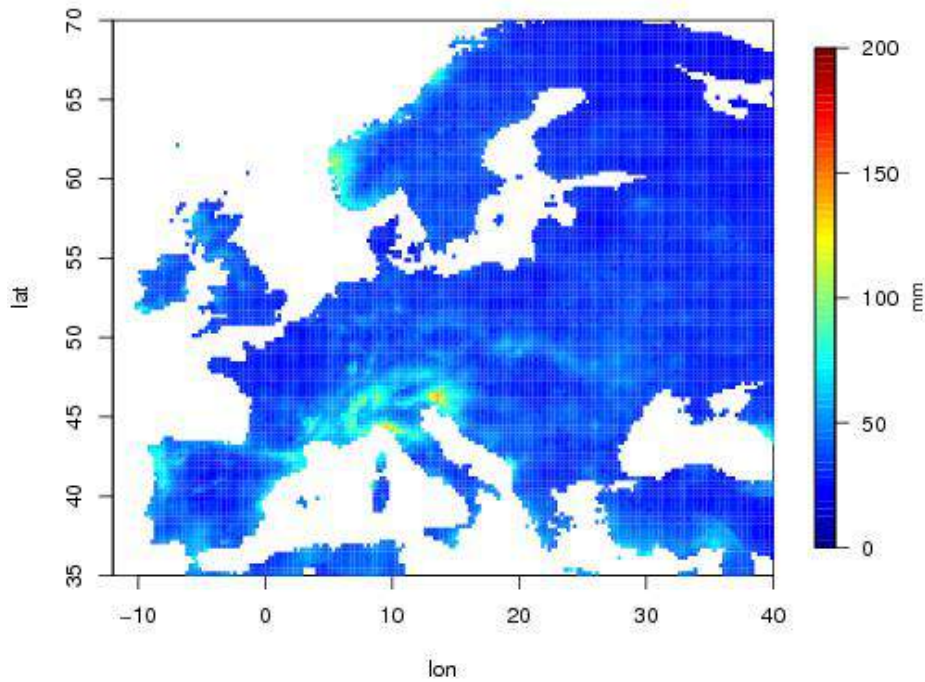


Figure 5.11. 5-year return values of 24-hour precipitation intensity based on the E-OBS data set. Units in mm.

5.3.3 Detection of heavy precipitation events

A detection algorithm for gridded data sets was developed, which identifies heavy precipitation events of various durations and spatial extents. The approach is based on a method that has been originally developed for the detection of windstorms (Leckebusch et al. 2008). The method was extended for the RAIN project to account for the special characteristics of heavy precipitation, in particular for the fact that rain accumulates over time.

In a first step the algorithm identifies all grid boxes in which the rainfall exceeds the design rainfall. For this, aggregation periods starting from a single time step up to 72- hours are considered. All identified grid boxes which are located within the same continuous rain area (i.e. which are not separated by rain free grid boxes) are considered as belonging to the same event and form a cluster. The centre of mass is calculated for each cluster. The clusters are then tracked in time using a nearest neighbor approach. Thus, each detected event can consist of several grid boxes and can last for several time steps. A severity index (SI) is assigned to all events. It is calculated only from grid boxes and time steps where the design rainfall was exceeded and is defined as follows:

Equation 5-6

$$SI = \sum_t^T \sum_k^K \frac{precip_{k,t}}{annualprecip_k} * A_k ,$$

where T is the considered time range, K is the number of affected grid boxes and A_k is the area of grid box k. Thus, the severity index takes the affected area, and the amount of precipitation accumulated over the duration of the event into account. It is normalized by the long-term mean annual precipitation sum expected for the grid box. The severity index can be used to compare the strength of the identified events. The detection algorithm also stores additional information for each event,

such as the date, location, affected area, duration, severity and maximum precipitation (Table 5.2: Reanalysis products used for the analysis.Figure 5.12).

Produced by WTRACK of IfM-FUB revision 226

DATE	INDEX	SIZE	AREA	LON	LAT	MEANPRE	STDV	MAXPREC	LONMAX	LATMAX	SI
Event: 200200001 Start: 2002010100 Length: 3 Area: 3.12 SI: 6.87											
2002010100	1	51	3.03	37.20	39.70	17.38	2.03	20.70	36.63	39.38	1.75
2002010200	1	52	3.06	37.09	40.01	20.50	1.15	26.30	20.88	70.13	2.07
2002010300	1	52	3.09	37.27	39.71	29.65	3.43	36.20	37.13	39.88	3.04
Event: 200200002 Start: 2002010800 Length: 4 Area: 1.54 SI: 3.21											
2002010800	2	11	0.31	18.50	68.64	15.44	2.84	18.60	16.63	68.38	0.11
2002010900	2	49	1.43	15.96	67.69	32.94	11.87	64.00	13.63	66.88	0.75
2002011000	2	53	1.54	16.43	67.89	65.76	17.18	112.30	13.63	66.88	1.73
2002011100	2	44	1.30	15.85	67.70	30.48	9.75	59.20	13.63	66.88	0.62
Event: 200200003 Start: 2002021400 Length: 4 Area: 0.62 SI: 1.19											
2002021400	3	17	0.55	13.85	65.17	8.40	3.17	15.50	13.13	65.38	0.09
2002021500	3	19	0.62	14.06	65.17	36.21	3.20	41.90	14.13	64.88	0.48
2002021600	3	19	0.62	14.06	65.19	42.61	3.02	47.40	13.13	65.38	0.56
2002021700	3	12	0.39	14.13	65.19	5.80	0.77	6.70	13.88	65.38	0.05
Event: 200200004 Start: 2002031900 Length: 3 Area: 0.10 SI: 0.24											
2002031900	4	2	0.10	9.61	49.14	43.00	0.80	43.80	9.88	48.88	0.10
2002032000	4	2	0.10	9.64	49.11	44.43	6.50	50.90	9.88	48.88	0.10
2002032100	4	2	0.10	9.62	49.13	20.71	1.70	22.40	9.88	48.88	0.05

Table 5.4. Output of precipitation detection scheme.

As small scale and short-duration can be as harmful for infrastructure as long-term large-scale events, no size or duration thresholds are implemented in the detection algorithm.

An example for a historic severe precipitation event, as it is detected by the heavy precipitation detection algorithm is shown in Figure 5.12. Precipitation accumulated for the period August 11 2002 to August 13 2002 based on the E-OBS data set. Color denotes grid boxes exceeding 50-year return levels. Units mm. Precipitation accumulated over 3 days is shown for the period between the 11th of August and the 13th of August 2002. Shading denotes areas where the 50-year return levels were exceeded. In August 2002 record-breaking rainfall amounts and intensities occurred in Central Europe. They resulted in a large-scale flooding event (e.g. Ulbrich et al. 2003).

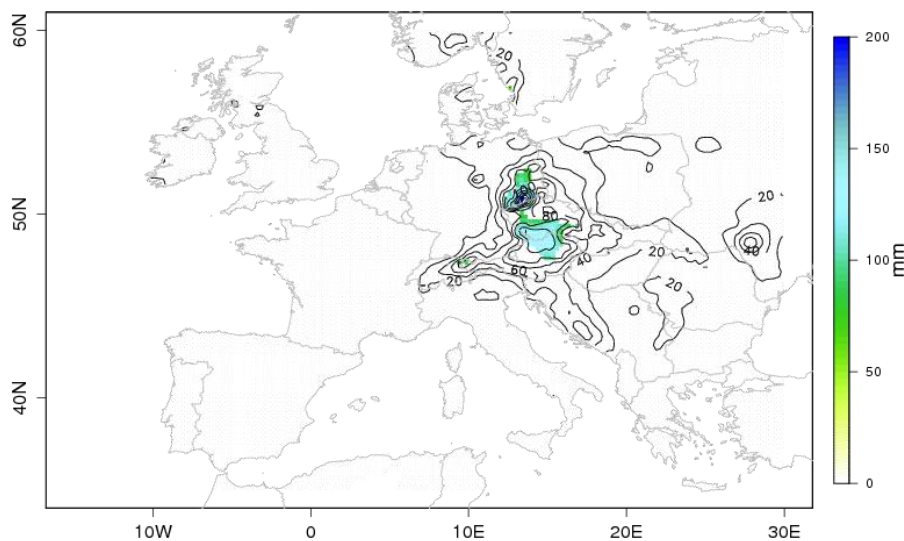


Figure 5.12. Precipitation accumulated for the period August 11 2002 to August 13 2002 based on the E-OBS data set. Color denotes grid boxes exceeding 50-year return levels. Units mm.

The event was triggered by a cyclone on a passage from the Mediterranean into Central Europe. Such so-called “Vb” cyclones are known to be able to transport huge amounts of water into Central Europe and have been associated with several flood events in the past. Figure 5.12 shows that the 50-year return levels were exceeded in a large area over central Europe.

Comparing all events detected in the E-OBS dataset, which exceeded the 50-year return levels, the most extreme events have been identified. The highest severity index was calculated for an event effecting Spain, which took place in November 1997. It had a severity index of 49.9 and was also described in the literature (Lorente et al. 2008). The longest duration of an event in the data set was 11 days. It occurred over Estonia in August 1987. The largest extent (152300km²) is associated with an event which occurred in September 1992 with its centre over Eastern Europe.

6. Conclusions and recommendations

6.1 Conclusions

The stakeholder interviews and the past cases that were studied allow us to answer the questions raised in the introduction. We will review them one by one in the following sections.

- How were critical infrastructure impacted by severe weather in EU?

Extreme weather affects critical infrastructure in two ways. Either extreme weather can damage components of the infrastructure, or impair its functioning without causing structural damage.

The damaging severe weather types that were mentioned most often by stakeholders are extreme winds, flooding and freezing precipitation. Roads and railways can be affected by floods that cause erosion or by landslides. Particularly vulnerable components are tunnels, bridges and sections next to slopes. In addition, trees or other objects can be blown onto them. For railways, the catenary and other electric installations are additional components sensitive to extreme weather. In case of roads, heat and cold spells have deteriorating effects on the road surface.

Electrical power supply is most often affected by damage to the transmission lines by extreme winds or freezing precipitation. In addition, power generation may be affected by extreme weather too. Power supply is also one of the great concerns of providers of telecommunication services, which may independently be affected by outages of various communication systems. A high redundancy of networks spatially limits the consequences of such impacts.

For roads and railways, functioning can be impaired or limited without structural damage. This makes them more vulnerable than power or telecommunications. For instance, this is the case when traffic is rendered impossible because of snow accumulations. Dense fog has the same effect of thwarting transport. Slippery conditions because of freezing precipitation, snow or hail may lead to an accumulation of traffic accidents on roads that yield the network unusable. Preventive measures such as reduced speeds limit the network's capacity.

- Which severe weather events have had the greatest impact on CI in the EU?

According to the interviewed stakeholders, **windstorms**, **heavy rainfall (especially when leading to river floods)**, **snow and snow storms** and **freezing precipitation** are the extreme weather phenomena with the greatest impact on critical infrastructure. It is possible that stakeholders are somewhat biased towards those events that they know to have occurred, thereby underestimating the impact of rare events such as major coastal floods or tornadoes. The event that was judged to have the highest societal impact by the most stakeholders is windstorms.

- Which CI are most vulnerable to extreme weather?

All four CI types are vulnerable to extreme weather. However, road and railway systems are judged to be more sensitive than power and telecommunications. The likely reason is the susceptibility of the vehicles and trains which may be affected even in cases without any structural damage to the systems.

- Which measures have CI operators taken to prevent or respond to extreme weather impacts?

Interviewed CI operators have indicated many types of impact, which can broadly be categorized into two categories: preventive measures and measures taken once a warning for imminent extreme weather has been issued.

As **preventive measures**, they invest in **increasing the resilience of their systems**. This is done by creating network redundancy or by strengthening structural components of their infrastructure on the basis of regulations that ensure their resistance and that of the system. In some cases, CI operators mention that they cooperate with climate scientists to ascertain that these regulations take possible future changes of severe weather into account. Additionally, action plans are developed that make an optimal response of personnel possible once an event occurs.

A second type of measures are those taken **when an event is approaching** and are aimed at **reducing its impact**. This requires a good early warning of the event that is properly communicated and understood. To that aim, a vast majority of stakeholders have arrangements with weather services. The measures that are typically taken include the increase of redundancy of the network or taking measures that increase resistance at the cost of reducing capacity. Another way to respond is to actively inform users of the CI network of possible outages in order to help them reduce impact on their end. Finally, recover quickly from the event are taken, which primarily involve the allocation of personnel and equipment.

Examples of measures that were mentioned by the interviewees are listed in this table:

Response:	Preventive	Upon warning
Railways	Use tailored or public weather forecasts Investigate climate change and choice of new infrastructure Build protective infrastructure: avalanche barriers, rockfall fences, tunnels and galleries Stabilize slopes with anchors or concrete Install alarm systems for rock falls Install avalanche warning commission Reduce train services	Reduce train speed Check switch heaters before cold spells Preventively close stations or tracks Deploy more personnel
Roads	Consider of climate (change) when construction new infrastructure components Monitor weather forecasts and observations Construct IT systems warnings for drivers) Monitor roads for weather-induced wear and tear	Reduce traffic speed Close bridges Contractors on stand-by Prohibit lorries to drive in winter storms

	<p>Decrease speed limits during winter weather, storms</p> <p>Make sure priority with which snow is removed is set</p> <p>Ensure availability of snow disposal sites</p>	
Telecom networks	<p>Protect antennas against icing and lightning</p> <p>Ensure network has high redundancy</p>	<p>Pre-warn response teams for repairs</p> <p>Phone warnings to clients</p>
Power grids	<p>Use weather forecasts and warnings</p> <p>Install dedicated Load dispatch centres to monitor weather</p>	<p>Start additional power plants</p> <p>Increase network redundancy by using more power lines</p> <p>Stop wind turbines</p> <p>Call extra personnel to manage network usage</p> <p>Ensure that replacements are available for broken equipment</p>
Emergency managers	<p>Receive weather warnings from authorities</p> <p>Develop emergency response scripts</p>	<p>Put personnel on stand-by</p> <p>Check communication network, power supply</p> <p>Communicate emergency routes</p> <p>Check equipment</p> <p>Cancel major public events</p> <p>Rehearse procedures and scripts</p>

6.2 Recommendations

The results presented here leave a number of questions unanswered, which can be formulated as focal points for the remainder of the RAIN project Hazard Identification work package.

Although the List of Past cases presented in Chapter 3 indicates that extreme weather impacts on CI occur in many areas in Europe, the distribution of the risk of events across Europe is uncertain. It is recommended and foreseen that RAIN will develop maps and gridded data sets that will show this distribution.

It was also noted that the effectiveness of measures that CI operators can take when an event is likely or imminent, depends on the quality of the warnings, their communication and the extent to which they are correctly understood. To that aim it is recommended and foreseen that the RAIN partners will perform an assessment of early warning systems.

Finally, some CI managers mentioned that they take climate change effects into account when establishing the regulations according to which their system and its components should be designed. However, for many of the severe weather phenomena discussed herein, an analysis of the effects on climate change on extreme weather probabilities has not been made with the latest suite of regional and global climate models, or not at all. Again, it is recommended and foreseen that RAIN will perform these analyses.

7. References

- Anderson, P.L., Meerschaert, M.M. (1998). Modeling river flows with heavy tails. *Water Resources Research* 34(9):2271–2280. doi:10.1029/98WR01449
- Anziani, A. (2010). Rapport d'information fait au nom de la mission commune d'information sur les conséquences de la tempête Xynthia, rapport d'étape 10/6/2010 No 554, Sénat, France.
<http://www.senat.fr/rap/r09-647-1/r09-647-1.html>
- Apel, H., Aronica, G.T., Kreibich, H., Thielen, A.H. (2009). Flood risk analyses—how detailed do we need to be?. *Natural Hazards* 49(1):79–98. doi:10.1007/s11069-008-9277-8
- Bates, P., De Roo, A.P. (2000). A simple raster-based model for flood inundation simulation. *Journal of Hydrology* 236(1–2):54–77. doi:10.1016/S0022-1694(00)00278-X
- Bersani, C., Gerard, F., Gondran, O., Helias, A., Martin, X. et al. (2010). Tempete Xynthia retour d'expérience, évaluation et propositions d'action tome I: rapport, May 2010.
<http://www.ladocumentationfrancaise.fr/var/storage/rapports-publics/104000293/0000.pdf>
- Bertin X., Bruneau, N., Breilh, J.-F., Fortunato, A.B., Karpytchev, M. (2012). Importance of wave age and resonance in storm surges: The case Xynthia, Bay of Biscay. *Ocean Modelling* 42:16–30. doi:10.1016/j.ocemod.2011.11.001
- B. Feuerstein et al., 2011: Towards an improved wind speed scale and damage description adapted for Central Europe. *Atmospheric Research*, 100, 547 – 564
- Blackburn, M., Methven, J., Roberts, N. (2008). Large-scale context for the UK floods in summer 2007. *Weather* 63(9):280–288. doi:10.1002/wea.322
- Blöschl, G., Nester, T., Komma, J., Parajka, J., Perdigão, R.A.P., (2013). The June 2013 flood in the Upper Danube Basin, and comparisons with the 2002, 1954 and 1899 floods. *Hydrol Earth Syst Sci* 17, 5197–5212. doi:10.5194/hess-17-5197-2013
- Bonelli P, Lacavalla M, Marcacci P, Mariani G & Stella G. (2011). Wet snow hazard for power lines: a forecast and alert system applied in Italy. *Natural Hazards and Earth System Sciences* 11: 2419–2431
- Breilh, J.F., Chaumillon, E., Bertin, X., Gravelle, M. (2013). Assessment of static flood modeling techniques: application to contrasting marshes flooded during Xynthia (western France). *Natural Hazards and Earth System Sciences* 13(6):1595–1612. doi:10.5194/nhess-13-1595-2013.
- Brönstrup, C. (2014): Sechs Tote in NRW: Schwerstes Unwetter seit Jahren - Welt - Tagesspiegel. [online] Tagesspiegel.de. Available at: <http://www.tagesspiegel.de/weltspiegel/sechs-tote-in-nrw-schwerstes-unwetter-seit-jahren/10016822.html> [Accessed 18 Nov. 2014].
- Buishand, T.A. (1989). Statistics of extremes in climatology. *Statistica Neerlandica* 43(1):1–30. doi:10.1111/j.1467-9574.1989.tb01244.x

Caron, J. F., Zwack, P., & Pagé, C. (2005). A diagnostic study of the GEM operational forecast of the european windstorm'Lothar'. Part I: The diagnostic tool. Mon. Wea. Rev.

Chatterton, J., Viavattene, C., Morris, J., Penning-Rowell, E., Tapsell, S. (2010). The costs of the summer 2007 floods in England. Environment Agency, Bristol, UK, 51 pp.
https://www.gov.uk/government/uploads/system/uploads/attachment_data/file/291190/scho1109brja-e-e.pdf

Coles, S., Bawa, J., Trenner, L., & Dorazio, P. (2001). An introduction to statistical modeling of extreme values (Vol. 208). London: Springer.

Danske Bank: Skog & Ekonomi. Temaartikel 2: Brandkatastrofens effekt på marknaden. Nummer 3, September 2014. <http://www.danskebank.se/PDF/Skog-och-Lantbruk/Skog-och-Ekonomi/2014/Skog-och-Ekonomi-Nr3-2014.pdf>

Deltares (2014). SOBEK User Manual.
http://content.oss.deltares.nl/delft3d/manuals/SOBEK_User_Manual.pdf

Deutschebahn.com, (2014): Interim Report January – June 2014. [online] Available at:
http://www.deutschebahn.com/file/7586374/data/zb2014_dbgroup.pdf [Accessed 20 Nov. 2014].

Donat, M. G., Leckebusch, G. C., Pinto, J. G., & Ulbrich, U. (2010). Examination of wind storms over Central Europe with respect to circulation weather types and NAO phases. International Journal of Climatology, 30(9), 1289-1300.

DWD (2014). Berichte des Deutschen Wetterdienstes 242,C. Stein and G. Malitz Das Hochwasser an Elbe und Donau im Juni 2013, Wetterentwicklung und Warnmanagement des DWD, Hydrometeorologische Rahmenbedingungen, Deutscher Wetterdienst, Fachinformationsstelle und Deutsche Meteorologische Bibliothek, Frankfurter Straße 135, 63067 Offenbach

Ebita, A., Kobayashi, S., Ota, Y., Moriya, M., Kumabe, R., Onogi, K., ... & Ishimizu, T. (2011). The Japanese 55-year Reanalysis" JRA-55": an interim report. Sola, 7, 149-152.

EC, Humanitarian aid and civil protection, Slovenia-Severe Weather-International assistance, Available on
http://ercportal.jrc.ec.europa.eu/ercmaps/ECDM_20140206_Slovenia_SevereWeatherAssistance.pdf

Environment Agency (2007). Review of 2007 summer floods. Environment Agency, Bristol, 60 pp.
https://www.gov.uk/government/uploads/system/uploads/attachment_data/file/292924/geho1107bnmi-e-e.pdf

EQE (1999). EQE Summary Report: The European storms Lothar and Martin December 26-28, 1999.

EQECAT (2007). Europe Windstorm Kyrill Causes Losses in Western Europe. Website last accessed on 28 Dec. 2014. <<http://www.eqecat.com/catwatch/europe-windstorm-kyrill-loss-western-europe-2007-01-18/>>

Ervine, D.A., MacLeod, A.B. (1999). Modelling a river channel with distant floodbanks. Proceedings of the Institution of Civil Engineers-Water and Maritime Engineering 136(1):21–33. doi:10.1680/iwtme.1999.31265

ESWD entry for the event: <http://www.eswd.eu>

EUMETRAIN E-TRAIN-WIKI: http://www.zamg.ac.at/etrainwiki/doku.php?id=20_february_2010_-_catastrophic_flash_flood_in_madeira_island

FAZ (2013). Frankfurter Allgemeine Zeitung, Website last accessed on 9 Dec. 2014, <http://www.faz.net/aktuell/gesellschaft/ungluecke/hochwasser/bildergalerie-bilder-vom-hochwasser-am-5-juni-12210540/das-autobahnkreuz-an-der-12210744.html>

FFSA / GEMA (2011). La tempête Xynthia du 28 février 2010 – Bilan chiffré au 31 décembre 2010. <https://www.ffsa.fr/sites/upload/docs/application/pdf/2011-06/bilanxynthia28022011.pdf>

Fink, A. H., Brücher, T., Ermert, V., Krüger, A., & Pinto, J. G. (2009). The European storm Kyrill in January 2007: synoptic evolution, meteorological impacts and some considerations with respect to climate change. *Natural Hazards and Earth System Science*, 9(2), 405-423.

Focus (2013). Nach Hochwasser: Sperrung von ICE-Strecke dauert an, Website last accessed on 9 Dec. 2014, http://www.focus.de/panorama/welt/verkehr-nach-hochwasser-sperrung-von-ice-strecke-dauert-an_aid_1038115.html

Focus (2007). Orkan „Kyrill“ fegt über Deutschland und Europa. Website last accessed on 3 Dec. 2014. <http://www.focus.de/panorama/welt/wetter_did_14486.html>

Forstén J. (2002). Sähköntoimitusvarmuuden parantaminen (Improving the delivery reliability of electricity). Ministry of Trade and Industry of Finland, Espoo, 36 pp [in Finnish]

Fragoso, M., Trigo, R. M., Pinto, J. G., Lopes, S., Lopes, A., Ulbrich, S., and Magro, C.: The 20 February 2010 Madeira flash-floods: synoptic analysis and extreme rainfall assessment, *Nat. Hazards Earth Syst. Sci.*, 12, 715-730, doi:10.5194/nhess-12-715-2012, 2012.

Freer, J., Beven, K.J., Neal, J., Schumann, G., Hall, J., Bates, P.D. (2013). Hydrological flood uncertainty and risk research. In: Rougier, J., Sparks, S., Hill, L.J. (eds) *Risk and Uncertainty Assessment for Natural Hazards*, Cambridge University Press, Cambridge, 190–233

French Wikipedia: http://fr.wikipedia.org/wiki/Le_Grand-Bornand

Gazeta.pl, (2008): Traba powietrzna szaleje nad Polska. Sa ranni, dwie osoby nie zyja. [online] Available at:

http://wiadomosci.gazeta.pl/wiadomosci/1,130438,5593623,Traba_powietrzna_szaleje_nad_Polska__Sa_ranni__dwie.html [Accessed 9 Dec. 2014].

Glogovcan T. (2014). Captured in ice and snow. In SINFO-Slovenian Information, February 2014, published by the Slovenian Government Communication Office.

Grochala, R., 2012: Analiza trab powietrznych z 15 sierpnia 2008 w Polsce. [online] Available at: <http://lubiepogode.files.wordpress.com/2012/02/grochala2012.pdf> [Accessed 20 Nov. 2014].

Grunwald S. and H.E.Brooks, 2011: Relationship between sounding derived parameters and the strength of tornadoes in Europe and USA from reanalysis data. *Atmospheric Research*, 100, 479 – 488.

Gumbel, E.J. (1958). *Statistics of Extremes*. Columbia University Press, New York, 397 pp

Haavasoja T and Pilli-Sihvola Y. (2010). Friction as a Measure of Slippery Road Surfaces. In *Proceedings of SIRWEC 15th International Road Weather Conference*, Quebec City, Canada, 5-7 February 2010. Available at: <http://www.sirwec.org/Papers/quebec/11.pdf>.

Hanna, E., Mayes, J., Beswick, M., Prior, J., Wood, L. (2008). An analysis of the extreme rainfall in Yorkshire, June 2007, and its rarity. *Weather* 63(9):253–260. doi:10.1002/wea.319

Haylock, M.R., Hofstra, N., Klein Tank A.M.G., Klok, E.J., Jones P.D. and New, M. (2008). A European daily high-resolution gridded dataset of surface temperature and precipitation. *J. Geophys. Res (Atmospheres)*, 113, D20119, doi:10.1029/2008JD10201

Hoppula P. (2005). Tykkylumi ja otolliset säätilanteet sen aiheuttamille puustovaurioille (Crown snow-load and favourable weather conditions for forest damage caused by it). MSc thesis, University of Helsinki, Helsinki, 87 pp [in Finnish]

Horritt, M.S., Bates, P.D. (2002). Evaluation of 1D and 2D numerical models for predicting river flood inundation. *J Hydrol* 268(1–4):87–99. doi: 10.1016/S0022-1694(02)00121-X

http://www.sawa-project.eu/uploads/documents/NVE_Report7-11.pdf

Hoskins, B. J., & Coutinho, M. M. (2005). Moist singular vectors and the predictability of some high impact European cyclones. *Quarterly Journal of the Royal Meteorological Society*, 131(606), 581-601.

Hoskins B. J., Hodges K. I., (2002). New Perspectives on the Northern Hemisphere Winter Storm Tracks. *J. Atmos. Sci.*, 59: 1041–1061.

Huibregtse, J.N., Morales Napoles, O., de Wit, M.S. (2013). Flooding of tunnels: quantifying climate change effects on infrastructure. *Proceedings 11th International Conference on Structural Safety and Reliability (ICOSSAR2013)*, New York, June 2013, 1463–1470

Hunter, N.M., Bates, P.D., Horritt, M.S., Wilson, M.D. (2007). Simple spatially-distributed models for predicting flood inundation: A review. *Geomorphology* 90(3–4):208–225. doi: 10.1016/j.geomorph.2006.10.021

iDNES.cz, (2009): Vlaky do Ostravy zastavil blesk, vypalil zabezpecovaci zarizeni - iDNES.cz. [online] Available at: http://zpravy.idnes.cz/vlaky-do-ostravy-zastavil-blesk-vypalil-zabezpecovaci-zarizeni-pxz-/domaci.aspx?c=A090629_192154_domaci_abr [Accessed 20 Nov. 2014]. Heavy snowfall

Ihalainen A. & Ahola A. (2003). Pyry- ja Janika-myrskyjen aiheuttamat puuston tuhot (Forest damage caused by the storms Pyry and Janika). *Metsätieteen aikakauskirja* 3/2003: 385–401 [in Finnish]

- Inness, P. M., Dorling, S. (2012). Operational weather forecasting. John Wiley & Sons.
- Insee (2014). Résultats du recensement de la population 2010. <http://www.insee.fr/fr/bases-de-donnees/default.asp?page=recensement/resultats/2010/rp2010.htm>
- Joe, H. (2014). Dependence Modeling with Copulas. Chapman & Hall/CRC, London, 480 pp
- Juga I, Hippi M, Moisseev D, Saltikoff E. (2012). Analysis of weather factors responsible for the traffic “Black Day” in Helsinki, Finland, on 17 March 2005. Meteorological Applications vol. 19: 1-9.
- Juga I, Hippi M, Nurmi P, Karsisto V. (2014). Weather factors triggering the massive car crashes on 3 February 2012 in the Helsinki metropolitan area. In proceedings of 17th International Road Weather Conference, La Massana, Andorra, January 30 to February 1, 2014. Available from <http://www.sirwec.org/Papers/andorra/21.pdf>.
- Kosiba, K.A., and J. Wurman, 2013: The Three-Dimensional Structure and Evolution of a Tornado Boundary Layer. Wea. Forecasting, 28, 1552–1561.
- Kalnay, E., Kanamitsu, M., Kistler, R., Collins, W., Deaven, D., Gandin, L., ... & Joseph, D. (1996). The NCEP/NCAR 40-year reanalysis project. Bulletin of the American meteorological Society, 77(3), 437-471.
- Kanamitsu, M., Ebisuzaki, W., Woollen, J., Yang, S. K., Hnilo, J. J., Fiorino, M., & Potter, G. L. (2002). Ncep-doe amip-ii reanalysis (r-2). Bulletin of the American Meteorological Society, 83(11), 1631-1643.
- Katz, R.W., Parlange, M.B., Naveau, P. (2002). Statistics of extremes in hydrology. Advances in Water Resources 25(8–12): 1287–1304. doi: 10.1016/S0309-1708(02)00056-8
- Keraunos Website - Orage diluvien du 14 juillet 1987 au Grand-Bornand (Haute-Savoie) : <http://www.keraunos.org/actualites/faits-marquants/1970-1989/orage-14-juillet-1987-grand-bornand-catastrophe-crue-eclair-inondation-camping-haute-savoie.html>
- Kim, B., Sanders, B. F., Schubert, J. E., Famiglietti, J. S. (2014) Mesh type tradeoffs in 2D hydrodynamic modeling of flooding with a Godunov-based flow solver. Advances in Water Resources 68:42–61. doi:10.1016/j.advwatres.2014.02.013
- Klawa, M., & Ulbrich, U. (2003). A model for the estimation of storm losses and the identification of severe winter storms in Germany. Natural Hazards and Earth System Science, 3(6), 725-732.
- Kolen, B., Slomp, R., Jonkman, S.N. (2013). The impacts of storm Xynthia February 27–28, 2010 in France: lessons for flood risk management. Journal of Flood Risk Management 6(3): 261–278. doi: 10.1111/jfr3.12011
- Kolen, B., Slomp, R., van Balen, W., Terpstra, T., Bottema, M., Nieuwenhuis, S. (2010). Learning from French experiences with storm Xynthia: Damages after a flood. HKV and Rijkswaterstaat, www.helpdeskwater.nl/publish/pages/26374/xynthia_e_25-10.pdf
- Kuroiwa D. (1965). Icing and snow accretion on electric wires. Cold Regions Research and Engineering Laboratory, Research Report 133.

- KZGW (2010). Główne założenia metodyk dotyczących opracowania map zagrożenia powodziowego. www.kzgw.gov.pl/files/file/Wiadomosci/Metodyki_MZP_KH_.pdf
- Lahti K., Lahtinen M. & Nousiainen K. (1997). Transmission line corona losses under hoar frost conditions. *IEEE Transactions on Power Delivery* 12: 928–933
- Leckebusch, G. C., Renggli, D., & Ulbrich, U. (2008). Development and application of an objective storm severity measure for the Northeast Atlantic region. *Meteorologische Zeitschrift*, 17(5), 575-587.
- Lemieux, C. (2009). *Monte Carlo and Quasi-Monte Carlo Sampling*. Springer, New York, 382 pp
- Leutbecher, M., Barkmeijer, J., Palmer, T. N., & Thorpe, A. J. (2002). Potential improvement to forecasts of two severe storms using targeted observations. *Quarterly Journal of the Royal Meteorological Society*, 128(583), 1641-1670.
- Ljubljana and Slovenia Covered in Ice, Available on <http://www.ljubljana.si/en/living-in-ljubljana/focus/86867/detail.html>
- Lorente P., Hernández, E. Queralt, S. Ribera P. (2008). *Advances in Geosciences, European Geosciences Union (EGU)*, 16, pp.73-80
- Lumbroso, D. M., Vinet, F. (2011). A comparison of the causes, effects and aftermaths of the coastal flooding of England in 1953 and France in 2010. *Natural Hazards Earth System Sciences* 11(8), 2321–2333. doi:10.5194/nhess-11-2321-2011
- Markosek J. (2014). Severe freezing rain in Slovenia. In 20th WGCEF meeting, Geneva, 3 October 2014
- Marsh, T. (2008). A hydrological overview of the summer 2007 floods in England and Wales. *Weather* 63(9):274–279. doi:10.1002/wea.305
- Marsh, T. J., Hannaford, J. (2007). *The summer 2007 floods in England and Wales – a hydrological appraisal*. Centre for Ecology & Hydrology, Wallingford, 32 pp. http://www.ceh.ac.uk/documents/ceh_floodingappraisal.pdf
- Mattéi, J.M, Vial, E., Rebour, V., Liemersdorf, H., Türschmann, M. (2001). Generic results and conclusions of re-evaluating the flooding protection in French and German nuclear power plants. *Eurosafe Forum 2001*.
- Maurer, H., Rudzikaite, L., Kiel, J., Partzsch, I., Pelikan, V. et al. (2012) *WEATHER Case studies – Synthesis Report*. http://www.weather-project.eu/weather/downloads/Deliverables/WEATHER-D6_Case-Studies_v1-0-prel-fin.pdf
- MAZ (2013) *Märkische Allgemeine Zeitung*, “Nach Sommerhitze Unwetter“, Website last accessed on 9 Dec. 2014. <http://www.maz-online.de/Brandenburg/Nach-Sommerhitze-Unwetter>
- Merz, B., Elmer, F., Kunz, M., Mühr, B., Schröter, K., Uhlemann-Elmer, S., (2014). The extreme flood in June 2013 in Germany. *Houille Blanche* 5–10. doi:10.1051/lhb/2014001

- Meteo France (2010). La tempête Xynthia des 27-28 février 2010.
<http://www.meteofrance.fr/climat-passe-et-futur/bilans-climatiques/bilan-2010/la-tempete-xynthia-des-2728-fevrier-2010>
- MetOffice (2012). Heavy rainfall/flooding - June 2007.
<http://www.metoffice.gov.uk/climate/uk/interesting/june2007>
- Metsätuhotyöryhmä (2003). Työryhmämuistio MMM 2003:11 (The working group memorandum MMM 2003:11). Ministry of Agriculture and Forestry of Finland, Helsinki, 35 pp [in Finnish]
- Milojevic, A., Kovats, S., Leonardi, G., Murray, V., Nye, M., Wilkinson, P. (2014). Population displacement after the 2007 floods in Kingston upon Hull, England. *Journal of Flood Risk Management*, published online, doi:10.1111/jfr3.12111
- Möllmann, A.F.D., Vermeer, P.A. (2007). Reliability analysis of a dike failure. *Proceeding of the 18th European Young Geotechnical Engineers' Conference, Ancona, Italy, 17–20 June 2007*
- MP (2013) Berliner Morgenpost, "Gewitter über Berlin flutet U-Bahnhof in Steglitz, Website last accessed on 9 Dec. 2014, <http://www.morgenpost.de/berlin-aktuell/article118702060/Gewitter-ueber-Berlin-flutet-U-Bahnhof-in-Steglitz.html>
- Munichre.com, (2014): Comparatively few major natural catastrophe losses in first half-year | Munich Re. [online] Available at: <http://www.munichre.com/en/media-relations/publications/press-releases/2014/2014-07-09-press-release/index.html> [Accessed 20 Nov. 2014].
- Munich RE, (2013). *Topics Geo 2013, Naturkatastrophen 2013, Analysen, Bewertungen, Positionen*, Münchener Rückversicherungs-Gesellschaft, Königinstraße 107, 80802 München, Bestellnummer 302-08120, 2014
- Munich Re, (2002). *Winter storms in Europe (II)*. Munich.
- Murray R.J., Simmonds I., (1991). A numerical scheme for tracking cyclone centres from digital data. Part I: development and operation of the scheme. *Aust. Meteor. Mag.* 39: 155–166.
- Nature World News: Sweden's Massive Forest Fire Lit by Record Temperatures (Aug 11 2014), accessed 2.12.2014: <http://www.natureworldnews.com/articles/8493/20140811/swedens-forest-fire-massive-lit-record-temperatures.htm>
- Naulin, M., Kortenhaus, A., Oumeraci, H. (2012). Failure Mechanisms of Flood Defence Structures. Status Report Of Activity 2.2 & 2.3, XtremRisk, https://www.tu-braunschweig.de/Medien-DB/hyku-xr/23_xtremrisk_2-2_2-3_fm_final_all.pdf
- Neal, R., Bell, S., Wilby, J. (2011). Emergent disaster response during the June 2007 floods in Kingston upon Hull, UK. *Journal of Flood Risk Management* 4(3):260–269. doi:10.1111/j.1753-318X.2011.01110.x
- Nelsen, R. B. (2006). *An Introduction to Copulas*. Springer, New York, 276 pp

Nto.pl, (2008): Traba powietrzna nad autostrada A4. [online] Available at: <http://www.nto.pl/apps/pbcs.dll/article?AID=/20080815/REGION/844275154> [Accessed 20 Nov. 2014].

NVE (2011). Preliminary Flood Risk Assessment in Norway - An example of a methodology based on a GIS-approach. Norwegian Water Resources and Energy Directorate, 46 pp.

ONLINE, R. (2014): Schäden nach Unwetter in Düsseldorf: Hier fährt die Rheinbahn ab Donnerstag wieder. [online] RP ONLINE. Available at: <http://www.rp-online.de/nrw/staedte/duesseldorf/hier-faehrt-die-rheinbahn-ab-donnerstag-wieder-aid-1.4304070> [Accessed 20 Nov. 2014].

Ozga-Zielińska, M., Brzeziński, J., Ozga-Zieliński, B. (1999). Zasady obliczania największych przepływów rocznych o określonym prawdopodobieństwie przewyższenia przy projektowaniu obiektów budownictwa hydrotechnicznego: długie ciągi pomiarowe przepływów. Institute of Meteorology and Water Management, Warsaw, 45 pp

Palmer, T., and Hagedorn, R. (2006). Predictability of weather and climate. Cambridge.

Paprotny, D. (2014). Trends in storm surge probability of occurrence along the Polish Baltic Sea coast. arXiv:1410.2547

Pedreras, R., Garcin, M., Krien, Y., Climent, D.M., Mugica, J., Francois, B. (2010). Tempete Xynthia: compte rendu de mission préliminaire. BRGM/RP-58261-FR. <http://www.lafautesurmer.net/2010-04-08-Rapport-BRGM.pdf>

Pineau-Guillou, L., Lathuiliere, C., Magne, R., Louazel, S., Corman, D., Perherin, C. (2012). Sea levels analysis and surge modelling during storm Xynthia. *European Journal of Environmental and Civil Engineering* 16(8):943–952. doi:10.1080/19648189.2012.676424

Pinto, J. G., Ulbrich, U., Leckebusch, G. C., Spanghel, T., Meyers, M., & Zacharias, S. (2007). Changes in storm track and cyclone activity in three SRES ensemble experiments with the ECHAM5/MPI-OM1 GCM. *Climate Dynamics*, 29(2-3), 195-210.

Pitt, M. (2008). The Pitt Review: lessons learned from the 2007 flood. http://webarchive.nationalarchives.gov.uk/20100807034701/http://archive.cabinetoffice.gov.uk/pitt-review/_/media/assets/www.cabinetoffice.gov.uk/flooding_review/pitt_review_full%20pdf.pdf

Posthumus, H., Morris, J., Hess, T.M., Neville, D., Phillips, E., Baylis, A. (2009). Impacts of the summer 2007 floods on agriculture in England. *Journal of Flood Risk Management* 2(3):182–189. doi:10.1111/j.1753-318X.2009.01031.x

Poulter, B., Halpin, P.N. (2008). Raster modelling of coastal flooding from sea-level rise. *International Journal of Geographical Information Science* 22(2):167–182. doi:10.1080/13658810701371858

Prior, J., Beswick, M. (2008). The exceptional rainfall of 20 July 2007. *Weather* 63(9):261–267. doi: 10.1002/wea.308

Pristov N., Strajnar B., Cedilnik J., Jerman J., Smerkol P., Licer M. and Fettich A. (2014): Limited area modeling in Slovenia -2014, IN 36th EWGLAM and 21st SRNWP Meeting, Offenbach, 29 September-2 October, 2014

Rauhala J, Juga I. (2010). Wind and snow storm impacts on society. In Proceedings of SIRWEC 15th International Road Weather Conference, Quebec City, Canada, 5-7 February 2010. Available from <http://www.sirwec.org/Papers/quebec/20.pdf>.

Satellite wind data: <http://manati.star.nesdis.noaa.gov/datasets/RSCATData.php>

Schölzel, C., Friederichs, P. (2008). Multivariate non-normally distributed random variables in climate research – introduction to the copula approach. *Nonlinear Processes in Geophysics* 15(5):761–772. doi:10.5194/npg-15-761-2008

Schröter, K., Kunz, M., Elmer, F., Mühr, B., and Merz, B. (2014). What made the June 2013 flood in Germany an exceptional event? A hydro-meteorological evaluation, *Hydrol. Earth Syst. Sci. Discuss.*, 11, 8125-8166, doi:10.5194/hessd-11-8125-2014

Schweckendiek, T., Kanning, W. (2009). Updating piping probabilities with survived loads. In Van Gelder, P., Proske, D., Vrijling, H. (eds), *Proceedings of the 7th International Probabilistic Workshop*, Delft, the Netherlands, 25–26 November 2009

Segond, M.L., Wheeler, H.S., Onof, C. (2007). The significance of spatial rainfall representation for flood runoff estimation: A numerical evaluation based on the Lee catchment, UK. *Journal of Hydrology* 347(1–2):116-131. doi: 10.1016/j.jhydrol.2007.09.040

Simmons, A., Uppala, S., Dee, D., & Kobayashi, S. (2007). ERA-Interim: New ECMWF reanalysis products from 1989 onwards. *ECMWF newsletter*, 110(110), 25-35.

Skogsbranden i Västmanland 2014. Wikipedia (in Swedish), accessed 2.12.2014: http://sv.wikipedia.org/wiki/Skogsbranden_i_Västmanland_2014.

Slovenia Is Still Frozen Solid: 'This Is Crazy, Really Crazy', Available on <http://www.businessinsider.com/photos-of-ice-storm-in-slovenia-2014-2>

SMHI, 2014a: Tidig och varm vår (Jun 3 2014): <http://www.smhi.se/nyhetsarkiv/tidig-och-varm-var-1.75564>

SMHI, 2014b: Juni 2014 - Nordliga vindar gav kyligt och ostadigt väder (Jul 10 2014): <http://www.smhi.se/klimatdata/manadens-vader-och-vatten/2.1118/juni-2014-nordliga-vindar-gav-kyligt-och-ostadigt-vader-1.75690>

SMHI, 2014d: 2000-talets hittills högsta temperatur i Sverige (Aug 5 2014): <http://www.smhi.se/nyhetsarkiv/2000-talets-hittills-hogsta-temperatur-i-sverige-1.76636>

SMHI, 2014c: Rekordvarm julimånad i nordväst (Aug 8 2014): <http://www.smhi.se/klimatdata/manadens-vader-och-vatten/sverige/2.1118/juli-2014-rekordvarm-manad-i-nordvast-1.76471>

SMHI, 2014e: Augusti blev extremt regnig i västra Götaland (Aug 29 2014): <http://www.smhi.se/nyhetsarkiv/augusti-blev-extremt-regnig-i-vastra-gotaland-1.77419>

Sobey, R.J. (2001). Evaluation of Numerical Models of Flood and Tide Propagation in Channels. *Journal of Hydraulic Engineering -ASCE* 127(10):805–824. doi: 10.1061/(ASCE)0733-9429(2001)127:10(805)

Solantie R. (1994). Effect of weather and climatological background on snow damage of forests in Southern Finland in November 1991. *Silva Fennica* 28: 203–211.

Stuttgarter Zeitung, 30 July 2013: *Das Unglück kam aus dem Nichts*. <http://www.stuttgarterzeitung.de/inhalt.katastrophe-von-1972-das-unglueck-kam-aus-dem-nichts.a6298d57-b9a3-48dc-9c7d-96efd3b631dc.html>

SWR, 2006: News Report of 15 August 2006: <http://www.youtube.com/watch?v=M2vfxZ072q4>

Tagesschau.de, (2014): Unwetter: Verheerende Schäden am Schienennetz. [online] Available at: <http://www.tagesschau.de/inland/unwetter-164.html> [Accessed 20 Nov. 2014].

Tatge, Y., (2009). Looking Back, Looking Forward: Anatol, Lothar and Martin Ten Years Later. AIR WORLDWIDE, 9 Sept. 2009. Website last accessed 28 Dec. 2014. <<http://www.air-worldwide.com/Publications/AIR-Currents/Looking-Back,-Looking-Forward--Anatol,-Lothar-and-Martin-Ten-Years-Later>>

T. Chmielewski, H. Nowak and K. Walkowiak, 2013: Tornado in Poland of August 15 2008: Results of post-disaster investigation. *Journal of Wind Engineering and Industrial Aerodynamics*, 118, 54 – 60.

Ulbrich, U., Brücher, T., Fink, A., Leckebusch, G.C., Krüger, A. and Pinto, J.G. (2003). The central European floods of August 2002: Part 1 – Rainfall periods and flood development, *Weather*, 58, 371-377.

Ulbrich, U., Fink, A. H., Kława, M., Pinto, J. G. (2001). Three extreme storms over Europe in December 1999. *Weather*, 56(3), 70-80.

Ulbrich, U., Leckebusch, G. C., & Pinto, J. G. (2009). Extra-tropical cyclones in the present and future climate: a review. *Theoretical and Applied Climatology*, 96(1-2), 117-131.

Union of the Electricity Industry (2006). *Impacts of Severe Storms on Electric Grids*. Brussels.

Uppala, S. M., Kållberg, P. W., Simmons, A. J., Andrae, U., Bechtold, V., Fiorino, M., ... & Woollen, J. (2005). The ERA-40 re-analysis. *Quarterly Journal of the Royal Meteorological Society*, 131(612), 2961-3012.

Valinger E. & Lundqvist L. (1992). The influence of thinning and nitrogen fertilization on the frequency of snow and wind induced stand damage in forests. *Scottish Forestry* 46: 311–320

Vinet, F., Lumbroso, D., Defossez, S., Boissier, L. (2012). A comparative analysis of the loss of life during two recent floods in France: the sea surge caused by the storm Xynthia and the flash flood in Var. *Natural Hazards* 61(3): 1179–1201. doi: 10.1007/s11069-011-9975-5

Vorogushyn, S., Merz, B., Apel, H. (2009). Development of dike fragility curves for piping and micro-instability breach mechanisms. *Natural Hazards and Earth System Sciences* 9(4):1383–1401. doi:10.5194/nhess-9-1383-2009. Wikipedia (2009). Während des Sturms Kyrill am 18.1.2007

umgeknickter Strommast bei Magdeburg-Ottersleben. Website last accessed on 3 Dec. 2014.
<http://upload.wikimedia.org/wikipedia/commons/9/97/Strommast.JPG>

Wilkens, A. (2014). Mobilfunknetze Hielten "Kyrill" Stand. Heise Online, 19 Jan. 2007. Website last accessed 28 Nov. 2014. <<http://www.heise.de/newsticker/meldung/Mobilfunknetze-hielten-Kyrill-stand-136374.html>>.

WMO (2009). 'Guide to hydrological practices', Report, WMO-No 168, vol.II.

Zhou Y., Niu S., Lü J & Zhou L. (2012). Meteorological conditions of ice accretion based on real-time observations of high voltage transmission line. Chinese Science Bulletin 57: 812–818.

Appendix A. Technical details of physical and statistical methods to be used by TU-Delft

A. De Saint-Venant equations in hydraulic modelling

One-dimensional flow in advanced hydraulic models is described by continuity equation (A.1) and momentum equation (A.2). In case of momentum equation, the five components describe inertia, convection, water level, bed friction and wind friction, respectively.

$$\frac{\partial Q}{\partial x} + \frac{\partial A}{\partial t} - q = 0 \quad (\text{A.1})$$

$$\frac{\partial Q}{\partial t} + \frac{\partial(Q^2/A)}{\partial x} + gA \frac{\partial h}{\partial x} + \frac{gQ|Q|}{C^2RA} - W \frac{\tau}{\rho} = 0 \quad (\text{A.2})$$

where Q – discharge (m^3/s); x – distance (m); A – wetted area (m^2); t – time (s); q – lateral discharge per unit length (m^2/s); g – gravity acceleration (m/s^2); h – water level above reference level (m); C – Chezy coefficient ($\text{m}^{1/2}/\text{s}$); R – hydraulic radius (m); W – flow width (m); ρ – water density (kg/m^3); τ – wind shear stress (N/m^2).

Two-dimensional flow is described by three equations: continuity (A.3), momentum in x direction (A.4) and momentum in y direction (A.5).

Są to tzw. równania wód płytkich. In case of momentum equation, the six components describe acceleration, horizontal pressure in x direction, horizontal pressure in y direction, advection, bottom friction and wall friction (Bates and De Roo 2000, Deltares 2014).

$$\frac{\partial h}{\partial t} + \frac{\partial(ud)}{\partial x} + \frac{\partial(vd)}{\partial y} = 0 \quad (\text{A.3})$$

$$\frac{\partial u}{\partial t} + u \frac{\partial u}{\partial x} + v \frac{\partial u}{\partial y} + g \frac{\partial h}{\partial x} + g \frac{u|V|}{C^2d} + au|u| = 0 \quad (\text{A.4})$$

$$\frac{\partial v}{\partial t} + u \frac{\partial v}{\partial x} + v \frac{\partial v}{\partial y} + g \frac{\partial h}{\partial y} + g \frac{v|V|}{C^2d} + av|v| = 0 \quad (\text{A.5})$$

where x, y – distance (m), u – velocity in direction x (m/s), v – velocity in direction y (m/s), V – velocity: $\sqrt{u^2 + v^2}$ (m/s); d – water depth (m); a – wall friction coefficient (1/m).

Example of techniques available for selecting a parametric distribution for a certain data set

There are several methods of analysing the quality of input data and calculating probability distributions. An example procedure, which contains several steps, is as follows:

The input data set should consist of at least 30 elements and be homogenous in terms of the cause and conditions behind the events.

Statistical tests are performed on the input data to ensure homogeneity:

- Test for outlying elements (Grubbs-Beck test)
- Test for independence (Wald-Wolfowitz runs test)
- Test for stationarity (Student's t-test using Spearman's rank correlation coefficient)

The data are fitted to distributions using maximum likelihood estimation (MLE):

- Gumbel
- Generalized extreme value
- Lognormal
- Gamma
- Log-gamma

The output distributions are tested for statistical significance using Kolmogorov-Smirnov's test

The best-fitting distribution is chosen utilizing Akaike Information Criterion test.

Appendix B: Interview guideline

The following guideline was used to conduct semi-structured interviews with stakeholders. A semi-structured interview allows for a diversion of the interview from the main structure that is provided by the guideline.

Paragraphs	Issue	Aspects	Elements to consider
1. Organisation	A. Interviewee	<ul style="list-style-type: none"> • Organisation • Name of the interviewee • Function/role • Experience with weather forecast process 	
	B. Type of organisation	<ul style="list-style-type: none"> • Rail • Road • Power grids • Telecom and data grids • Other land based CI operators 	
2. Inventory of functional consequences	A. Identified functions that can be affected by extreme weather events	<ul style="list-style-type: none"> • Flow of road traffic • Train services • Power transmission • Information flow • Emergency management 	
	B. Identified infrastructure that can be affected by extreme weather events		
	C. Expected consequences for the identified functions (which service can't be continued) and identified infrastructure failures (which element is expected to be out of function)	<ul style="list-style-type: none"> • Detail the consequences 	
	D. Identified extreme weather events that are relevant for the organisation	<ul style="list-style-type: none"> • For which functions • For which assets/part of infrastructure • Which extreme weather event will lead to an operational failure with a high impact on society 	<ul style="list-style-type: none"> • Wind storms • Heavy rainfall • Coastal floods • River floods • Landslides • Tornadoes • Large hail • Thunderstorm gusts • Lightning • Snow (or snow storms) • Freezing Rain and Icing • Wildfires • Heat or cold waves • Dense fog • Other
	E. What intensity of an event would lead to these consequences?	<ul style="list-style-type: none"> • Name thresholds, if possible. 	

	F. What kind of preventive measures are implemented against the identified weather events?	<ul style="list-style-type: none"> • Arrangement with a weather service e.g., to provide early warning? • Emergency plan for warning case? 	
	G. What kind of preventive measures should be developed against the identified weather events?		
	H. What kinds of response measures are implemented for each type of extreme weather event?		
	I. What kind of response measures should be developed for each type of extreme weather event?		

(questions about arrangements with weather services omitted²)

3. Present arrangements	A. What kind of essential framework arrangements are made with weather services?		<ul style="list-style-type: none"> • Contract? • MoU? • Detailed working procedures? • Shared IT-systems? • Dedicated forecasts? • Involvement of weather service in emergency management? • If no: go to question 4
-------------------------	--	--	---

(questions about arrangements with weather services omitted)

4. Experiences	A. Which extreme weather events with severe effects occurred during the last 25 years?		
----------------	--	--	--

² The interview also included a sizeable number of questions relating to arrangements of stakeholders with weather services. The analyses of the responses to these questions are topic of a forthcoming RAIN report.